MODIFICATION OF VESICULAR STOMATITIS VIRUS G PROTEIN FOR TARGETED GENE DELIVERY INTO PSCA-POSITIVE TUMOR CELLS

DISSERTATION

zur Erlangerung des akademischen Grades

Doctor rerum naturalium

(Dr. rer. nat.)

eingereicht an der

Fakultät Mathematik und Naturwissenschaften

der Technischen Universität Dresden

von

Serap Güneş

geboren am 17.07.1981 in Kocaeli

Gutachter: 1. Prof. Dr. med. habil. Ernst Peter Rieber
                 2. Prof. Dr. rer. nat. habil. Gerhard Rödel
                 3. Prof. Dr. med. habil. Hinrich Abken

Tag der Einreichung   : 05.04.2007
Tag der Disputation   : 21.06.2007

ACKNOWLEDGEMENTS

PUBLICATIONS

Temme A., Rodriguez J.A., Hendruschk S., Gunes S., Weigle B., Schakel K., Schmitz M., Bachmann M., Schackert G., Rieber E.P. (2006)

Nuclear localization of Survivin renders HeLa tumor cells more sensitive to apoptosis by induction of p53 and Bax.

Cancer Letters, Nov 3, [Epub ahead of print]

Morgenroth A., Cartellieri M., Schmitz M., Gunes S., Weigle B., Bachmann M., Abken H., Rieber E.P., Temme A.

Targeting of tumor cells expressing the prostate stem cell antigen (PSCA) using genetically engineered T cells

The Prostate (in Press)

ABBREVIATIONS

AAV	Adeno-associated virus
Ab	Antibody
Ad	Adenovirus
ADA	Adenosine deaminase
Ag	Antigen
AMI	scFv against PSCA
ATCC	American Type Culture Collection
bp	Base pair
BSA	Bovine serum albumin
CA	Capsid protein
PCa	Prostate cancer
CAR	Coxsackie and Adenovirus receptor
CFTR	Cystic fibrosis transmembrane conductor regulator
CMV	Cytomegalovirus
Cryy	C-receptor 1-related gene/protein y
C-terminus	Carboxy terminus
Cy3	Indocarbocyanin
D-MEM	Dulbecco's Modified Eagle's Medium
DMSO	Dimethylsulfoxyde
DNA	Desoxyribonucleic acid
dNTP	Desoxynucleotide
dsDNA	Double-stranded DNA
DSMZ	German Collection of Microorganisms and Cell Culture

E.coli	Escherichia coli
ECL	enhanced chemiluminescence
EDTA	Ethylenediaminetetraacetic acid
e.g.	*exempli gratia* (Latin; for example)
EGFP	Enhanced green fluorescence protein
ER	Endoplasmic Reticulum
et al.	*et alia* (Latin; and others)
EtBr	ethidium bromide
etc.	*et cetera* (Latin; and so forth)
Fab	Variable fragment
FACS	Fluorescence activated cell sorter
Fc	Constant domain
Fig.	Figure
FITC	Fluorescein-Isothiocyanat
FSC	Forward scatter
g	Centrifugal force
Gag	Retroviral group-specific antigen
GALV	Gibbon Ape Leukemia Virus
GAM	Goat anti-mouse
GBM	Glioblastoma Multiforme
GM-CSF	Granulocyte-macrophaeg colony stimulating factor
gp	Glycoprotein
GPI	Glycosylphosphatidylinositol
HEK cells	Human Embryonic Kidney cells
HEPES	[4-(2-hydroxyethyl)-1-piperazine]-ethanesulfonic acid

HER2	Human epidermal growth factor receptor 2
HMW-MAA	High-molecular weight melanoma-associated-antigen
hr	Hour
HRP	Horseradish peroxidase
HSV	Herpes Simplex Virus
HTLV	Human T Cell Leukemia Virus
ICP	Infected cell protein
i.e.	*id est* (Latin; that is)
Ig	Immunoglobulin
IL	Interleukin
INF	Interferon
IRES	Internal ribosome entry site
kb	Kilobase
kDa	Kilodalton
LATs	Latency-Associated Transcripts
LB medium	Luria Bertani medium
LMO-2	LIM domain only-2
LTR	Long terminal repeat
M	molar
MA	Matrix protein
min	Minute
MLV	Murine Leukemia Virus
mM	minimolar
MMP	matrix metalloprotease
MOI	multiplicity of infection

MoMuLV	Moloney Murine Leukemia Virus
mRNA	Messenger RNA
MTX	Methotrexate
NB	nanobeads
NC	Nucleocapsid protein
Ni-NTA	Nickel- Nitriltriacetic acid
N-terminus	Amino terminus
OD	optical density
PAGE	Polyacrylamide gel electrophoresis
PBS	Phosphate buffered saline
PCR	Polymerase chain reaction
PEG	polyethylene-glycol
PEI	Polyethylenimine
PFA	Paraformaldehyde
PH domain	Pleckstrin homology domain
phOx	4-ethoxymethylene-2-phenyl-2-oxazolin-5-one
PLL	Poly-L-lysine
Polybrene	Hexadimethrinbromide
PS	Phosphatidylserine
PSA	Prostate Specific Antigen
PSCA	Prostate stem cell antigen
PVDF	Polyvinylidenfluorid
Ψ	Packaging signal "Psi" of a retroviral RNA
RNA	Ribonucleic acid
RT	Room temperature

scFv	single-chain antibody variable fragment
SCID	Severe Combined Immune Deficiency
SDS	Sodium dodecyl sulfate
SSC	Side scatter
ssDNA	Single-stranded DNA
STET	TRIS NaCl EDTA Triton X-100 buffer solution
SU	Surface subunit
TAA	Tumor-Associated Antigen
TBE buffer	Tris-Borate-EDTA buffer
TBS buffer	Tris-buffered saline
TBS-TT	TBS-Tween 20-Triton X-100
TE	Tris-EDTA buffer
TIL	Tumor-infiltrating lymphocyte
TK	Thymidine kinase
TM	Transmembrane subunit
V_H chain	Variable heavy chain
V_L chain	Variable light chain
VSV-G	Vesicular Stomatitis Virus G protein
wt	Wild type
ZZ domain	Immunoglobulin G-binding domain from Protein A (Staphylococcus aureus)

1.   SUMMARY

Gene therapy is a promising treatment option for cancer. Ideally, a therapeutic gene is delivered specifically into tumor cells sparing the neighboring normal cells. For this purpose gene delivery vectors are designed that can recognize structures, which are exclusively expressed on tumor cells (*i.e.* the tumor-associated antigens -TAA-). Retroviral vectors are commonly used for gene therapy by modifying the envelope protein responsible for the recognition of the target cell. The Vesicular Stomatitis Virus G protein (VSV-G) is a well-liked choice for pseudotyping the retroviral vectors since it confers on the viral particle stability to allow concentration to high titers necessary for the clinical applications. However, the main drawback of VSV-G, the ubiquitously expressed receptor and thus the broad target range, hinders the use of this protein for targeted gene therapy.

In this thesis, we aimed to modify the VSV-G for targeted gene therapy against Prostate Stem Cell Antigen (PSCA) -expressing tumors. Therefore we followed two approaches. The first approach comprised of the fusion of a single-chain antibody fragment against PSCA to the N-terminus of VSV-G. In the second approach the VSV-G was modified by insertion of a small epitope.

We could demonstrate that two positions in the N-terminal region of VSV-G protein permit insertion of a ten amino acid long epitope. These mutant VSV-G proteins were successfully assembled into retroviral particles. We demonstrated that the mutant retroviral particles can be used for targeting to PSCA-positive cells using nanobeads. The nanobeads were chemically coupled to antibodies against the epitope in the VSV-G protein and PSCA on the tumor cell. These bispecific nanobeads allowed the recruitment of mutant retroviral particles to the PSCA-positive cells. Our results point out the potential of these mutant retroviral particles in targeted gene delivery. Further studies will be necessary to assess the efficiency of *in vivo* targeted gene therapy using these mutant retroviral particles.

2. INTRODUCTION

2.1. Gene Therapy

Gene therapy is a molecular approach in medicine whose aim is to cure or slow down the progression of a disease by transferring genetic material into specific cells. Among the first candidates for gene therapy were the monogenic diseases, where the delivery of a functional gene copy substitutes for a defective gene. Accompanied by increased knowledge of the molecular mechanisms underlying diseases, several other target diseases also entered the scene of gene therapy, including infectious diseases and cancer. The first clinical gene transfer trial comprised marker gene transfer to tumor-infiltrating lymphocytes (TILs) in 1989 [4]. In this first study, TILs were isolated from patients and a bacterial Neomycin resistance gene was transferred by a retroviral vector into these cells. Gene-marked TILs were re-infused into patients and the fate of engineered cells was observed by subsequent periodic blood sampling from patients. This study was followed by several other gene marking studies [5] . It was in 1990 when Blaese *et al.* conducted the first therapeutic gene therapy trial on two girls suffering from adenosine deaminase (ADA) deficiency – a form of severe combined immune deficiency (SCID). ADA deficiency is an inherited genetic disorder which leads to inability to degrade adenosine. This in turn causes toxicity to T cells and results in immunodeficiency. In this trial both patients received infusions of autologous gene-corrected T lymphocytes. The clinical outcomes of this study were encouraging [5,6].

Currently, nearly thousand clinical gene therapy protocols are applied worldwide [7]. And surprisingly the initial targets, monogenic diseases, constitute only a small fraction of the diseases treated by gene therapy approaches (Figure 1A) [1]. Most of the protocols (67%) intend to treat cancer, which reflects both the urgent need for new cancer treatment modalities and also the already existing knowledge of the disease biology. In general, cancer gene therapy trials employ three approaches to eliminate tumor cells. The first approach aims at boosting the patient's immune system to recognize and defeat tumor cells. Here, tumor cells can be modified to express molecules that enhance an anti-tumor immune response. Several molecules have been used so far, including tumor-specific (TSA) or tumor-associated (TAA) antigens and cytokines. To date, Interferon (IFN) γ [8] and Interleukin (IL)-2 [9,10] encoding genes are used in the treatment of several cancers, such as prostate cancer, melanoma and lymphoma (Figure 1B).

The second strategy aims at destroying tumor cells by facilitating a cell cycle arrest or by inducing programmed cell death (apoptosis). Most cancer cells bear defects in tumor suppressor genes, which control the cell cycle and the apoptosis. Therefore, it is possible to eliminate tumor cells by delivering into tumor cells

genes whose products either restore the function of a tumor suppressor gene such as p53 or induce apoptosis.

The third approach for treating cancer by transfer of genes is the so-called suicide gene therapy. Here, genes encoding enzymes, such as the thymidine kinase (TK) of the Herpes Simplex Virus (HSV), are transferred into tumor cells. The modified tumor cells become capable of phosphorylating the prodrug ganciclovir, which can be administered intratumorally or systemically. This initiates a phosphorylation cascade whose end product triphosphate ganciclovir is a toxic nucleoside analogue, which interferes with the DNA replication [11].

Gene therapy is an up-and-coming option for many hereditary and infectious diseases as well as cancer, and yet incurable diseases such as AIDS. Although the preferential methods may vary for each disease, all gene therapy applications share the common requirement for a delivery vehicle that ensures a selective and highly efficient gene transfer into the target cells.

A

Indications Addressed by Gene Therapy Clinical Trials

- Cancer diseases 67% (n=842)
- Vascular diseases 9% (n=113)
- Monogenic diseases 8.4% (n=106)
- Infectious diseases 6.4% (n=81)
- Gene marking 4% (n=50)
- Other diseases 3.7% (n=47)
- Healthy volunteers 1.7% (n=21)

The Journal of Gene Medicine, © 2007 John Wiley and Sons Ltd   www.wiley.co.uk/genmed/clinical

B

Gene Types Transferred in Gene Therapy Clinical Trials

- Cytokine 27% (n=335)
- Antigen 16% (n=203)
- Tumor suppressor 11% (n=141)
- Suicide 7.8% (n=98)
- Deficiency 5.8% (n=73)
- Drug resistance 4.4% (n=56)
- Receptor 3.7% (n=47)
- Replication inhibitor 3.6% (n=45)
- Others 18% (n=223)
- Unknown 3.1% (n=39)

The Journal of Gene Medicine, © 2007 John Wiley and Sons Ltd   www.wiley.co.uk/genmed/clinical

Figure 1. Gene therapy clinical trials

Distribution of (A) indications addressed by the gene therapy clinical trials and (B) the therapeutic genes transferred (http://www.wiley.co.uk/genmed/clinical/).

2.2. Gene Therapy Vectors

The main objective of the gene therapy is to transport therapeutic genetic material into the target cells. Accordingly, gene transfer vehicles, so-called vectors, are needed. An ideal gene therapy vector should allow selective and efficient transfer of a gene. Furthermore, it should be easy to handle and cost-effective to produce, and last but not least, it should cause no adverse immune responses in the host [12].

2.2.1. Non-viral vectors

Gene delivery vectors can be broadly categorized into two groups: non-viral and viral vectors. Non-viral vectors are appealing since they are non-infectious, and are not very toxic to the cells. They can be easily prepared and produced at large scales. The size of the genetic material that can be transferred using a non-viral vector is theoretically unlimited, whereas in the case of viral vectors the packaging capacity is defined. Another advantage of non-viral vectors compared to the viral gene transfer systems is their safety. In general, the non-viral vectors do not induce a specific immune response and are usually less immunogenic than viral vectors. However, the low gene transfer efficiency achieved with non-viral vectors remains an obstacle for clinical applications.

The simplest way of transferring DNA into a cell is to inject naked DNA. Naked DNA was shown to be taken up by muscle cells but the transfection efficiency was low [13,14]. Moreover, expression of the transgene was transient. Genetic material transfer using non-viral vectors can also be performed by chemical or physical methods [15]. The physical transfection methods include electroporation [16-18] and gene bombarding [19]. Electroporation relies on the generation or opening of pores on the target cell membrane by electrical shock, followed by the entry of the DNA into the cells. In gene bombarding the DNA, which is coupled to gold particles, is 'shot' into the target cells under high pressure. Chemical transfection methods include calcium phosphate precipitation [20]. In calcium phosphate precipitation [21], [4-(2-hydroxyethyl)-1-piperazine]-ethanesulfonic acid (HEPES) - buffered solution containing phosphate ions is used together with calcium chloride to form complexes with DNA. Calcium phosphate/DNA complexes precipitate onto the monolayer cells in culture.

DNA can also be delivered using lipids and polymers. These DNA packages are internalized by the target cell via the endocytotic pathway. Anionic and neutral liposomes have been used for DNA transfer, but are now outnumbered by cationic liposomes [22-28]. Cationic liposomes can interact with the negatively charged DNA and form complexes spontaneously. Cationic liposome/DNA complexes still bear absolute positive charges that protect the DNA from degradation by enzymes and interact with the negatively charges phospholipids in the target cell membrane

and release their contents into the target cells [29-31]. Alternatively, cationic polymers can be formed into complex with DNA for delivery [32]. The most commonly used cationic polymers are poly-L-lysine (PLL) and its derivatives polyethylenimine (PEI) [33-36], polybrene and chitosan [37-39]. Cationic polymers are synthetic molecules and therefore can be readily modified for ligand-targeted binding to defined cell types [40,41].

Despite the safety advantage of non-viral vectors, their gene transfer efficiency must be improved to become ideal gene therapy vectors. Actually, most studies and clinical trials [7] focus on viruses as gene delivery vehicles (Figure 2). Viruses have naturally evolved to transfer genes into host cells. Adenoviruses, Herpes Simplex viruses, Adeno-associated viruses and retroviruses (including lentiviruses) are among the most commonly used viruses in gene therapy.
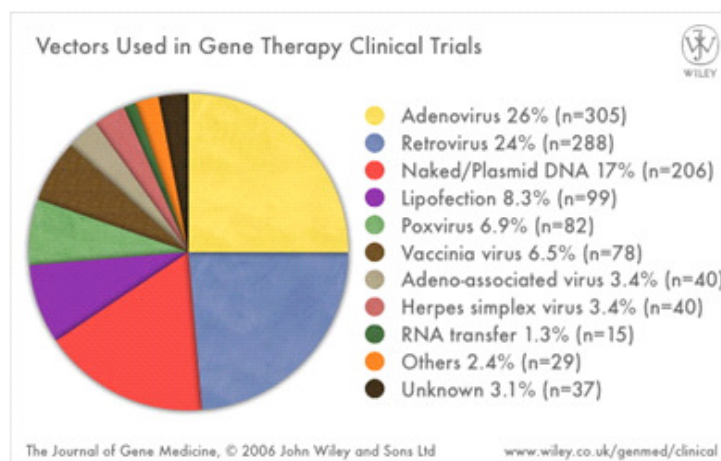
Figure 2. Gene therapy vectors used in clinical trials [1].

2.2.2. Viral vectors

During evolution viruses have acquired advanced mechanisms to deliver their genetic material to their host cells such as the ability to overcome cellular barriers (*i.e.* the plasma membrane, and degradation by lysosomes after internalization). Therefore, viruses offer great opportunities in the gene therapy field, where efficient gene delivery plays a decisive role [42] . There are several viruses which have been adopted for gene therapy.

2.2.2.1.   *Adenoviruses*

Adenoviruses (Ad) are non-enveloped, linear double-stranded DNA viruses. An approximately 36kb long adenoviral genome is encapsulated in an icosahedral protein coat. Adenovirus entry into the host cell is mediated by two main interactions. The knob domain of the 182 kDa fiber protein in the viral coat

interacts with the "Coxsackie and Adenovirus receptor" (CAR) in the target cell [43-45]. Virus internalization occurs by means of receptor-mediated endocytosis via the interaction between Arg-Gly-Asp motives in the penton base and the cellular integrins [46,47]. Adenoviruses can infect both dividing and non-dividing cells with equal efficiency. Also, recombinant adenoviruses can be produced at very high concentrations and they have a high capacity for foreign DNA (approximately 8.5kb). However, adenovirus-mediated therapeutic gene expression is transient since no integration into the host genome takes place.

Adenoviruses have been extensively used in various gene therapy approaches and are under continuous development [48,49]. Three generations of adenoviral vectors have been generated to decrease the cytopathic effects and immune responses. The first-generation adenoviral vectors lack the E1 region, whose products control the activation of DNA synthesis and the late viral gene expression [50]. These E1-deleted adenoviral vectors are replication-deficient, but are still immunogenic. To reduce the adverse immunological effects of adenoviral vectors the second-generation adenoviral vectors were generated by deleting the E2 or E4 region from the E1-deleted viruses [51-54]. Further improvement has been attempted with the so-called "gutless" vectors (third-generation) which retain only the *cis*-acting inverted terminal repeats and a packaging signal from the wild-type virus [55]. Production of gutless vectors requires a complementing packaging cell line [56-59] or a helper virus [60-62], which provides the necessary viral structural proteins *in trans*.

A limitation of adenoviruses as gene therapy vectors is that the majority of the human population already has faced infections with wild-type adenoviruses. Therefore, the presence of neutralizing antibodies against different serotypes remains an obstacle for gene therapy using adenoviral vectors. Nevertheless, adenoviral vectors constitute the most commonly used vectors in clinical gene therapy trials (Figure 2) [63-68].

2.2.2.2. Adeno-associated viruses

Adeno-associated virus (AAV) – a member of the parvovirus family- is a single-stranded non-enveloped DNA virus with a 4.5 kb genome. Usually the AAV serotype 2 is used as a template for AAV vectors. Wild-type AAV 2 is non-pathogenic to humans and integrates into the long arm of chromosome 19 in human cells [69,70]. However, the recombinant AAV (rAAV) loses this specificity and integrates at other sites [71]. All but 145bp of the AAV genome, the terminal repeats containing a promoter, can be removed to insert foreign genes, yet the AAV genome size may not be exceeded. Unfortunately, this packaging capacity is often too small for therapeutic genes, limiting the applications of rAAV as gene therapy vector. AAV-derived vectors require a helper virus (mostly Ad) for viral replication. Difficulties in complete removal of the helper virus from the viral stocks

still hinders the use of AAV-derived vectors for human gene therapy [72]. Nonetheless, rAAV vectors have been introduced into the Phase I clinical trials in cystic fibrosis treatment [73,74] delivering the cystic fibrosis transmembrane conductance regulator (CFTR) gene. These studies demonstrated that AAV-derived vectors were well tolerated by the patients. On the other hand, a patient died in a Phase I trial using rAAV to deliver Hemophilia B (Factor IX) through intrahepatic artery [75] and the study was abandoned. This incident led to some apprehensions about the safety of rAAV-mediated gene therapy.

2.2.2.3.   *Herpes Simplex Virus-1*

Herpes Simplex Virus-1 (HSV-1) is a natural human pathogen with a 150kb double-stranded DNA genome. Non-essential genes can be removed and the virus can then carry up to 50kb of foreign genes, which enables several genes to be packaged [76]. HSV-1 infection has two phases: the lytic replication and the latent state. The lytic infection, which generally takes place in epithelial cells, results in virus replication and lysis of the host cell, hence the name. However, sometimes the virus proceeds along the nerves and commences the latent state in the neurons. The latent virus shuts off the host cell protein synthesis and allows the production of only a small set of RNA species (Latency-Associated Transcripts or LATs) [77-80].

HSV-1 can infect both dividing and non-dividing cells but integration into the host genome does not occur. Although it can infect a broad range of cells, HSV exhibits a natural tropism to neurons, where it can persist as an intranuclear episome during the lifetime of the host. A disadvantage of HSV-1–derived vectors is their cytotoxicity owing mainly to proteins called "the infected cell proteins" (ICP) [81]. Recombinant HSV-1 vectors are produced with deletions in the ICP genes to reduce toxicity. The biggest concern in the use of HSV-1 vectors for human gene therapy is the safety of this natural pathogen.

There are two generations of HSV-1 vectors. The first-generation vectors contain mutations in a single gene and can replicate only in dividing cells. For instance, HSV1716 is a first-generation vector in which one copy of the ICP34.5 gene is deleted. ICP34.5 is normally found as two copies located in the inverted repeat regions and plays an important role in pathogenicity in neurons. HSV1716 is used in clinical trials for recurrent high-grade glioma, where viral replication was shown to take place only in glioma cells [82]. To further reduce the risk of reverts to the wild-type virus, in the second-generation vectors more genes are deleted or mutated. G207 is a second-generation HSV-1-derived vector in which both copies of ICP34.5 are deleted and a lacZ marker gene is inserted destructively into the gene encoding the large subunit of viral ribonucleotide reductase. It has been tested in malignant glial tumors and exhibited anti-tumor effects without any virus-related toxicity [83].

2.2.2.4. Retroviruses

Retroviruses [42,84-88] are enveloped, single-stranded positive-sense RNA viruses with a diploid genome (Figure 3). Retroviruses are divided into two groups according to the complexity of their genomes: simple (*e.g.* Murine Leukemia Virus –MLV) and complex retroviruses (*e.g.* Human Immunodeficiency Virus –HIV). All retroviruses contain at least three coding regions – *gag*, *pol* and *env* (Figure 4). The *gag* (group-specific antigen) region encodes a precursor protein, which gives rise to the capsid (CA), the matrix (MA) and the nucleocapsid (NC) proteins. The *pol* gene (which overlaps at the 3' end with the 5' end of *gag*) encodes for the reverse transcriptase, which generates a DNA copy of the RNA genome, and the integrase, the enzyme catalyzing the integration of the provirus into the host genome. The product of the third region *env* is the envelope protein, which consists of a surface subunit (SU) and a transmembrane (TM) subunit. Moreover, there is a small coding region called *pro,* common to all retroviruses, coding for the protease that is responsible for the cleavage of the viral proteins. Complex retroviruses, such as Human T Cell Leukemia Virus (HTLV) or HIV, contain additional coding regions for accessory proteins which enable them to infect post-mitotic or quiescent cells.
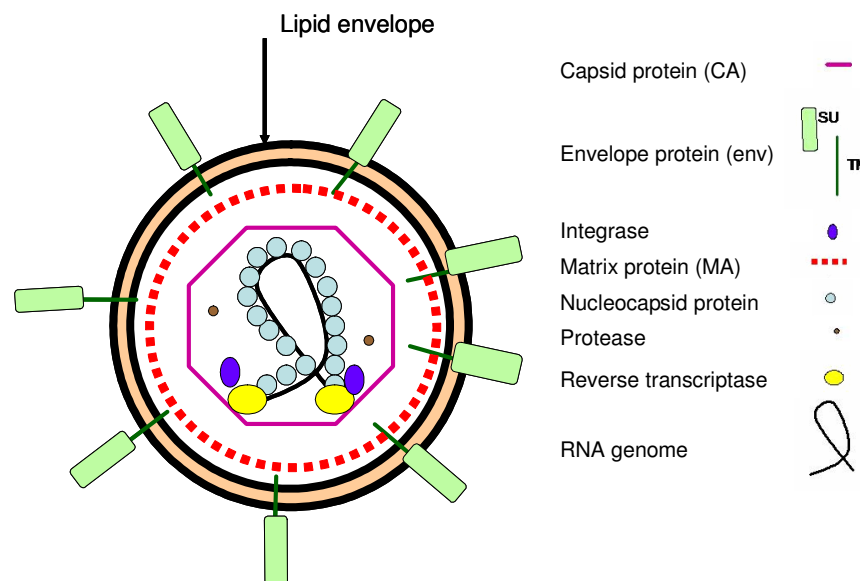
Figure 3. Structure of a retrovirus.

The retrovirus-derived vectors are generated by the removal of non-essential coding regions from the virus genome. The essential *gag-pol* and *env* regions can be supplied *in trans*. To reduce the reversion to the wild-type replication-competent retrovirus, these essential coding regions are supplied on different transcriptional units. The only sequences necessary *in cis* are the packaging signal (Ψ), the long-terminal repeats (LTRs) and the elements directing the reverse

transcription such as the primer-binding site. LTR regions exist as two copies, each on one side of the viral genome and contain the promoter elements that regulate the transcription of the genes and regions responsible for the polyadenylation of proviral transcripts. Removal of the non-essential genes allows packaging of approximately 7-8kb foreign DNA.
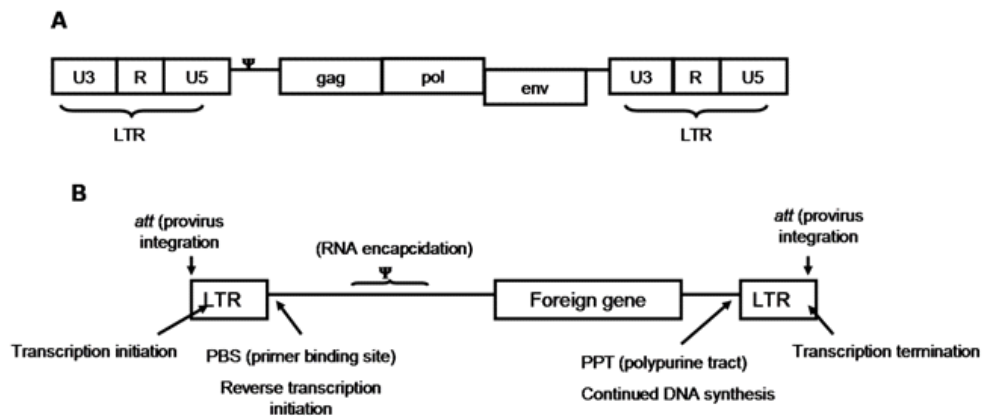
Figure 4. Genomic organization of retroviruses and retroviral vectors.

A: The genome structure of a prototypical retrovirus. B: *cis*-acting elements of a typical retroviral vector. Modified from Buchschacher, G. L. and Wong-Staal F. 2000 [89].

The natural tropism of retroviruses is defined by the envelope protein. In general, the envelope proteins consist of two subunits. The surface subunit (SU) binds to the target cells via its receptor and brings the transmembrane unit (TM) into the vicinity of the cell membrane. Then, the TM subunit mediates fusion of the retroviral envelope with the target cell membrane. Target specificity can therefore be manipulated by modifying the SU portion. Moreover, viral particles can be assembled using the envelope protein from another virus [90-92]. Although several viral envelope proteins have been used to alter the retroviral tropism, most of the studies concentrated on Vesicular Stomatitis Virus G protein (VSV-G) [93]. VSV-G confers a broad target range [94] and stability on the retroviral particle, paving the way for the concentration of the virus to high titers by ultracentrifugation [95].

Retroviral vectors are the prototype viral vectors used in human gene therapy [96]. The results of the first trial encouraged further work with retroviral vectors and a few years later retroviral vectors were used to treat a lethal form of Severe Combined Immune Deficiency (X-linked SCID) [97-100]. The outcomes were auspicious, yet three of the patients developed T-cell leukemia-like symptoms [101]. Careful analysis of the proviral integration sites in these patients revealed a single copy of provirus integration at or near the Lim domain only-2 (LMO-2) gene [102], whose gene product is a central regulator of hematopoiesis. This led to concerns about the insertional mutation risk in the retroviral gene delivery.

Nevertheless, retroviruses continue to make up 24% of the clinical protocols used in human gene therapy.

2.3. Targeting retroviral gene delivery vectors

An essential feature of an ideal gene therapy vector is the ability to distinguish between target (*e.g.* tumor cells) and non-target cells. There are mainly two steps in gene delivery that may be modified to achieve a targeted tropism. One way is to control expression of the therapeutic gene at the transcriptional level by making use of tissue- or tumor-specific promoters so that the delivered gene is only expressed in target cells [103,104]. For instance, Vile *et al.* [104] demonstrated successfully that melanoma cells can be targeted with retroviral vectors under the transcriptional control of the murine tyrosinase gene promoter region. Another approach to achieve targeted gene delivery into the target cells is to re-define the viral host range [105-107], thus the virus can only infect a selected cell type while leaving the neighboring non-target cells untouched.

2.3.1. Modification of the viral envelope proteins for targeted gene therapy of tumor cells

Promising target structures for the selective transduction via modified viruses are the so-called "tumor-associated antigens (TAA)" (*i.e.* HER2/neu on mammary carcinoma cells, the high-molecular-weight melanoma-associated-antigen (HMW-MAA) on malignant melanoma cells). Ideally, these antigens are exclusively expressed on the tumor cells.

Target cell tropism can be achieved by several genetic modifications of the viral envelope proteins, for example by introducing engineered domains derived from growth factors, domains from adhesion molecules and other targeting devices such as single-chain variable fragments (scFv). In a recent approach Ohno *et al.* [106,107] modified the Sindbis virus envelope protein by inserting two tandem repeats from the immunoglobulin G-binding domain (ZZ-domain) of Protein A from Staphylococcus aureus. After conjugating chimeric viruses with monoclonal antibodies against CD4 and EGFR, respectively, selective infection of CD4-positive lymphoblastoid cells and EGFR-positive glioma cells were obtained. The ZZ-domain was also used to modify the ecotropic and the amphotropic Moloney Murine Leukemia Virus (MoMuLV) envelope proteins. When tethered to an anti-HER2 monoclonal antibody these chimeric viral particles specifically bound to HER2/neu-positive cells. However, the fusion capacity of the chimeric envelope protein was severely impaired. Therefore, it was necessary to co-express the wild-type envelope protein [108]. Recently, Morizono *et al.* [109] used a ZZ-domain-modified Sindbis virus envelope protein to pseudotype lentiviruses. The lentiviral particles were conjugated to anti P-glycoprotein antibodies. Then the conjugated

chimeric lentiviral particles were successfully used for selective *in vivo* transduction of melanoma cells. The IgG-binding domain allows this system to be extended with other antibodies targeting a broad spectrum of cell types. On the other hand, a clinical application in humans can be hindered by a variety of IgG antibodies present in human serum that likely compete with the binding of the conjugated targeting antibody. An alternative approach to confer target specificity and to avoid interference with serum antibodies is the direct fusion of a single-chain variable fragment to the viral envelope protein. Following this approach, Martin *et al.* [110,111] modified the amphotropic 4070SU protein by fusing a single-chain antibody fragment against the high-molecular-weight melanoma-associated-antigen (HMW-MAA) expressed on melanoma cells. They introduced a matrix metalloprotease (MMP) cleavage site between the scFv and the envelope protein. The modified viral particles bound to the melanoma cells and the MMP enzymes on the target cell surface cleaved off the scFv. The virus was then free to transduce the target cell. Although a successful binding of the viral particles to melanoma cells was demonstrated, the transduction efficiencies were not convincing.

2.3.2. Pseudotyping retroviral vectors

A widely used approach for targeting viral vectors to specific cell types or to expand the tropism is to exchange the envelope proteins. This procedure, the so-called pseudotyping, allows adopting the known tropism of a certain virus. To date, several envelope proteins have been tested for altering the tropism of retroviral vectors [112-114], in particular, the Gibbon Ape Leukemia Virus (GALV) [113-115] envelope protein and the VSV-G protein [93,95,116-119]. Although some studies suggest GALV envelope protein as a promising alternative [120-122] to VSV-G due to comparable transduction efficiencies and the identified cellular receptor, VSV-G continues to be the leading choice for pseudotyping retroviral particles [123].

2.3.2.1. *Vesicular Stomatitis Virus G protein (VSV-G)*

The VSV-G protein from Indiana serotype contains 511 amino acids, and is a Type-I membrane protein [124]. This envelope protein possesses a single transmembrane domain and exposes its amino terminus on the exterior side of the membrane and its carboxy terminus on the interior side.

During maturation, the VSV-G precursor first inserts into the Endoplasmic Reticulum (ER) where the signal peptide is cleaved and the protein trimerizes [125,126]. Most of the folding and also the N-glycosylations occur at this step while the protein is still in the ER [127]. Only the correctly folded, glycosylated [128,129], and trimerized proteins are transported to the Golgi apparatus. Misfolded VSV-G

proteins are retained in the ER associated with ER chaperons like BiP and calnexin [130-132]. In the Golgi apparatus the post-translational modifications are further processed and the VSV-G protein is transported to the cell membrane. There is a very tight regulation on the transport of the protein [126]. Therefore, any modification to target the VSV-G to a specific receptor must maintain three features of the protein. First of all, the proper folding must be retained. Second, the trimerization must take place. Last but not least, a vital step in the viral infection, the fusion capacity, must be preserved despite the mutation.

VSV-G-mediated viral infection starts with the binding of VSV-G protein to its yet unidentified ubiquitously expressed cellular receptor [124]. It has been shown by saturation experiments in Vero cells that VSV-G facilitates the viral entry over a specific receptor [133]. Schlegel *et al.* proposed phosphatidylserine (PS) as the cellular receptor since purified PS inhibited VSV binding and infection [134]. However, Coil *et al.* [135] reported being unable to reproduce these results. A following study from Carneiro *et al.* [136] confirmed a direct interaction between VSV-G and PS before the acidification in the endosomal vesicle, but did not point out PS as the cellular receptor. Using the information from other Rhabdoviruses that are known to bind to PS, a similar PS-binding domain (called the p2-like peptide) is located in VSV-G between the amino acid residues 134 and 161 [137-139].

Following the interactions with the receptor, virus is internalized into endosomal vesicles, which shortly thereafter acidify. The acidic pH triggers drastic conformational changes in the VSV-G protein and generates a fusion-active form [140-142]. VSV-G-mediated fusion of the viral envelope with endosomal membrane occurs in a narrow pH range, between 5.8 and 6.2. Histidine residues 148 and 149 are protonated in this pH range and these positively charged residues were shown to interact with PS [136,141]. All viral fusion proteins including VSV-G share some characteristics [143,144]. There are two main classes of viral fusion proteins: Class-I proteins (such as Influenza HA) and Class-II proteins (such as the Alphavirus E1 protein). These two classes differ in the number of units in the envelope oligomers and in the initial fusion step. The Class-I proteins form trimers of two-chain monomers whereas the Class-II proteins exist as dimers and are associated with another viral protein. In Class-I proteins the fusion peptide is generated by proteolytic cleavage of the N-terminus of the protein, however Class-II proteins are not cleaved – rather their associated proteins are. Despite all the structural differences between the classes, both types of proteins are synthesized in an energetically metastable conformation favoring the post-fusion conformation (irreversible conformational change). Another common property of both fusion protein classes is the post-fusion structure, which appears as trimers. The VSV-G protein, despite sharing several features with already defined viral fusion proteins, has some distinct characteristics [145]. It forms like the Class-I fusion proteins trimers in the viral membrane, but is not

synthesized in metastable conformation and the conformational change leading to fusion is reversible.

Fusion of the endosomal membrane with the viral envelope, releases the viral capsid into the cytoplasm. The viral genome is then transported to the nucleus and the viral genes are expressed.

The VSV-G is a common choice to extend the tropism of retroviral vectors and to improve particle stability. However, for clinical applications of VSV-G-pseudotyped retroviral particles the tropism must be restricted to defined target cell populations. In recent years, efforts were made to identify regions in the VSV-G protein that could be modified without affecting protein function but on the other hand could be useful for altering the tropism of the retroviral particle [146,147]. Yet, most of the introduced modifications affected the function of the VSV-G protein negatively: Mutations in the ectodomain were reported to interfere with intracellular transport, whereas many of the transmembrane mutants fail to induce fusion [126,148]. N-terminal fusion of a single-chain antibody fragment to the VSV-G retained the intracellular transport capacities of the wild-type protein, but the fusion and in turn the transduction efficiency was inefficient [149]. Recently, a study reported successful incorporation of His-tag into the ectodomain of VSV-G in a transposon-based procedure [150]. One of the insertions was made at amino acid position 24 (precursor peptide) and the modified protein was successfully incorporated into retro- and lentiviral particles. Interestingly, Guibinga *et al.* [146] showed that VSV-G mutant with an insertion of ten amino acid-long collagen binding domain at this position displays a temperature-sensitive phenotype. The mutant was transported to the surface of transfected cells only at permissive (30°C) temperature. Taken together these results emphasize the need of deeper understanding of the VSV-G structure.

2.3.3. Nanoparticles as targeted therapy tools

Still in its infancy, the nanotechnology offers invaluable tools for the targeted gene delivery. Nanoparticles may be composed of gold, silica or iron oxide cores [26,151-154]. Surface of the nanoparticles are generally modified to enhance DNA or vector binding and the complex stability. The molecules used commonly to surface-modify nanoparticles include among others polysaccharides, starch, dextran and oleic acid (www.chemicell.de).

Iron oxide-derived magnetic nanoparticles are of special clinical interest when the gene delivery vehicle or the genetically engineered targets cells are to be concentrated or purified. Chan *et al.* [155] made use of the ability of lentiviruses to capture packaging cell surface proteins during budding. The packaging cell surface was biotinylated, and the lentiviruses labeled with biotin were concentrated with streptavidin-coupled magnetic beads. The virus was concentrated up to 10^2-

10^3 fold depending on the type of the envelope protein used (VSV-G or the amphotropic envelope proteins, respectively). The authors have also has engineered HEK 293T packaging cells to express B7.1 (CD80) on the surface. They serially conjugated paramagnetic nanoparticles to protein A-biotin and B7.1 binding CTLA 4-immunoglobulin. The modified lentiviral particles were then captured by the modified-nanoparticles. The authors showed enhanced transduction of primary and established leukemia cells with this system.

In addition to their utility as helper molecules for enhanced infection or vector purification, nanoparticles were tested for cellular labeling, drug delivery, imaging, hyperthermia, and as hybrid vectors for cell / vector separation and not to mention transfection [156,157]. Okon *et al.*[158] analyzed the biodegradation of iron-dextran nanoparticles in rat, and suggested that nanoparticles appear as good targeting tools for both *in vitro* and *in vivo* biomedical applications. Recently nanoparticles were used for anti-cancer therapy. Here, nanoparticles were injected transperineally into the prostate [159]. Using alternating magnetic field applicator the nanoparticles were used to obtain hyperthermic to thermoablative temperatures that either render the prostate cancer cells sensitive to apoptosis or lead to direct cell killing, respectively. Kohler *et al.* [160] used iron nanoparticles to target the chemotherapeutic drug methotrexate (MTX) to cancer cells. The authors have modified the surface of nanoparticles with folic acid. Folic acid receptors are found at high densities on cancer cells. With this system they could show receptor-mediated endocytosis of the particle/drug complex and release of MTX in the cell. The therapeutic effect was strictly cancer cell-specific.

2.4. Gene therapy targeting prostate cancer and Prostate Stem Cell Antigen (PSCA)

Prostate cancer (PCa) is among the most commonly diagnosed cancers in men in USA, and is estimated to be the second leading cause of male deaths in 2006 [161]. Radical prostatectomy, radiation and androgen ablation therapies are the current treatment options for the advanced prostate cancer. However, following regression after the hormone depletion therapy some of the patients experience recurrence. Despite the advancements in detection methods and the therapy modalities, there is no effective treatment for patients with recurrent hormone-resistant disease or patients who has metastatic disease at the time of diagnosis. Therefore, new therapy options are urgently needed.

The prostate gland is a readily accessible organ, which allows easy application of the gene therapy vectors. In case of a suicide gene therapy, the by-stander effect, which is the diffusion of toxic products from the target cell to the neighboring cells mainly through gap junctions, is not very detrimental since prostate is an accessory organ. All these features make prostate cancer a suitable candidate for the gene therapy [162].

Several prostate specific proteins were analyzed for their suitability as anti-cancer targets. In analyses of mRNA and protein levels regarding the specificity and expression density, the "Prostate Stem Cell Antigen" (PSCA)- appeared as an appealing candidate for targeted immunotherapy against prostate cancer [163-169]. PSCA is a 123 amino acid GPI-anchored protein. It shares 30% homology with the Stem Cell Antigen-2, from which the name is deduced [168]. Although the function of PSCA in the prostate tissue and its role in prostate carcinogenesis is yet unknown, the elevated protein expression level in prostate cancer and prostate metastasis to bone, in pancreatic cancer and human transitional cell carcinoma indicates its potential as target antigen [163,164,166,167,170]. In addition, Saffran *et al.* [171] pointed out to an anti-tumor effect of an anti-PSCA antibody where they demonstrated tumor regression of the human prostate cancer xenografts in mice. The same anti-PSCA antibody was also shown to inhibit prostate tumor growth *in vivo* by a Fc-independent mechanism [172]. Taken together, the current knowledge suggests PSCA as a good candidate for antibody-based anti-tumor therapy for advanced prostate cancer.

2.5. Aim

The aim of this project was to generate ligand-modified VSV-G proteins for targeted anti-tumor therapy using retroviral vectors. Two strategies were employed for the targeted therapy: Direct recruiting of the viral particles onto the tumor cells (Figure 5) and bringing the viral vector in the vicinity of the target tumor cells via nanoparticles (Figure 6). In the first strategy the VSV-G protein was modified by a N-terminal insertion of a single-chain antibody fragment against the target tumor-associated antigen, the PSCA. The scFv fragment allows the direct connection of the modified retroviral particle and the tumor cell. In the second approach, the VSV-G protein was modified by insertion of a small peptide. The linker molecules between the vector and the tumor cell were superparamagnetic nanoparticles, which are coupled to anti-PSCA and anti-myc antibodies. Both approaches should be followed in the same way, where functional properties of the modified envelope proteins such as intracellular transport, fusion and virus assembly should be assessed in a step-wise manner.
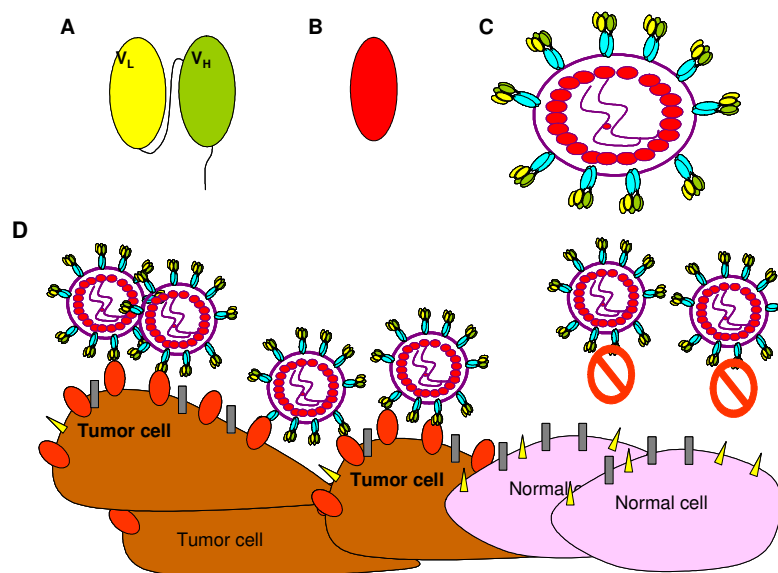
Figure 5. Targeting strategy using scFv-modified viral particles.

Single-chain antibody fragment (A) against the tumor-associated antigen PSCA (B) is fused to the N-terminus of the VSV-G protein. The modified VSV-G proteins are used to pseudotype retroviral particles (C), which can then selectively bind to the PSCA on tumor cells whereby normal cells lacking the target molecule are spared. (D)
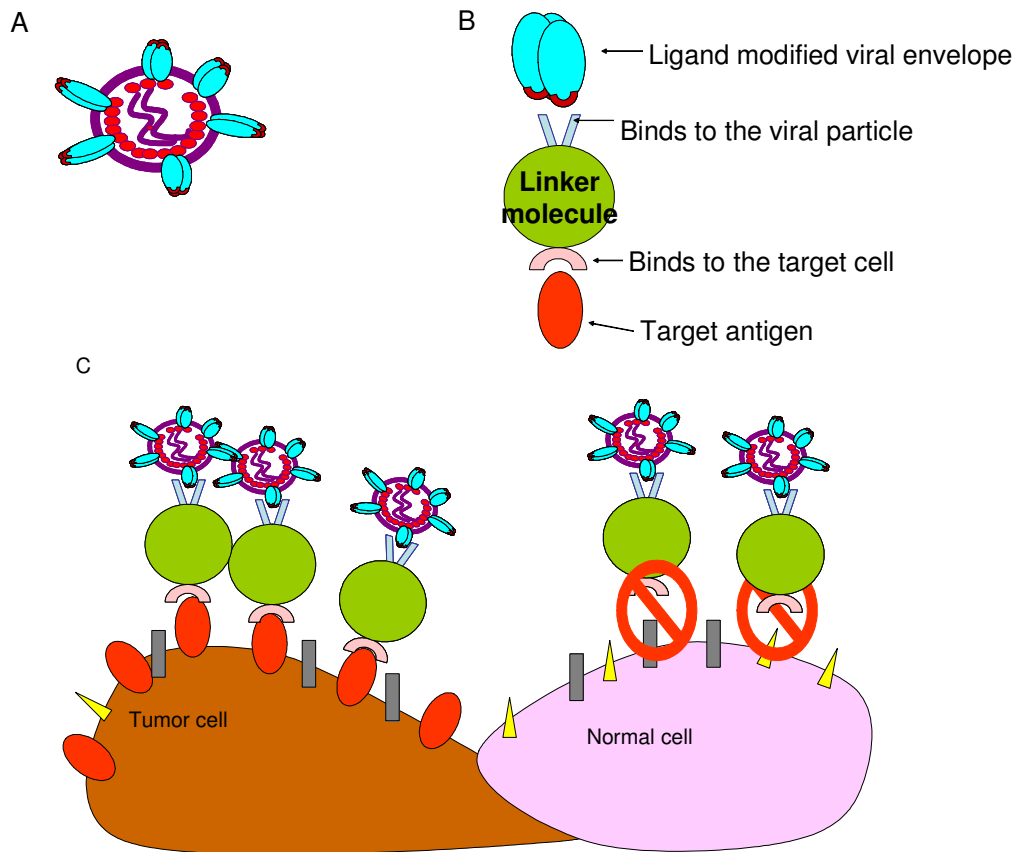
Figure 6. Targeting strategy using ligand-modified viral particles and the nanobeads.

A: Retroviral envelope proteins can be modified by insertion of a ligand or an epitope. B: Linker molecules (*e.g.* bispecific diabodies or nanobeads) can be generated, which are able to bind to the ligand-modified viral particle and a target molecule on the tumor cell simultaneously. C: Ligand-modified viral particles can be directed specifically to the tumor cell that expresses the target molecules whereby normal cells lacking the target molecule are spared.

3.   MATERIALS

3.1.   Chemicals

The chemicals were purchased from Sigma (Taufkirchen, Germany), Merck AG (Darmstadt, Germany), Gerbu (Gaiberg, Germany) or Roth (Karlsruhe, Germany). Chemicals from other suppliers were stated when necessary.

3.2.   Primers

All primers were purchased from MWG-Biotech AG (Munich, Germany).

3.3.   anti-PSCA/ anti-myc superparamagnetic nanobeads

Superparamagnetic nanobeads coupled to anti-PSCA antibody (7F5, Dr. Agnieszka Morgenroth, Institute of Immunology) and anti-myc antibody (Invitrogen) were provided by Chemicell GmbH (Berlin, Germany).

3.4.   Enzymes

Enzyme	Supplier
DNase I	MBI Fermentas
Easy-A High Fidelity PCR Cloning Enzyme	Stratagene
Herculase high fidelity DNA polymerase	Stratagene
T4 DNA Ligase	Promega
Trypsin/EDTA	Sigma
Restriction endonucleases	Amersham Biosciences
RNase A	Roche

Table 1. Enzymes and their suppliers.

3.5.   DNA and Protein Markers

GeneRuler 100bp DNA ladder   Fermentas

GeneRuler 1kb DNA ladder   Fermentas

PageRuler prestained protein marker   Fermentas

Precision Plus Dual Color prestained protein ladder   BioRad

3.6.   Solutions and Buffers

Anode buffer I	300mM Tris-Base
	20% Methanol (v/v)
Anode buffer II	25mM Tris-Base
	20% Methanol (v/v)
Cathode buffer	25mM Tris-Base
	40mM 6-Amino capronic acid (Fluka)
6x Gel loading buffer	30% Gylcerin (v/v)
	0.25% Bromophenolblue (w/v)
	0.25% Xylenxyanol FF (w/v) (Fluka)
Lysis Buffer	50mM Tris-HCl (pH 8.0)
	300mM NaCl
	2mM EDTA
	1% NP-40
	Protease inhibitor tablet (1 tablet/ 10ml buffer; Roche)
Lysozyme	10mlg/ml chicken egg-white lysozyme in
	10mM Tris-HCl, pH 8.0
PBS	9.55g/l PBS Dry substance (Biochrome, Berlin)
PFA	4%; 4g/100ml PBS
Poly(ethylene)imine (PEI)	50% (w/v ; Sigma-Aldrich)
5x SDS sample buffer	50% Glycerin
	15% SDS (w/v)
	15% 2-Mercaptoethanol (v/v)
	0.15% Bromophenolblue (w/v)

Sodium butyrate	500mM sodium butyrate
	dissolved in 1x PBS and sterile filtered through 0.45µm filter
STET buffer	10mM Tris-HCl, pH 8.0
	1mM EDTA
	0.1M NaCl
	5% Triton X-100 (v/v)
Stripping buffer	100mM 2-Mercaptoethanol
	2% SDS
	62.5mM Tris-HCl, pH 6.2
TBE buffer	89mM Tris-HCl, pH 8.0
	89mM Boric acid
	2mM EDTA
TBS	10mM Tris-HCl, pH 7.5
	100mM NaCl
TBS-TT	TBS
	0.2% Triton X-100 (v/v)
	0.05% Tween 20 (v/v; Serva)
TE buffer	10mM Tris-HCl, pH 7.5
	1mM EDTA

3.7. Bacteria

E.coli TOP 10 F' (Stratagene, Amsterdam, Netherlands) bacteria were used for plasmid transformation experiments. For the Site-Directed Mutagenesis transformation experiments, Epicurian Coli® XL-1 Blue Competent bacteria, which were supplied with the ExSite PCR-Based Site-Directed Mutagenesis Kit (Stratagene) were used. Table 2 summarizes the genotypes of the bacteria used.

Bacteria	Genotype	Provider
E.Coli TOP 10F´	F´{*lac*Iq, Tn*10*(TetR)} *mcr*A (*mrr-hsd*RMS-*mcr*BC) 80*lacZ* M15 *lac*X74 *rec*A1 *ara*D139 (*ara-leu*)7697 *gal*U *gal*K *rps*L (StrR) *end*A1 *nup*G	Stratagene
Epicurian Coli® XL-1 Blue Competent bacteria	*recA1 endA1 gyrA96 thi-1 hsdR17 supE44 relA1 lac* [F´ *proAB lac*IqZΔ*M15* Tn*10* (Tetr)]	Stratagene

Table 2. Bacteria strains and their genotypic features.

3.8. Culture Media

LB medium   1% Trypton (w/v) (Becton Dickinson)

                                                       0.5% Yeast extract (w/v) (Becton Dickinson)

   1% NaCl (w/v)

   pH 7.0

LB Agar   LB medium

   15g/l Agarose (Becton Dickinson)

D-MEM complete   D-MEM high glucose (4500mg/ml; Invitrogen)

   10% FCS (v/v) (heat-inactivated)

   100µg/ml Penicillin/Streptomycin

3.9. Antibodies

Antibody	Dilution	Supplier
Anti- goat IgG (H+L)-Cy3 conjugate (donkey)	1:100	Jackson Immuno Research Labs
Anti- mouse IgG (H+L)-FITC conjugate (sheep)	1:100	Jackson Immuno Research Labs
Anti-c-myc Alexa 488 conjugate (mouse)	1:500	Upstate
Anti-goat IgG HRP-conjugate (rabbit)	1:2000	Dako
Anti-La 4B6 (mouse)	Undiluted	Provided by Prof. Michael Bachmann (Institute of Immunology, Dresden)
Anti-mouse Ig HRP conjugate (rabiit)	1:1000	Dako
Anti-mouse IgG (Fab')2 –Cy3 conjugate (goat)	1:50	Dianova
Anti-p30 serum (goat)	1:250 (IB) 1:100 (IF)	Provided by Julian Bess (SAIC Frederick, NCI, USA)
Anti-VSV-G (P5D4, mouse)	1:2000 (IB) 1:5000 (IF)	Sigma
Anti-VSV-G 17-2-21-4 (mouse)	1:400	Provided by Prof. Jean Grünberg (University of Geneva, Switzerland)
Anti-VSV-G neutralizing (8G5, mouse)	1:500	Provided by Prof. Douglas S Lyles (West Forest University, USA)
Anti-VSV-G-Cy3 conjugate	1:5000	Sigma
IB: Immunoblotting. IF: Immunofluorescence.		

Table 3. Antibodies and the dilutions used.

3.10. Kit Systems

Kit system	Supplier
ECL Plus Western Blot Detection Kit	Amersham Biosciences
Fast Link DNA Ligation Kit	Epicentre
Invisorb Maxi Kit	Invitek
Invisorb Spin DNA Extraction Kit	Invitek
µMACS *c-myc* isolation kit	Miltenyi Biotec
PCR 2.1 TA cloning kit	Invitrogen
RNeasy Mini Kit	Qiagen
Super Script First-Strand Synthesis System for RT-PCR	Invitrogen

Table 4. Kit systems and the suppliers.

3.11. Cell Lines

The cell lines HEK 293, HEK 293T, HT1376, and RT4 were purchased from American Type Culture Collection (ATCC; Manassas, VA, USA) and were cultured as recommended by the supplier (Table 5). The PSCA-positive HEK 293-PSCA cell line was generated in the Institute of Immunology. HEK 293 cells were transfected with a plasmid encoding a glycosylphosphatidylinositol-anchored (GPI) PSCA and Geneticin resistance gene. The cell line was cultured under antibiotic selection.

Cell line	Supplier	Origin	Features
HEK293	ATCC; CRL-1573	Human embryonic kidney cells	Adherent, epithelial
HEK 293T	ATCC;	Derivative of HEK293	Adherent, epithelial
RT4	ATCC; HTB-2	Human bladder, transitional cell papilloma	Adherent, epithelial
HT1376	ATCC; CRL-1472	Human bladder carcinoma	Adherent, epithelial

Table 5. Cell lines and their basic features.

3.12. Plasmids

pcz-VSV-Gwt encoding the VSV-G protein was kindly provided by Dr. Lindemann (Institute of Virology, Dresden). pMD.G2 plasmid coding for VSV-G protein was a gift from Prof. Trono (University of Geneva). The plasmid pRevCMV_PSCA_IRES2_EGFP encoding a GPI-anchored PSCA and EGFP separated by an IRES was generated at the Institute of Immunology.

3.13. Other materials

Sterile 0.45µm filters were purchased from Schleicher & Schuell (FP 30/0,45 CA-S).

4. MOLECULAR BIOLOGICAL METHODS

4.1. Polymerase chain reaction

Polymerase chain reaction (PCR) allows the amplification of DNA using a pair of oligonucleotides complementary to the 5' and 3' ends of the target DNA sequence. Basic components of DNA amplification by PCR are; a template DNA, DNA polymerase, oligonucleotide primers, dNTP and an appropriate buffer. For the amplification of the DNA sequence, the template DNA is first denatured where the hydrogen bonds connecting the DNA strands are broken at high temperature (95°C). Then the temperature is lowered to favor annealing of the oligonucleotide primers to their complementary sequences on the single-stranded DNA (ssDNA; generally around 50-60°C). In the next step – the elongation step-, the thermostable polymerase synthesizes the DNA sequence between the oligonucleotide primers (72°C). This reaction is repeated generally 25-30 times to achieve large amounts of target DNA sequence. In the last cycle, elongation step is typically extended up to 15 min to ensure complete synthesis of all available fragments. By PCR, it is possible to introduce mutations in the target sequence, as well as to modify ends of a DNA sequence for the ease of cloning into an appropriate vector. In Table 6 PCR conditions and primers used in this thesis are depicted.

Primer name	5'→ 3' sequence	PCR conditions	Used in generation of
AMI forward	TTTTT**CTCGAG**CCATGGAGACAGACACACT	95ºC →2min **95ºC → 30sec** <u>**60ºC → 30sec** 34 cycles</u> **72ºC → 2.5min** 72ºC → 5min	pAMI-G
AMI reverse	AAAAA**CTCGAG**GGCACTATTCAGAT		
AMI forward	TTTTT**CTCGAG**CCATGGAGACAGACACACT	95ºC → 2min **95ºC → 30sec** <u>**60ºC → 30sec** 34 cycles</u> **72ºC → 2.5min** 72ºC → 5min	pAMI-L-G
AMI linker reverse	AA AAA **CTC GAG** *GCC TCC GCT GCC GCC* GGC GCT ATT CAG ATC CTC		
VSV-G-linker fuso2 forward	TTTT**CTAGA**<u>TCTGAGCTTGCACTTGAGCTT</u>CACCATGTGCTGGTTGATGAATAC	95ºC → 2min **95ºC → 30sec** <u>**68ºC → 30sec** 35 cycles</u> **72ºC → 1.5min** 72ºC → 7min	pAMI-L-sG-1
VSV-G-XbaI reverse	TTTTT**TCTAGA**TTACTTTCCAAG		
VSV-G-linker fuso3 forward	TTTT**CTAGA**<u>TCTGAGCTTGCACTTGAGCTTT</u>CCATGGACATCACCTTCTTCTCA	95ºC → 2min **95ºC → 30sec** <u>**68ºC → 30sec** 35 cycles</u> **72ºC → 1.5min** 72ºC → 7min	pAMI-L-sG-1
VSV-G-XbaI reverse	TTTTT**TCTAGA**TTACTTTCCAAG		
VSV-G XbaI forward	TTT T**TT CTA GA**A CTG GAA AAATG	94ºC → 2min 94ºC → 30sec <u>**54 ºC → 30sec** **68ºC → 105 sec** 35 cycles</u> **72ºC → 1.5min** 72ºC → 7min	pAMI-G and pAMI-L-G
VSV-G XbaI reverse	TTT T**TT CTA GA**T TAC TTT CCA AG		

Table 6. PCR primers and PCR conditions.

4.1.1. Ex-Site PCR-based Site-directed mutagenesis

The Site-Directed Mutagenesis is a molecular biological technique to insert a desired mutation into a DNA sequence. Oligonucleotide primers containing that particular mutation are designed and the mutations are incorporated into the template by PCR. Myc epitope inserted-VSV-G protein-encoding DNA sequences were generated by ExSite PCR-Based Site-Directed Mutagenesis (Figure 7). Main components of this procedure were the mutagenesis buffer, two oligonucleotide primers -one of which was phosphorylated-, dNTP mix, a DNA polymerase blend and a template plasmid DNA. The components were mixed and the plasmid DNA was amplified by PCR using the primers and the conditions listed in Table 7. Subsequently, *Dpn*I restriction enzyme was used to digest the parental double-

stranded DNA (dsDNA) and the hybrid dsDNA, which consists of one parental and one mutated strand. *Dpn*I recognizes the sequence 5'-G$_{m6}$ATC- 3' and digests the DNA fragments containing methylated adenine. Cloned Pfu DNA polymerase was then used to remove the 3' overhangs of the mutated DNA. Mutated DNA was intramolecularly ligated for 1hr at 37°C with T4 DNA ligase and the ligated DNA was used to transform Epicurian Coli XL-1 Blue supercompetent bacteria.
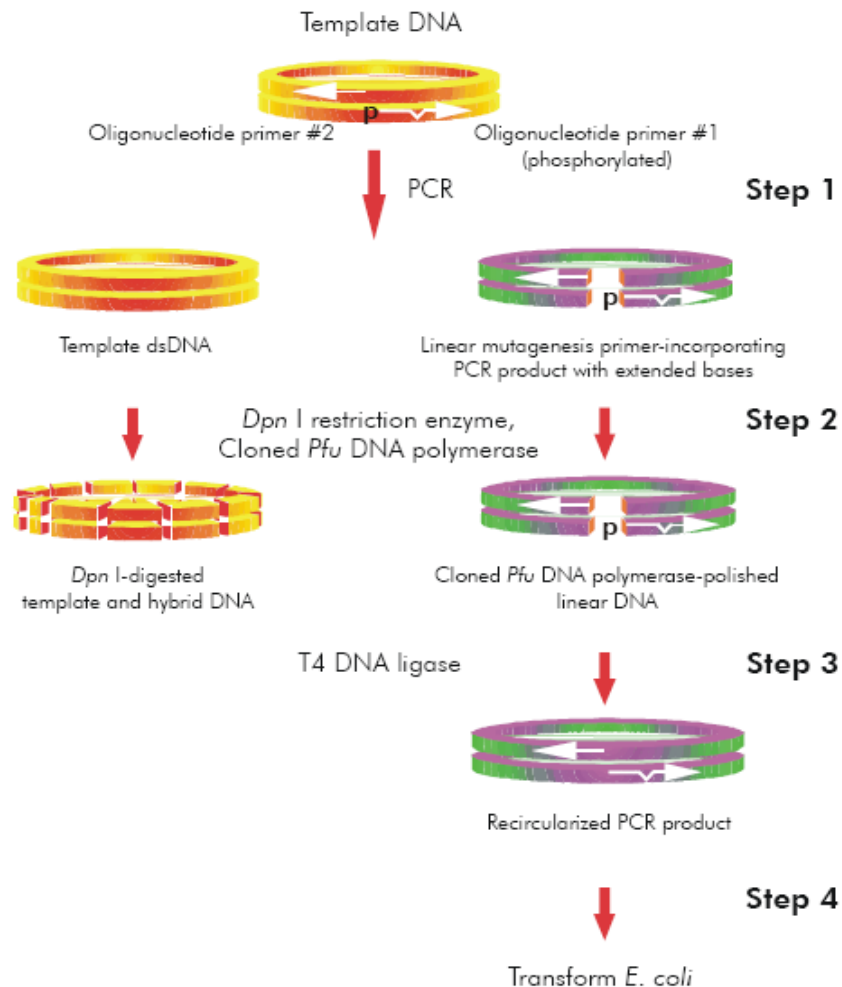
Figure 7. ExSite™ PCR-based Site-Directed Mutagenesis (www.stratagene.com).

ExSite PCR-based Site-Directed Mutagenesis is performed in four steps. In step 1, the template DNA is amplified with oligonucleotide primers containing the desired mutation. *Dpn*I restriction enzyme digests the parental plasmids at the sequence 5´-G$_{m6}$ATC-3´ and *Pfu* DNA polymerase removes the 3' overhang from the mutated DNA (Step 2). The modified DNA is intramolecularly ligated in Step 3 by T4 DNA ligase. The ligated DNA is then transformed into XL1-Blue supercompetent cells (Step 4).

Primer designation	5'→3' sequence	PCR conditions		
VSV-G myc 17 forward	**GAACAAAAACTCATCTCAGAAGAGGATCTGCAG**TTCACCATAGTTTTTCCACACAAC	94℃ → 4 min 50℃ → 2 min 68℃ → 7.5 min		
VSV-G myc 17 reverse	CTTGCAATTCACCCCAATG	94℃ → 1 min 54℃ → 2 min 68℃ → 7.5 min	18 cycles	
		68℃ → 15 min		
VSV-G myc 28 forward	**GAACAAAAACTCATCTCAGAAGAGGATCTGCAG**AACTGGAAAAATGTTCCTTCTAATT	94℃ → 4 min 50℃ → 2 min 68℃ → 7.5 min		
VSV-G myc 28 reverse	TCCTTTTTGGTTGTGTGG	94℃ → 1 min 54℃ → 2 min 68℃ → 7.5 min	18 cycles	
		68℃ → 15 min		
VSV-G myc 208 forward	**GAACAAAAACTCATCTCAGAAGAGGATCTGCAG**GGAGAGCTATCATCCCTGGGAAAG	94℃ → 4 min 50℃ → 2 min 68℃ → 7.5 min		
VSV-G myc 208 reverse	GTCCTCTGAGAAGGTG	94℃ → 1 min 54℃ → 2 min 68℃ → 7.5 min	18 cycles	
		68℃ → 15 min		
VSV-G myc 266 forward	**GAACAAAAACTCATCTCAGAAGAGGATCTGCAG**CCTGAATGCCCAGAAGGGTCAAGT	95℃ → 45 sec 95℃ → 45 sec 54℃ → 45 sec	24 cycles	
VSV-G myc 266 reverse	GAATCTGGCTGCAGCAAAG	72℃ → 7 min		
		72℃ → 10 min		
VSV-G myc 278 forward	**GAACAAAAACTCATCTCAGAAGAGGATCTGCAG**TCTCAGACCTCAGTGGATGTAAGT	95℃ → 45 sec 95℃ → 45 sec 54℃ → 45 sec	24 cycles	
VSV-G myc 278 reverse	TGGAGCAGAGATACTTGACCC	72℃ → 7 min		
		72℃ → 10 min		

Table 7. Primers for ExSite PCR-based Site-directed Mutagenesis

4.1.2. Generation of La epitope-modified VSV-G proteins

La epitope was inserted into VSV-G coding sequence in pMD.G2 by PCR amplification. Briefly, for each construct La sequence was inserted into VSV-G coding sequence by PCR amplification of N- and C-terminal flanking regions using the conditions and the primers depicted in Table 8. The primer pairs were designed to insert the La epitope and restriction enzyme sites for the cloning. PCR products were first cloned into pGemT vector separately and brought together in pGemT using *Xho*I restriction site. The La epitope-modified VSV-G sequence was then cut out from pGemT using the internal restriction sites (*Hin*d III and *Age*I) into pMD.G2 vector, which was also digested with the same enzyme combination.

La-modified VSV G protein designation	Primer designation	5'→3' sequence	PCR conditions		
VSV G La 17 N terminus	VSV-G 5F	GACCTCCATAGAAGACACC	95°C 5min		
	VSV-G 4B6 XVIII 12R	*CTCGAG*CTTGCAATTCACCCCAATG	95°C 30 sec 57°C 45sec 68°C 1min	30 cycles	
			68°C 5min		
VSV G La 17 C terminus	VSV-G 4B6 XVIII 11F	*CTC**GAGAAAGAAGCACTGAAGAAAATA ATAGAAGACCAACAAGAATCCCTAAACA AA**TTCACCATAGTTTTTCCAC	95°C 5min		
			95°C 30 sec 53°C 45sec 68°C 1min	30 cycles	
	VSV-G 4R	GGAGCAGCAATATCGACT	68°C 5min		
VSV G La 31 N terminus	VSV-G 5F	GACCTCCATAGAAGACACC	95°C 5min		
	VSV-G (XhoI) 2R	*CTCGAG*AACATTTTTCCAGTTTCC	95°C 30 sec 50°C 45sec 68°C 45sec	30 cycles	
			68°C 5min		
VSV G La 31 C terminus	VSV-G 4B6 XVIII 3F	*CTC**GAGAAAGAAGCACTGAAGAAAATA ATAGAAGACCAACAAGAATCCCTAAACA AA**CCTTCTAATTACCATTATTGC	95°C 5min		
			95°C 30 sec 52°C 45sec 68°C 1min 45sec	30 cycles	
	VSV-G 4R	GGAGCAGCAATATCGACT	68°C 5min		
VSV G La 209 N terminus	VSV-G 5F	GACCTCCATAGAAGACACC	95°C 5min		
	VSV-G (XhoI) 6R	*CTCGAG*GTCCTCTGAGAAGAAGGT	95°C 30 sec 53°C 45sec 68°C 1min 45sec	30 cycles	
			68°C 5min		
VSV G La 209 C terminus	VSV-G 4B6 XVIII 7F	*CTC**GAGAAAGAAGCACTGAAGAAAATA ATAGAAGACCAACAAGAATCCCTAAACA AA**GGAGAGCTATCATCCCTGGG	95°C 5min		
			95°C 30 sec 53°C 45sec 68°C 45 sec	30 cycles	
	VSV-G 4R	GGAGCAGCAATATCGACT	68°C 5min		
VSV G La 27 N terminus	VSV-G 5F	GACCTCCATAGAAGACACC	95°C 5min		
	VSV-G (XhoI) 10R	*CTCGAG*TGGGCATTCAGGGAATCT	95°C 30 sec 56°C 45sec 68°C 1min 45sec	30 cycles	
			68°C 5min		
VSV G La 275 C terminus	VSV-G 4B6 XVIII 9F	*CTC**GAGAAAGAAGCACTGAAGAAAATA ATAGAAGACCAACAAGAATCCCTAAACA AA**GAAGGGTCAAGTATCTCT	95°C 5min		
			95°C 30 sec 53°C 45sec 68°C 45 sec	30 cycles	
	VSV-G 4R	GGAGCAGCAATATCGACT	68°C 5min		

Table 8. Primers for PCR-based insertion of La epitope in VSV-G ectodomain.

La-epitope insertion mutants were generated by PCR amplification of VSV-G coding sequence from pMD.G2 plasmid. The La sequence is written bold and the restriction endonuclease recognition sites are written italic.

4.2. Restriction endonuclease digestion of DNA fragments

Restriction endonucleases are enzymes, which recognize specific DNA sequences and introduce double-stranded breaks in DNA. Depending on the sequence recognized by the restriction endonuclease and the type of strand break generated, the DNA fragments may have either "sticky" or "blunt" ends. The sticky-end DNA fragments have overhanging nucleotide sequences, which can be ligated to another DNA fragment possessing a complementary overhang. On the other hand, the blunt-end DNA fragments have no overhangs and can therefore be ligated to any blunt-end DNA fragment regardless of the restriction endonuclease

used to generate these fragments. For analytical and preparative purposes restriction endonucleases were used with recommended buffers and the restriction digestion was performed under optimum conditions for each enzyme, *i.e.* temperature, salt concentration, presence of bovine serum albumin, *etc.*

4.3. Agarose electrophoresis of DNA fragments

Agarose electrophoresis allows the separation of DNA fragments in an agarose matrix using electrical field. The negatively charged DNA fragments are forced to move along the electrical field. In general, smaller DNA fragments move faster than larger DNA fragments, but also the conformation of DNA has an impact, such that the supercoiled circular DNA fragments move faster than the linear DNA fragments, which in turn move faster than the open-circular DNA fragments. Adjusting the percentage of agarose, it is possible to determine the pore size of the agarose matrix. High agarose concentration slows down the overall speed of DNA molecules in the matrix and thus permits a better separation of smaller DNA fragments. Separated DNA fragments can be visualized with ethidium bromide (EtBr), a dye that intercalates with DNA and fluoresces under UV light.

The agarose (Serva) concentration was adjusted to 0.8-1.5% (w/v) in 0.5xTBE buffer, depending on the length of the fragments to be separated. Agarose was dissolved in buffer by heating and 0.2µg/ml EtBr was added after the gel cooled down. The gel was prepared in a horizontal gel electrophoresis chamber (Amersham Biosciences) and the samples were loaded after mixing with 6x gel loading buffer at 1:5 ratio. For estimation of the DNA fragment length, DNA ladders were run on the same gel. The gel chamber was filled with 0.5x TBE buffer and samples were run under 7V/cm electrode distance. The bands were visualized by UV-transilluminator (Biostep; Jahnsdorf).

4.3.1. Isolation of DNA fragments from agarose gel

DNA fragments separated in an agarose gel can be extracted to isolate a specific band. The band corresponding to the target DNA fragments was cut out with a scalpel. The agarose matrix was melted at 50°C with "the gel solubilizing buffer" supplied in the Invisorb Spin DNA Extraction Kit and DNA fragment in agarose was bound onto a filter. The filter was washed to remove unbound impurities. Elution buffer was added and the purified DNA was eluted by centrifugation. DNA fragment was then used for cloning immediately or stored at -20°C.

4.4. Cloning of DNA fragments

PCR products or DNA fragments obtained by digestion with restriction endonucleases can be cloned into vectors for further use. The cloning is

accomplished by ligation of either two compatible sticky-end DNA fragments or two blunt-end DNA fragments with DNA ligases in the presence of an appropriate buffer. In this study, ligations were performed with the Fast Link DNA Ligation Kit, unless otherwise stated. The insert DNA fragment and the vector DNA were digested with restriction endonucleases. The fragments were then separated from impurities by agarose gel electrophoresis and bands at correct sizes were isolated. Isolated insert and vector DNA were mixed at a 3:1 (Insert: Vector) ratio in the presence of recombinant ATP and the ligation buffer, and the mixture was incubated 5 min for sticky-end ligations or 15 min for blunt-end ligations at room temperature (RT). Then the ligase activity was ceased by incubation at 70°C for 15min. An aliquot (~2µl) of the ligation mixture was used to transform bacteria, and the rest was stored at -20°C.

4.4.1. Cloning of glycosylphosphatidylinositol (GPI)-anchored PSCA

A glycosylphosphatidylinositol anchored PSCA encoding pPSCA-IRES2-EGFP plasmid was first digested with *Hpa*I. After inactivating *Hpa*I, *Sma*I was added. The linearized plasmid was run on the gel and the DNA fragment containing PSCA was isolated. The gel-purified DNA fragment was then re-ligated using T4 DNA ligase and the plasmid was named pPSCA-IRES. The plasmid contains only a part of the IRES sequence.

4.4.2. Cloning of scFv anti-PSCA / VSV-G fusion protein

The single-chain antibody variable fragment against the tumor-associated antigen PSCA (AMI) was amplified from pSecTag 2B-AMI plasmid by PCR using AMI-forward and –reverse primers (Table 6). Primers were selected such that the Ig ĸ leader sequence from pSecTag2B, which directs the downstream protein for secretion, was also amplified. Shortly, anti-PSCA scFv and VSV-G encoding DNA sequences were amplified separately with PCR and were cloned into PCR vectors (pCRII or pCR3.1, respectively) using the TA Cloning Kit (Invitrogen). Restriction enzyme recognition sites were included in the PCR primers (Table 6) both to 5' and 3' ends of the sequences to facilitate further cloning. AM-I was amplified with primers coding for *Xho*I restriction site with or without linker, whereas the VSV-G amplification primers contained *Xba*I recognition site. First, AM-I coding sequence from pCRII vector was cloned into pcDNA3.1 following digestion of both plasmids with *Xho*I, which linearized pcDNA 3.1 (pAMI or pAMI-L). Next, VSV-G sequence was cloned into pAMI or p-AMI-L vectors using *Xba*I restriction enzyme, which cuts off VSV-G sequence from pCR 3.1 vector and linearized pAMI or pAMI-L. The plasmids were designated pAMI-G or pAMI-L-G, respectively.

VSV-G mediates binding of viral particles to the target cell surface via a ubiquitously expressed molecule [124]. Despite several evidence showing

particular sequences in VSV-G as being necessary for target binding, the exact sequence(s) responsible for the cellular target binding of VSV-G has not been yet identified. Therefore, VSV-G sequence contribution in the fusion protein was reduced to study whether it is possible to diminish wild-type VSV-G protein binding while enhancing specific targeting via AMI part of the fusion protein. pAMI-L was used as template for the fusion proteins with shortened VSV-G. The VSV-G sequence was amplified by PCR with primers, which encoded *Xba*I restriction site, an additional linker of 7 amino acids and generated 5'-end truncated VSV-G sequences. PCR products were cloned into pCR 2.1 vector using TA cloning kit. *Xba*I restriction sites were used to clone truncated VSV-G into linearized pAMI-L vector to generate pAMI-L-sG-1 and pAMI-L-sG-2.

4.5. Transformation of competent *E.coli* according to Hanahan [173]

Chemically competent *E.coli* bacteria were thawed on ice. 50µl of competent bacteria were mixed with 1µg of DNA and incubated 30 min on ice. Following the subsequent heat-shock for 2 min at 42°C in water-bath, 950 µl warm LB medium without antibiotics was added and the bacteria were grown 1hr at 37°C shaker. The 100 µl and 900 µl aliquots of bacteria were plated on LB-agar plates with antibiotic and incubated overnight at 37°C.

4.6. Plasmid mini preparation according to Holmes and Quigley [174]

Single-bacteria colonies were picked with a sterile tip and grown overnight (~18hrs) in 5 ml LB medium with antibiotic at 37°C shaker. Next day, 1.5ml of bacteria suspension was centrifuged to pellet down the bacteria and DNA was isolated according to protocol from Holmes & Quigley [174]. Briefly, bacteria pellet was re-suspended in 350µl of STET buffer and 25µl lysozyme solution was added. Suspension was boiled for 40sec and centrifuged at 14000rpm for 10min. Subsequently the pellet was removed with a sterile toothpick and 40µl sodium-acetate (2.5M, pH 5.2) and 420µl isopropanol were added to the supernatant. Following 5min incubation at RT the mixture was centrifuged. The supernatant was discarded and the pellet was washed with 250µl 70% ethanol. After removal of ethanol by centrifugation, DNA was re-suspended in 50µl H_2O and 2µl RNase A was added.

4.7. Plasmid maxi preparation from *E.coli*

For the amplification of plasmid DNA, 200µl of culture suspension from transformed *E.coli* was grown overnight in 100ml LB medium with antibiotics. Next day, the bacteria suspension was centrifuged and the plasmid DNA was isolated using the Invisorb Plasmid Maxi Preparation Kit according to manufacturer's instructions. Briefly, bacteria were pelleted and lyzed under alkaline conditions.

The crude bacteria lysate was cleared by centrifugation and DNA was bound onto a filter. Plasmid DNA free from impurities was eluted in a low-salt buffer. Concentration and purity of isolated DNA was measured by the optical density (OD) at 260nm and OD260/OD280 ratio, respectively (BioPhotometer, Eppendorf, Hamburg; using Eppendorf plastic cuvettes).

4.8. Sequencing of nucleic acids

DNA sequences were verified at the DNA Sequencing Facility of Max Planck Institute for Cell Biology and Genetic (MPI-CBG, Dresden) using insert- or vector-specific primers. The sequencing primers are listed in Table 9.

Primer designation	5'→3' sequence	Tm (^{o}C)
BGH reverse	TAGAAGGCACAGTCGAGG	56
M13 Universal (-21)	TGTAAAACGAACGGCCAGT	54
M13 reverse	GGAAACAGCTATGACCATG	56
T7 promoter	TAATACGACTCACTATAGGG	56
VSV G-SG forward	CATTGGGGTGAATTGCAAG	56
G-position 868 reverse	CAAGATCCTCTCAACGTC	50

Table 9. Sequencing primers and annealing temperatures.

4.9. Discontinuous Sodium Dodecyl Sulfate - Polyacrylamide Gel Electrophoresis (SDS-PAGE)

SDS-PAGE allows the separation of proteins according to their molecular weights. Protein samples were prepared in a reducing sample buffer. The reducing sample buffer contains anionic detergent SDS, which denatures the secondary and non-disulfide-bond depended structures in the protein, and 2-Mercapthoethanol, which reduces disulfide-bonds. In addition to its denaturing effect on protein, SDS assigns a negative charge to the protein in correlation with its mass. Due to this uniform mass: charge ratio proteins are separated mainly according to their sizes. With the help of a predefined protein molecular marker, it is possible to estimate the molecular weight of a sample. For SDS-PAGE Tris-HCl/Tris-Glycine buffer system was used. Acrylamid/N,N'-Methylenbisacrylamide (1:19, 40% stock

solution; Gerbu) concentration was adjusted depending on the experiment and varied between 8-12%. The protein samples were mixed with 5x SDS Sample buffer and were boiled at 95°C for 5-10 min before loading on the gels. BioRad Protean-3 chambers were used. The electrophoresis was performed at 60V for the collecting gel and 120V for the separating gel (BioRad Power Pac 3000). Precision Plus Dual Color (BioRad) or PageRuler (Fermentas) protein marker was used as the standard (Figure 8).
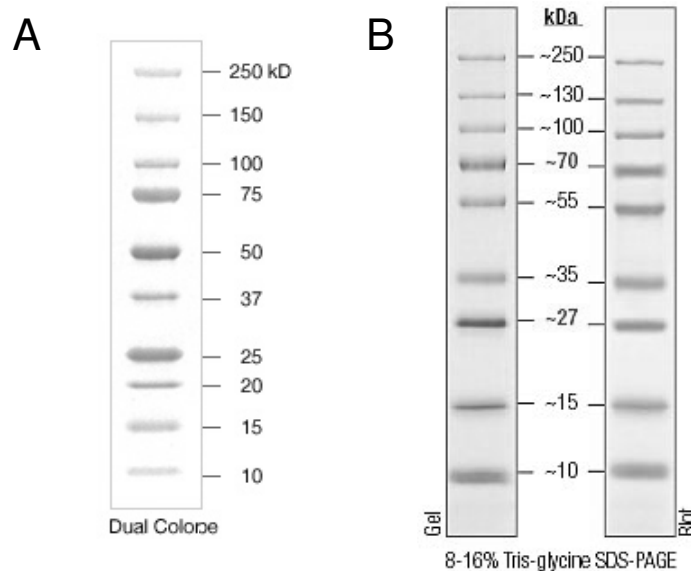
Figure 8. Protein molecular weight markers.

A: Precision Plus Dual Color protein marker (BioRad) with 70kDa and 25kDa as reference bands.
B: Fermentas PageRuler protein marker with 70kDa and 27kDa as reference bands.

4.10. Western blot analysis

Following the SDS-PAGE separation of proteins in a sample, the proteins were transferred onto a Polyvinylidenfluorid (PVDF) membrane for immunoblotting. SDS gel containing the separated proteins was placed face-to-face with a PVDF-membrane in a "sandwich model". In sandwich-model, from bottom to up 4 sheets of filter paper incubated in anode buffer-I, 4 sheets of filter paper incubated in anode buffer-II, PVDF-Membrane equilibrated in methanol and anode buffer-II, gel, and 8 sheets of filter paper incubated in cathode buffer were placed in a BioRad Trans-Blot SD Semi-Dry transfer apparatus. Under 25V current, proteins were transferred for 2 hours onto the membrane while preserving their organization in the gel. Non-specific reaction of antibodies was prevented by blocking the membrane overnight under agitation with 3% Bovine Serum Albumin (BSA) in Tris-buffered saline (TBS). Next day, the membrane was washed thoroughly with TBS under agitation before being incubated with the primary antibody against the protein of interest. The unbound antibody was removed by

successive washing and the membrane was then incubated with a horseradish peroxidase-labeled secondary antibody against the species in which the primary antibody was raised. Detection of the protein on the membrane was performed by enhanced chemiluminescence (ECL) reaction, where horseradish peroxidase acts as a catalyzer. Visualization was performed either with a light-sensitive Hyperfilm (Amersham) or with Fuji LAS 3000.

4.10.1. Detection of VSV-G protein

Total cell lysates were prepared by harvesting the cells in a lysis buffer. The VSV-G was detected by incubating the membrane with a mouse anti-VSV-G antibody (P5D4, 1:2000 diluted in 3%BSA-TBS) for 2hours at RT. The membrane was then washed with TBS-Tween 20-Triton X-100 (TBS-TT) and TBS. As secondary antibody rabbit anti-mouse Ig-HRP conjugate (DAKO) was used (diluted 1:1000 with 3%BSA-TBS). Following 1hour incubation at RT with the secondary antibody, the antibody-reactive bands were detected.

4.10.2. Detection of MLV capsid protein p30

Viral particles produced by the packaging cells contain the viral envelope protein and the capsid protein. The co-presence of MLV capsid protein p30 in the same blot was used to demonstrate that the whole viral particles were detected, and not only the viral envelope protein shed by the packaging cells. The membrane containing the purified viral supernatants, which was first used to detect VSV-G, was stripped under stringent conditions. The membrane was washed with TBS-TT and TBS, and was blocked overnight with 3%BSA-TBS. Next day, the membrane was washed and incubated 2 hours at RT with goat anti-MLV p30 serum (1:250 diluted in 3%BSA-TBS; NCI, USA). Following intensive washing with TBSTT and TBS, the membrane was incubated with rabbit anti-goat IG-HRP antibody (DAKO, 1:1000 in 3%BSA-TBS) for 1 hour at RT. The bands were detected with ECL reaction and using the Hyperfilm or with Fuji LAS 3000.

4.10.3. Binding of anti-PSCA/ anti-myc nanobeads to *myc*-modified virus

The myc epitope-modified VSV-G proteins were used to pseudotype retroviral particles. The packaging cell supernatant containing the viral particles was mixed with anti-myc / anti-PSCA nanobeads in orbital shaker for 30min at 37°C. The mixture was then centrifuged at 14000 rpm at 4°C for 30min. The pellet was re-suspended in SDS sample buffer and analyzed by SDS-PAGE and Western blotting. Anti-p30 serum and HRP conjugated rabbit anti-goat Ig was used to detect MLV capsid protein in the samples. The protein bands were visualized using ECL Plus kit and Fuji LAS 3000.

5. CELL BIOLOGICAL METHODS

5.1. Cell count determination

Cells were centrifuged and pelleted. The pellet was re-suspended in 1ml of culture medium, from which 10µl was taken out and mixed with 90µl of Trypan blue solution. Trypan blue dye is excluded from the membrane of viable cells, but not from that of dead cells. Thus the dead cells appear blue under the microscope. The viable cells were counted from 64 small squares of Neubauer chamber, and using the following formula the cell count was determined; (cell count / 4) x the dilution factor x 10^4.

5.2. Freezing and thawing of cell lines

Cells were pelleted by centrifugation and the pellet was re-suspended in 90% fetal calf serum (FCS)-10% Dimethylsulfoxyde (DMSO). Cell suspension was placed in a cryobox filled with 2-propanol, which ensures a cooling down process at 1°C/min rate. Then the cryobox was placed in -80°C refrigerator, for long-term storage cells were transferred into a liquid nitrogen tank. Frozen cells were thawed in a water-bath at 37°C and were taken into FCS. The suspension was centrifuged and the DMSO-containing supernatant was removed completely. The pellet was re-suspended in the respective culture medium.

5.3. Cultivation of cell lines

HEK 293T, HEK 239wt, and RT4 cell lines were cultured in high glucose DMEM. For cells transfected with an expression vector encoding for a selection marker, appropriate amount of the respective antibiotic was added to the culture medium. HEK 293-pPSCA cells, which were transfected with an expression vector conferring Geneticin resistance, were cultured in DMEM supplemented with G418 at 0,5µg/ml concentration. HT1376 cell line was cultured in DMEM high glucose medium in the presence of 1% non-essential amino acid solution (Biochrom, 100x). All media were supplemented with 10% FCS, 100µg/ml penicillin/streptomycin (Biochrom).

5.4. Transfection of cell lines

Transfections were performed using poly(ethylenimine) (PEI) solution (Sigma). PEI is a polycation, which binds to and precipitates DNA. Target cells were plated one day prior to the transfection. PEI was used (1mg/ml) to precipitate DNA in the culture medium for 20min at RT. The precipitate was used to transfect the cells overnight at 37°C or 32°C. Next day, the transfection medium was removed and

cells were incubated with culture medium containing sodium butyrate at a final concentration of 10mM for 8hours to induce Cytomegalovirus (CMV) promoter-dependent protein expression. Transfected cells were then cultured in the optimal culture medium until further analysis.

5.4.1. Generation of PSCA-positive HEK293 cell line

HEK293 wt cells were transfected with plasmid encoding a GPI-anchored PSCA and Geneticin (G418) resistance gene (pPSCA-IRES). The transfected cells were cultured under antibiotic selection (0.5µg/ml) at 37°C. The cell line was designated HEK293-PSCA. In addition, HEK 293-PSCA-IRES-EGFP cells were generated by transient transfection of HEK293 cells with pRevCMV_PSCA_IRES2_EGFP -a retroviral vector encoding for GPI-anchored PSCA and EGFP (separated by an Internal Ribosome entry site).

5.4.2. Viral particle preparation

One day prior to the transfection $4x10^6$ HEK293T cells were plated in 10cm dish. Next day, the virus packaging was performed as described by Soneoka *et al.* [3]. In this three-vector system, the packaging cells were co-transfected with retroviral vectors encoding *gag-pol* gene products (pHIT60), the gene of interest or the reporter gene (pcz-CFG2-fEGFPf) and the envelope protein (pcz-VSV-Gwt or myc-modified pcz-VSV.G). Conditioned medium containing the viral particles was collected 48 hours after transfection and filtered through a 0.45µm filter. The supernatant was either used immediately or stored at -80°C. The packaging cells were fed with fresh medium for a second virus harvest on the 3rd day after the transfection. Following the second harvest total cell lysates were prepared from the packaging cells.

5.5. Transduction of cell lines

Moloney Murine Leukemia Virus-(MoMuLV)-based retroviral vectors were produced (see chapter 5.4.2). pcz-CFG-5.1-MCS was used as the template for retroviral vectors. This retroviral vector contained the packaging signal Ψ, which is required for the assembly of newly-synthesized retroviral RNA into viral particles. Ψ is flanked on the 5'- and 3'- ends with LTRs, which contain the promoter elements in the viral genome. Supernatants containing the viral particles were harvested from the packaging cells 48 and 72 hours after transfection and pooled. Target cells were incubated overnight with the pooled supernatant in the presence of 8µg/ml Polybrene (Hexadimethrinbromide), when not otherwise stated. Next day, the medium was replaced.

5.5.1. Determination of virus titer

VSV-Gwt or modified VSV-G-pseudotyped EGFP-encoding viral particles were produced. The supernatants were harvested from the packaging cells and concentrated by 100fold (total volume 500µl) via ultracentrifugation. The concentrate was divided into 50µl aliquots and frozen at -80°C. On the same day target HEK293wt and HEK293-PSCA cells was plated at $2x10^4$ cells/ well in 48-well plates. The next day, one aliquot was thawed and titrated on the target cells by serial dilution (10^1 to 10^6) in a total volume of 1ml. Twenty-four hours later the medium was replenished and the cells were further cultivated. On day 2 after transduction, EGFP-positive colonies were counted and the titer (virus particle/ml) was calculated as follows: the number of EGFP-positive colonies x the dilution factor x 20.

5.5.2. Transduction of HEK293wt cells with *myc* epitope-modified viral particles in the presence of anti-myc antibody

HEK293T cells were plated in 24-well plates ($5x10^4$ cells / well) and grown overnight. Fresh supernatant from the packaging cells was used for transduction. Transduction was performed with 1ml supernatant (from 32°C packaging) and in the presence of one of the following antibodies at a final concentration of 1µg/ml: anti-Xpress, anti-c-myc or neutralizing anti-VSV-G antibody (8G5, a generous gift from Prof. Lyles, USA) and polybrene. Transduction was performed overnight, after which the medium was replenished. Transduction efficiencies were analyzed by flow cytometry 2 days after transduction.

5.5.3. Transduction of PSCA-positive cells with *myc*-modified viral particles in the presence of anti-myc/anti-PSCA antibody-coupled nanobeads

Viruses were produced at 37°C. The supernatant was harvested and filtered (0.45µm) and concentrated 100fold by ultracentrifugation. The viral particles were re-suspended in culture medium. VSV-G myc 17-pseudotyped retroviral particles (MLV$^{(G-myc\ 17)}$)were incubated 3hrs at RT in orbital shaker with magnetic beads and the mixture was used for transduction. When indicated the virus-magnetic bead mixture was incubated 1hr on a magnet and thereafter the precipitate and the supernatant were used promptly to transduce PSCA-positive and PSCA-negative cells, which were plated the previous day. VSV-G wt-pseudotyped retroviral particles were used without incubation with the nanobeads and in the presence of polybrene (8µg/ml). Next day the medium was replenished and the cells were further incubated at 37°C until the transduction efficiency was measured on 2 days post-transduction by FACS.

5.5.3.1. Confirmation of nanobeads internalization into PSCA-positive cells transduced with MLV$^{(G\text{-}myc\ 17)}$ particles

MLV$^{(G\text{-}wt)}$ and MLV$^{(G\text{-}myc\ 17)}$ particles were used for transduction of PSCA-negative and PSCA-positive cells in the excess of nanobeads. The transduced cells were cultivated for a week, in which the cells were splitted and washed intensively with PBS. On the last day, the cells were centrifuges and re-suspended in PBS and dried on Whatman paper. The Whatman paper was then scanned for documentation.

5.6. Preparation of cell lysates

Medium was removed from the cells. Cells were washed 2 times with PBS each for 5min. PBS was removed and cells were harvested directly in lysis buffer. All procedure was performed on ice. The cell lysates were either used immediately or was stored at -20°C.

5.7. Viral particle purification and concentration

5.7.1. Concentration of viral particles via ultracentrifugation

Viral particles were harvested from packaging cells at different time points and were pooled. Ultracentrifugation was performed with Beckman Coulter L60 ultracentrifuge using SW40Ti or SW28 rotors. The samples were centrifuged at 100 000 x g at 4°C for 2 hours. Then, the supernatant was discarded carefully, and the viral particles were re-suspended in culture medium.

5.7.2. Purification of *myc*-modified viral particles with µMACS *c-myc* isolation kit

Viral particles were produced with VSV-Gwt or c-myc-modified VSV-G envelope proteins. The particles were purified from medium from packaging cells via µMACS c-myc Isolation Kit (Miltenyi Biotec). Briefly, filtered (0.45µm) supernatant (~5ml) was mixed with 50µl of anti-myc magnetic beads. The mixture was incubated on ice for 30min under occasional mixing. During this incubation, µ column was equilibrated with 200µl lysis buffer and washed three times with PBS. At the same time, aliquots of elution buffer were placed in a pre-heated (95°C) thermo block. The mixture was then applied to the column and run through. The column was washed (2x 400µl wash buffer 1, 1x100µl wash buffer 2) and incubated 5min with 20µl pre-heated elution buffer. Samples were eluted in 50µl of pre-heated elution buffer and were analyzed by SDS-PAGE.

5.8. Immunofluorescence analysis

Immunofluorescence analysis enables the detection proteins using antibodies recognizing specific epitopes on them. In the indirect immunofluorescence analyses unlabeled primary antibodies are used to localize the protein of interest. Then the detection is achieved by fluorescent dye-labeled secondary antibody. The secondary antibody is specific to the species from which the primary antibody was obtained. In the direct immunofluorescence analysis, the proteins are detected by a fluorescence dye-labeled primary antibody.

5.8.1. Intracellular staining

For the detection of intracellular VSV-G protein expression, HEK293T cells were transfected with respective expression vectors. Two days after transfection cells were permeabilized 5min at RT with 0.37% paraformaldehyde (PFA) and 0.05% Triton X-100 and fixed for 15min at RT with 3.7% PFA. Cells were then washed 2 times with PBS each for 5 min and were incubated with Cy3 conjugated anti-VSV-G antibody P5D4 (diluted 1:5000) for 1 hr at RT. For the capsid protein detection, the cells were fixed with 3,7% PFA and stained with a goat anti-p30 serum (1:100) and revealed by donkey anti-goat IgG (H+L)-Cy3 antibodies.

5.8.2. Surface staining

Proteins expressed on the cell surface can be detected under native conditions, which do not disrupt the cell membrane. To detect VSV-G protein on the surface of transfected cells, HEK293T cells were incubated with anti-VSV-G antibody (17-2-21-4) (diluted 1:400), which recognizes an extracellular epitope, for 1 hr on ice. The cells were then washed with PBS and were incubated 1hr on ice (dark) with Cy3 conjugated goat anti-mouse Ig F(ab')$_2$ antibody (GAM-Cy3, diluted 1:50). Samples were then fixed with 4% PFA for 10min on ice. Accessibility of the *c-myc* epitope on the modified VSV-G protein was assessed using Alexa 448-coupled anti-c-myc antibody (1:500) for 1 hr on ice in dark. The cells were then fixed with 4%PFA for 10 min on ice. La epitope was on the transfected cells using anti-La antibody 4B6 (undiluted, 1 hr on ice) and Cy3 labeled goat anti-mouse Ig F (ab') 2 antibody (GAM-Cy3, diluted 1:50). Cells were then fixed with 4%PFA. PSCA expression was detected on cells from Glioblastoma Multiforme (GBM) patients. Cells were stained for 1hour on ice with anti-PSCA antibody 7F5 and then secondary antibody sheep anti-mouse Cy3. Cells were then fixed for microscopy. DNA counter staining was performed when applicable with Hoechst 33342 dye (10mg/ml stock solution diluted 1:1000) prior to the staining. The stainings were observed with a Zeiss Meta 510 Confocal Laser Scanning Microscope.

5.8.3. Binding of anti-PSCA/anti-myc nanobeads onto PSCA-positive cells

HEK293wt, HEK293-pPSCA, HT1376 and RT4 cells were plated at a density of 10^4/ well in 8-well chamber slides. On the subsequent day, cells were incubated with anti-PSCA /anti-myc magnetic beads either at 37°C 240 min. Cells were then washed with PBS to remove unbound magnetic beads. The bound magnetic beads were detected with a goat anti-mouse IgG F(ab')$_2$ antibody coupled to Cy3.

5.9. Confocal laser scanning microscopy

The confocal laser scanning microscopy was performed with a Zeiss Meta 510 Confocal Microscope (BIOZ, TU-Dresden).

5.10. Membrane fusion assay

VSV-G protein-mediated membrane fusion was demonstrated by a fusion assay. HEK 293T cells were co-transfected with VSV-Gwt or modified G protein expressing vector and an EGFP encoding expression vector in 24-well plates at 32°C or 37°C. The cells were incubated at RT for 10min with PBS adjusted to a certain pH (pH range 5.0 to 7.5 at 0.5 unit intervals). Then, cells were incubated at respective temperature for 3hrs with culture medium, before the fusion induction was repeated. After 3 hrs incubation following second fusion induction, cells were fixed and were observed with a Zeiss Axiovert 200M microscope.

5.11. Flow cytometry analysis

Flow cytometry enables analysis of cells using the principles of light scattering, light excitation and fluorochrome emission. Fluorescently labeled cells are forced under high pressure to intercept a laser beam, where they scatter light and fluorochromes are excited to a higher energy level. From the scattered light, it is possible to gain information about the cell volume (Forward cell scatter; FSC) and the cellular complexity such as granularity (Side scatter; SSC). Transduced cells were analyzed by a Becton Dickinson Flow Cytometer, and the transduction efficiency was determined in terms of EGFP or DsRed fluorescence gating on the living cells. For confirmation of the PSCA expression on the HEK293-PSCA cells, cells were natively stained with a monoclonal affinity-purified anti-PSCA antibody and a goat anti-mouse Cy3 conjugated antibody. The positive cell amount was measured by FACS.

5.12. Apoptosis analysis

Anti-PSCA/ anti-myc antibody-coupled nanobeads were analyzed for the induction of apoptosis in PSCA-negative and PSCA-positive cells. The cells were incubated

with nanobeads at 37°C for overnight to allow internalization. Next day, the cells were washed with PBS to remove unbound nanobeads. Cells were cultivated for an additional day before the apoptotic cell amount was measured in a SubG1 test. In SubG1 test internucleosomal DNA fragmentation is detected using propidium iodide.

6. RESULTS

6.1. Selection of model test system and tools

The aim of the project was to generate ligand-modified VSV-G proteins for targeting of tumor cells with expression of a surface tumor-associated antigen. In this project we choose prostate cancer as the model system and it's "Prostate Stem Cell Antigen (PSCA)" as the pilot target. PSCA expression is highly restricted to the prostate tissue in male with some expression in bladder and colon. Moreover, in first experiments we showed the presence of PSCA on the surface of glioblastoma cells obtained from surgery samples of Glioblastoma Multiforme (GBM) patients (Figure 9). We have also generated PSCA-positive HEK293 cells for our analyses. A GPI-anchored PSCA expressing vector was transfected into HEK293wt cells and the PSCA-positive cells were selected using Geneticin.
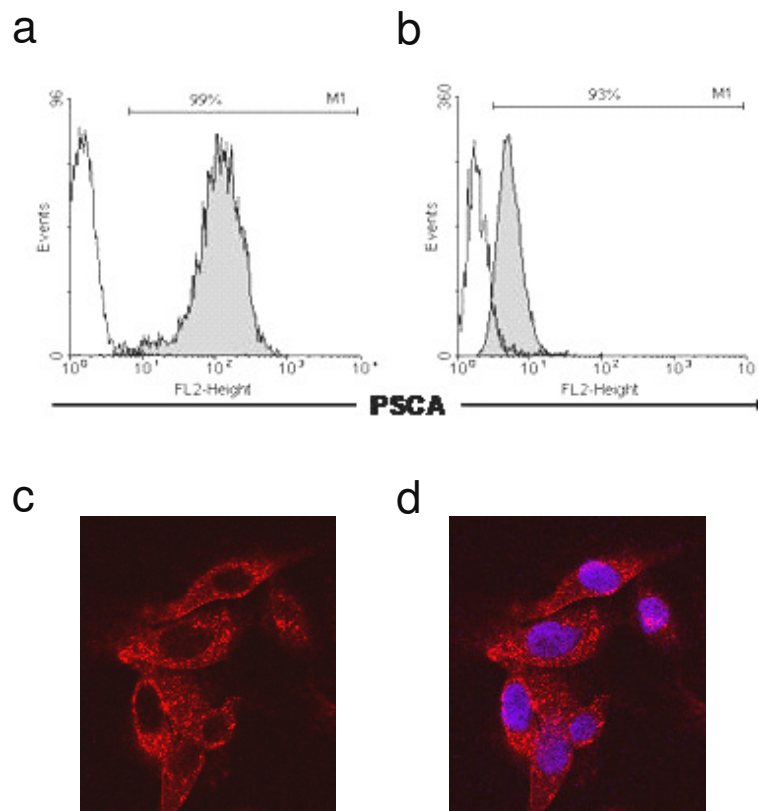

Figure 9. PSCA expression in GBM cells from patient.

PSCA-negative HEK293wt cells, and HEK293-PSCA cells and GBM cells from patient (4T1) were stained natively with anti-PSCA antibody and sheep anti-mouse Cy3 antibody. PSCA-positive cells were detected with flow cytometry (marked as M1) (a, b). PSCA-staining was also observed for 4T1 by indirect immunofluorescence using the same antibody combination as in flow cytometry detection. c: PSCA expression on natively stained 4T1 cells. d: 4T1 cells were stained with Hoechst 33342 and overlay is displayed. (a,b): open area: HEK293wt cells; gray area: HEK293-PSCA cells.

6.2. Generation of scFv anti-PSCA / VSV-G fusion protein for targeted gene delivery

The VSV-G mediates infection of a broad range of cells and thus despite the advantages of higher stability and high titer, VSV-G-pseudotyped particles are not suitable for selective targeting purposes. VSV-G fusion proteins were generated that were composed of a single-chain variable antibody fragment against PSCA and VSV-G protein. ScFv anti-PSCA (AM-I) was provided by Dr. Agnieszka Morgenroth at the Institute of Immunology (Dresden). AM-I was fused to VSV-G at the N-terminus. VSV-G is transported to the cell surface only as correctly folded trimers. To investigate the effect of fusion of AM-I to VSV-G, several different fusion proteins consisting of different VSV-G proportions and the scFv AM-I were generated. AM-I was fused either directly or with a small (5 amino acid-long) linker to VSV-G (Figure 10A and B). Besides, two more fusion proteins were produced in which AM-I was linked via an additional 7 long-long linker to N-terminally truncated VSV-G protein (Figure 10C and D).
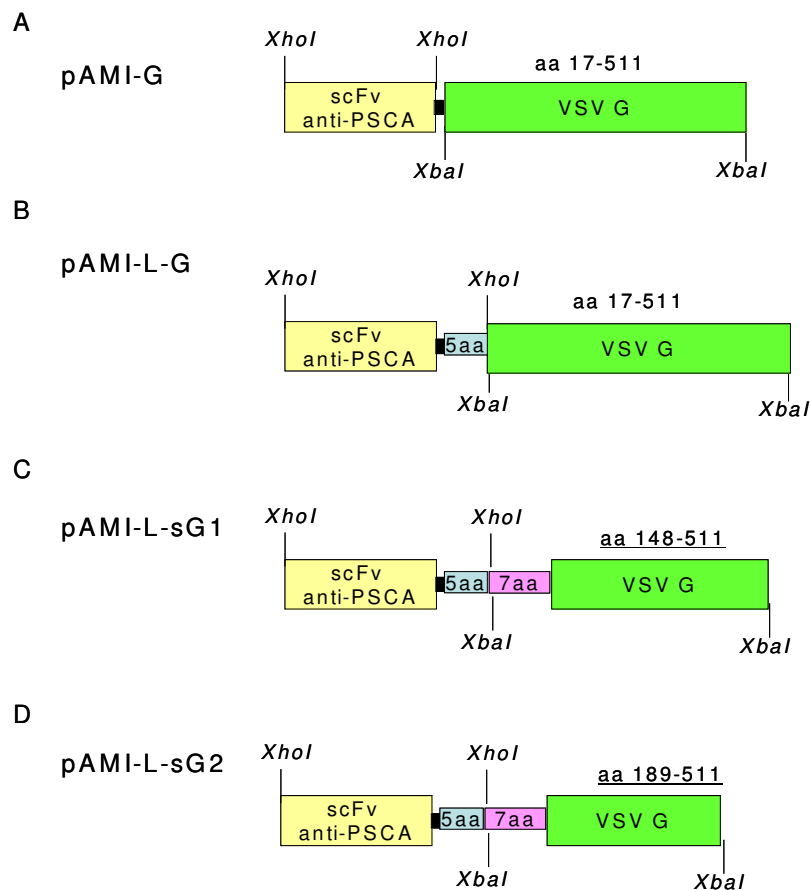

Figure 10. Schematic illustration of scFv anti-PSCA / VSV-G fusion proteins.

ScFv anti-PSCA was fused to the N-terminus of full-length VSV-G directly (A) or via a 5amino acid long linker (B). Two constructs (pAMI-L-sG1 and pAMI-L-sG2) contained VSV-G proteins, which were generated by N-terminal deletions of VSV-Gwt (C and D).

6.2.1. Intracellular and surface expression of scFv anti-PSCA/ VSV-G proteins

In first experiments we transfected the different scFv-AMI-VSV-G constructs in HEK293TZ cells and analyzed the expression of the fusion proteins by indirect immunofluorescence analysis. Only the modified protein expressed on cell surface can be packaged into viral particles. VSV-G depends on correct folding and trimerization for transport to the cell membrane. Intracellular and surface stainings were performed: For intracellular staining, transfected HEK293T cells were permeabilized and fixed. Cells were then stained with anti-VSV-G antibody directly coupled to Cy3 recognizing a cytoplasmic epitope in VSV-G (Figure 11).
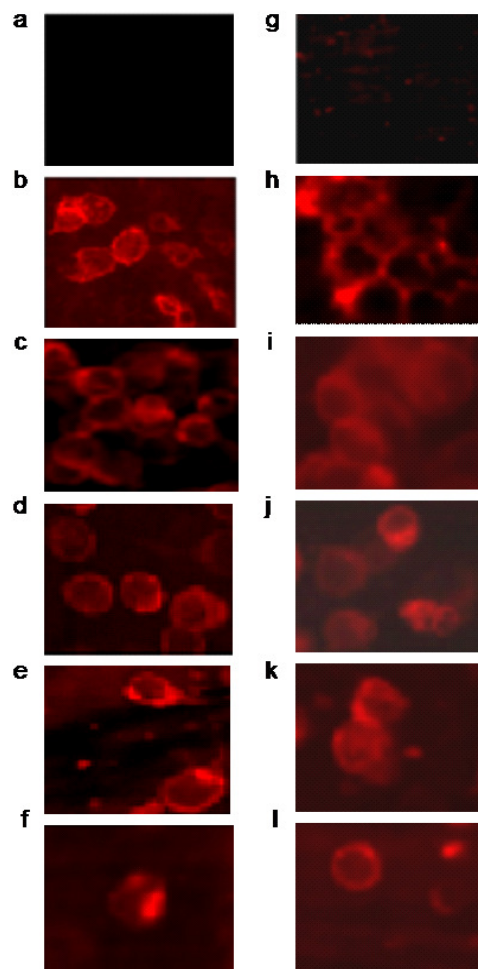

Figure 11. Intracellular staining of HEK293T cells.

HEK293T cells were transfected with VSVG-AMI fusion protein-encoding plasmids. Transfections were conducted at 37°C (A) or 32°C (B). VSVG staining was performed on fixed and permeabilized cells with anti-VSV-G antibody coupled to Cy3. In both cases, staining from 293T cells transfected with plasmids encoding a, g: mock transfected; b, h: pcz-VSV-G wt; c, i: pAMI-G; d, j: pAMI-L-G; e k: pAMI-L-sG-1; f, l: pAMI-L-sG-2.

The surface staining of the AMI–VSVG fusion proteins was investigated by the use of an anti-VSV-G antibody (17-2-21-4), which binds to the extracellular domain of VSV-G and secondary anti-mouse Ig F(ab)'$_2$-Cy3 (Figure 12A). A DNA counter-staining was performed with Hoechst 33342. The ectopically expressed fusion proteins were easily detected by intracellular staining. However, none of them was detectable on the plasma membrane. Prompted by this observation, we considered that the secondary or tertiary protein structure of the modified proteins was affected. Therefore, we decided to analyze the subcellular localization of the VSV-G constructs at a lower temperature. It is well known, that temperature-sensitive mutants of VSV-G experience problems either in folding or trimerization steps and are, therefore, not transported beyond the endoplasmic reticulum. However, this phenotype can be rescued by lowering the temperature to permissive temperatures, which allow correct folding or tolerate folding failures and enable subsequent transport of the protein to the cell membrane. Unfortunately, the intracellular transport could not be rescued for any of the AMI-VSV-G fusion proteins (Figure 12B). Consequently, studies with the AMI-VSV-G fusion proteins were not further pursued.
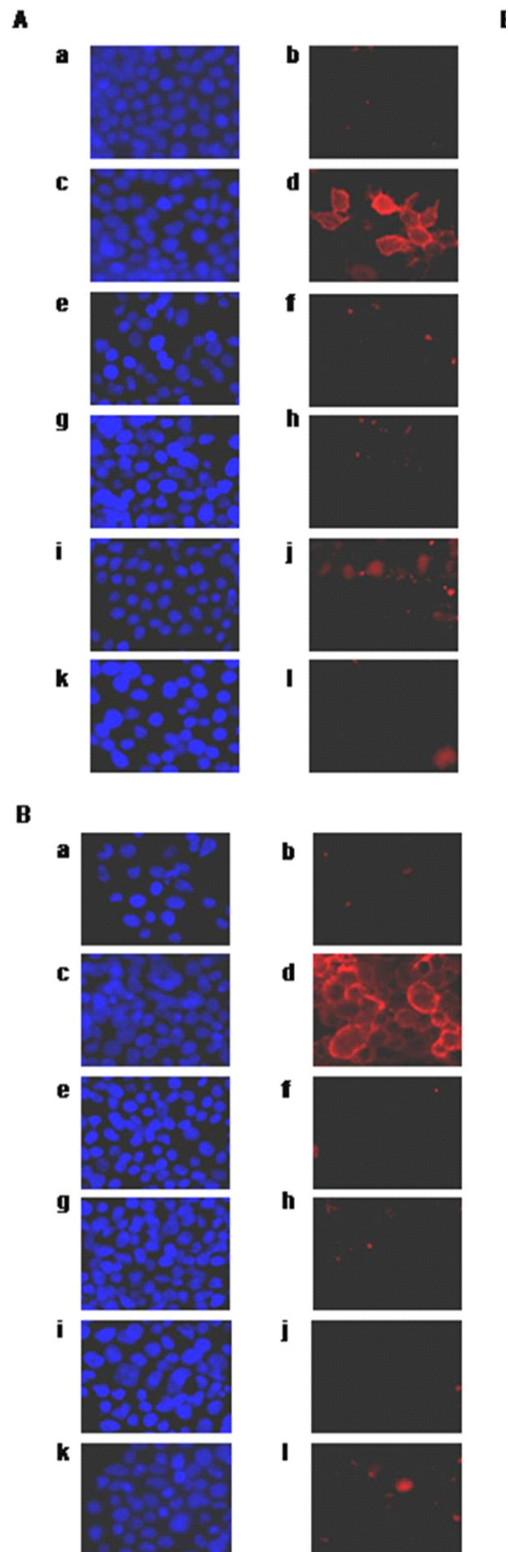
Figure 12. The extracellular staining of HEK293T cells.

HEK293T cells were transfected with VSVG-AMI fusion protein-encoding plasmids at 37°C (A) or 32°C (B) with a, b: mock transfected; c, d: pcz-VSV-G wt; e, f: pAMI-G; g, h: p-AMI-L-G; i, j: pAMI-L-sG1; k, l: pAMI-L-sG2. Staining was performed natively with anti-VSV-G antibody 17-2-21-4 and a Cy3-coupled goat anti-mouse antibody. DNA staining was performed with Hoechst 33342.

6.3. Generation of epitope-modified VSV-G proteins

Fusion of scFv against PSCA to VSV-G resulted in failure in transport of modified proteins to the cell surface. To eliminate the disruption in protein folding due to insertion of a large scFv molecule, modified VSV-G proteins were generated by inserting a small epitope in putative insertion-permissive sites. An epitope exposed on the surface of VSV-G can target the viral particle via linker molecules (such as antibodies or bispecific nanobeads), which bind both to the target cell and the viral particle. Nanobeads can be coupled to anti-epitope antibody and to an antibody recognizing an applicable tumor-associated antigen expressed on the tumor cell surface.

6.3.1. Selection of permissive sites in VSV-G protein for epitope insertion

Modification of VSV-G for selective targeting without interfering with its functions required identification of permissive sites in the protein. Epitope length may play a role in folding since the protein structure has a limited flexibility and cannot tolerate at every position any insertion. Any complication in folding will have its consequences in expression and function of the protein. Two different epitopes were chosen. The first epitope to be inserted was the ten amino acid long myc epitope (EQKLISEEDL). The myc epitope is commonly used to track proteins since it does generally not interfere with protein folding and function, and high-affinity anti-myc antibodies are available. The second epitope, the so-called La epitope consists of eighteen amino acids (EFEALKKIIEDQQESLNK) and was provided by Prof. M. Bachmann (Institute of Immunology, Dresden). The eighteen amino acid long La epitope is deduced from a region in the La protein to which high affinity antibodies were raised by Prof. M. Bachmann's group. Epitope insertion sites were chosen on the same basis as the myc-epitope insertion sites.

An ideal permissive site must allow insertion of an epitope without disturbing the folding, assembly into viral particles, virus internalization and subsequent fusion events. For this reason, VSV-G protein ectodomain sequences from VSV Indiana serotype strains and mutants were compared [175]. From the sequence comparison several non-conserved sites were identified as potential epitope-insertion permissive sites (Table 10), among which some located to neutralizing epitope sequences [176]. Moreover, amino acid position 17 in the precursor protein, which corresponds to the N-terminus of the mature protein, was included. An additional site at position 28 was chosen since epitope insertion at a close-by position was shown to be well-tolerated [147]. The epitope-modified VSV-G proteins were named by the amino acid number in precursor G protein (prior to proteolytic cleavage of 16 amino acid-long signal sequence in ER) after which the epitope is inserted. Table 11 depicts the designations of the modified VSV-G proteins with the positions of epitope insertion.

Amino acid position	San Juan	Mudd Summers	Orsay	tsG31	tsG31-PA	tsG31-PB	tsG31-PC
209	G	G	G	R	E	R	R
266	F	F	F	F	F	L/F	F
267	P	P	P	P	P	A/P	V/L
277	A	A	A	A	A	G	A/G
279	S	S	S	S	S	C/W/S	C/W/S
281	T	T	T	T	T	S/T	S

Table 10. Sequence comparison of VSV-G (Indiana) strains.

Accumulation of amino acid mutations in VSV-G protein from persistent infection isolates. Amino acid numbering was based on the precursor protein. tsG31 is a temperature mutant derived from VSV-G San Juan. tsG31-PA, tsG31-PB and tsG31-PC were derived from nude mice persistently infected with tsG31 [175]

Designation	Epitope	Position of amino acid residues flanking the insertion in the	
		Precursor VSV G	Mature VSV G
VSV G myc 17	*myc*	17-18	1-2
VSV G myc 28	*myc*	28-29	12-13
VSV G myc 208	*myc*	208-209	192-193
VSV G myc 266	*myc*	266-267	250-251
VSV G myc 278	*myc*	278-279	262-263
VSV G La 17	La	17-18	1-2
VSV G La 31	La	31-32	15-16
VSV G La 209	La	209-210	193-194
VSV G La 275	La	275-276	259-260

Table 11. Nomenclature of epitope-modified VSV-G proteins and the epitope insertion positions.

6.3.2. Insertion of *c-myc* epitope in permissive sites into VSV-G ectodomain

The myc epitope insertions were accomplished using the PCR-Based Site-Directed Mutagenesis Kit (Stratagene) according to manufacturer's instructions. For each site, VSV-G protein sequence in pcz-VSV-Gwt plasmid was amplified using a pair of primers introducing c-myc epitope and *Pst*I restriction site (inserting in total of 33 nucleotides).

6.3.2.1.   *Intracellular staining of myc-modified VSV-G-expressing cells*

HEK293T cells were transfected at 37°C with myc epitope-modified VSV-G protein encoding vectors. Cells were then stained for VSV-G expression. Transfected cells were fixed and permeabilized and stained with anti-VSV-G antibody coupled to Cy3. Figure 13 shows the protein expression in transfected cells. Effect of transfection temperature on protein expression was analyzed by transfection of cells also at 32°C and performing the same staining. VSV-G wt as well as all modified VSV-G proteins were detectable in transfected cells at both temperatures.
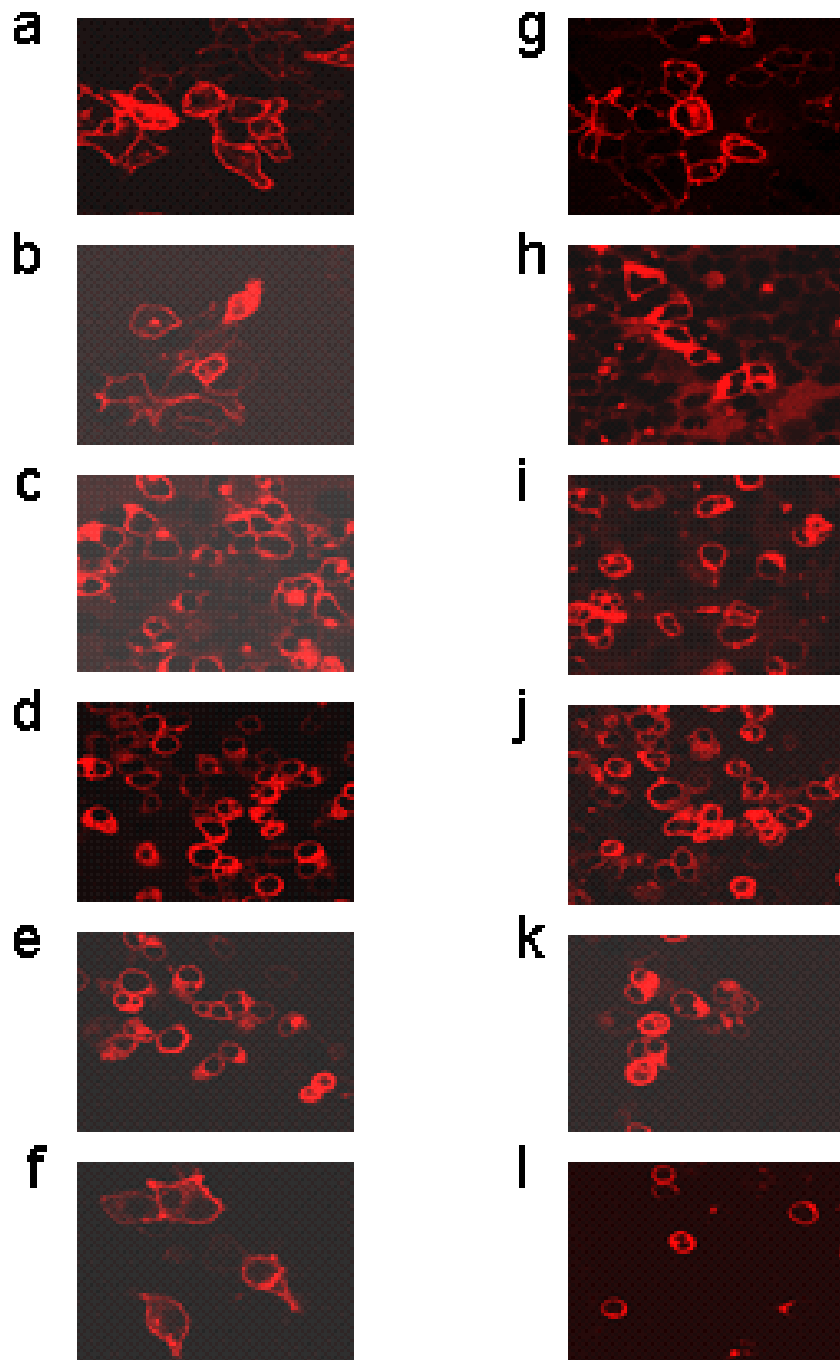
Figure 13. Intracellular expression of myc-modified VSV-G.

Intracellular staining of fixed and permeabilized HEK293T cells transfected with VSVG wt or VSV-G myc modified protein encoding plasmids was performed with anti-VSVG antibody (P5D4) coupled to Cy3. a, g: with VSV-G wt; b, h: with VSV-G myc-17; c, i: with VSV-G myc-28; d, j: with VSV-G myc-208; e, k: with VSV-G myc-266; f, l: with VSV-G myc-278 encoding vector. a-f: Transfection at 32 °C. g-l: Transfection at 37 °C.

6.3.2.2. *Surface expression of myc-modified VSV –G proteins*

Targeted gene delivery using linker molecules requires that the c-myc epitope is readily exposed on the viral particles. Therefore, first of all the surface expressions of modified envelope proteins on natively stained HEK293T cells were detected. Transfections were performed both at permissive (32°C) and restrictive (37°C) temperatures. Cells were stained first with Hoechst 33342 to visualize the nucleus. VSV-G staining was performed with anti-VSV-G antibody (17-2-21-4, kind gift of Prof. Grünberg, University of Geneva, Switzerland) recognizing an epitope in the extracellular domain of VSV-G. As expected, the VSV-G wt protein was readily detected on the cell surface. Interestingly, also the modified VSV-G myc 17 and VSV-G myc 278 proteins were detectable on the cell surface at both restrictive and permissive temperatures. However, the constructs VSV-G myc 28 was only detectable when the transfection was performed at the permissive temperature (Figure 14; a-c, f, g-h, l). The modified proteins VSV-G myc 208 and VSV-G myc 266 were not detected on the cell surface at both temperatures. (Figure 14; d-e, i-k).
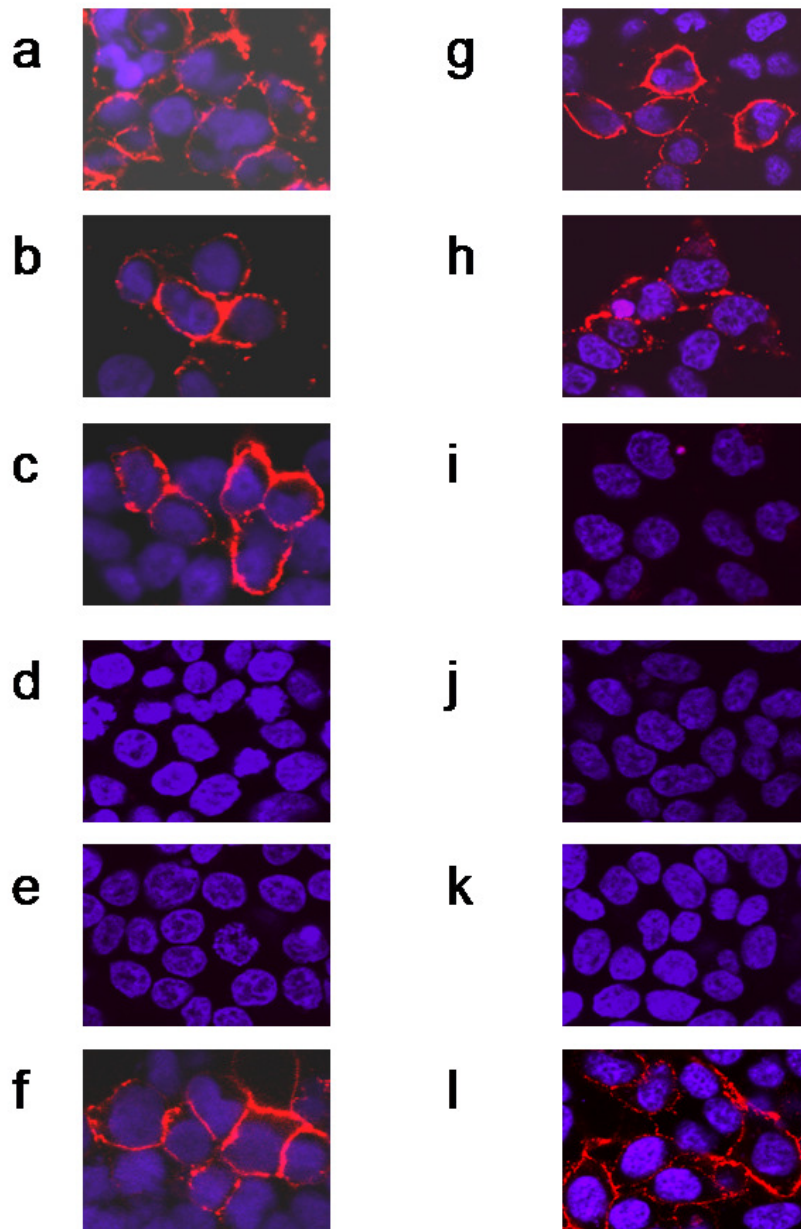
Figure 14. Surface expression of myc-modified VSV-G.

Native staining of non-fixed HEK 293T cells transfected with VSVG wt or VSV-G myc modified protein encoding plasmids was performed with anti-VSVG antibody (17-2-21-4) and as secondary antibody goat anti-mouse Ig F (ab')$_2$ antibody coupled to Cy3. a, g: with VSV-G wt; b, h: with VSV-G myc-17; c, i: with VSV-G myc-28; d, j: with VSV-G myc-208; e, k: with VSV-G myc-266; f, l: with VSV-G myc-278 encoding vector. a-f: Transfection at 32°C. g-l: Transfection at 37°C. DNA counter staining was performed prior to staining with Hoechst 33342.

6.3.2.3.   Detection of myc epitope in myc-modified VSV-G proteins

A crucial prerequisite for a nanobead-mediated selective retroviral transduction is the accessibility of the c-myc epitope on the viral particles. Therefore, HEK293T cells were transfected with VSV-G wt or VSV-G myc protein-encoding vectors and were stained natively with an anti-myc antibody directly coupled to Alexa 488. Transfections were performed at permissive and restrictive temperatures, respectively, in order to analyze temperature-mediated effects on the exposition of the myc epitope. As expected, in VSV-G wt-expressing cells no positive staining was observed. On the other hand, VSV-G myc 17, VSV-G myc 278 proteins were detected at both incubation temperatures, whereas VSV-G myc 28 was only detected on cells which were incubated at 32°C. These results closely resemble the native staining obtained with the 17-2-21-4-VSV-G antibody. The two modified proteins, VSV-G myc 208 and VSV-G myc 266, which were not detectable on cell surface at both temperatures, also did not expose the myc epitope at both temperatures (Figure 15). Table 12 summarizes the results of expression patterns of the myc epitope-modified VSV-G proteins.
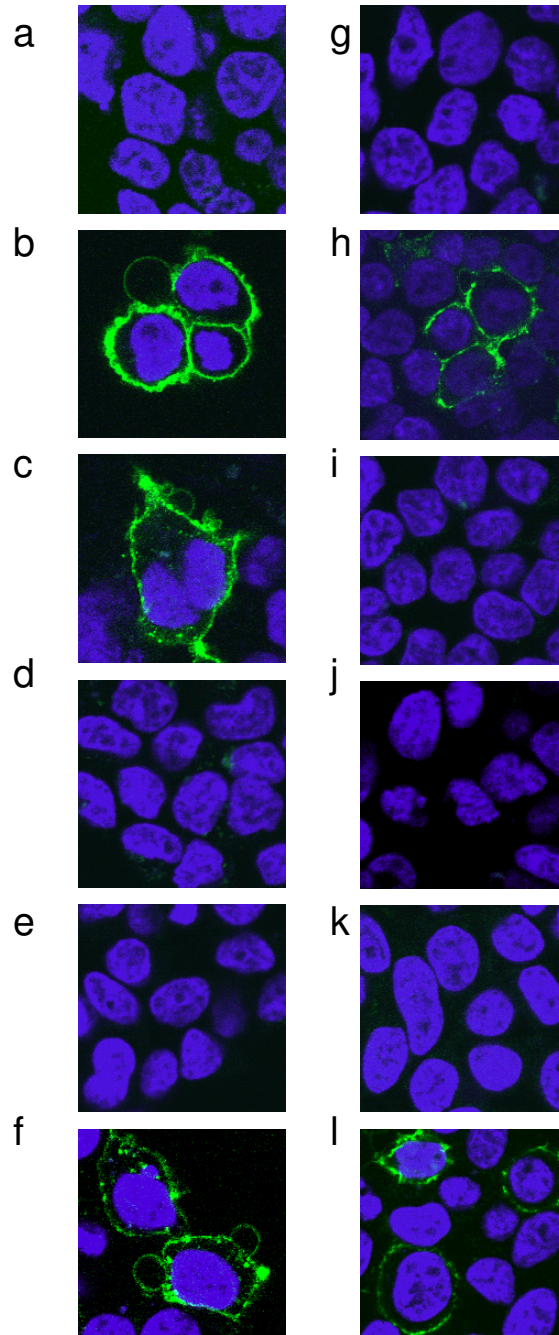
Figure 15. Availability of myc epitope on myc-modified VSV-G.

HEK293T cells transfected with VSV-G wt and VSV-G myc modified proteins-encoding plasmids: a, g: VSV-G wt; b, h: VSV-G myc 17; c, i: VSV-G myc 28; d, j: VSV-G myc 208; e, k: VSV-G myc 266; f, l: VSV-G myc 278. Surface expression of proteins was detected by native staining with anti-myc antibody coupled to Alexa 488. DNA counter staining was performed with Hoechst 33342. Transfections were performed either a-f: at permissive temperature 32°C or g-l: at restrictive temperature 37°C.

Designation	Intracellular expression	Surface expression	myc epitope accessibility
VSV-G wt	+	+	-
VSV-G myc 17	+	+	+
VSV-G myc 28	+	ts	ts
VSV-G myc 208	+	-	-
VSV-G myc 266	+	-	-
VSV-G myc 278	+	+	+

Table 12. Overview of results with myc-modified VSV-G proteins.

Also given is the accessibility of myc epitope by anti-myc antibody in native staining. ts: Temperature-sensitive expression, where protein or the epitope was only detectable at 32°C but not at 37°C. ts= temperature sensitive.

6.3.3. Insertion of La epitope in VSV-G ectodomain

6.3.3.1. Intracellular expression of La epitope-modified VSV-G proteins

HEK293wt cells were transfected with pMD2.G-La plasmids at 32°C or 37°C. Fixed and permeabilized cells were stained with Cy3 coupled anti-VSV-G antibody (Sigma). The cells were observed and pictures were taken with Zeiss LSM Meta 510 Laser Scanning Confocal Microscope. Figure 16 illustrates the intracellular expression of La-modified VSV-G proteins.
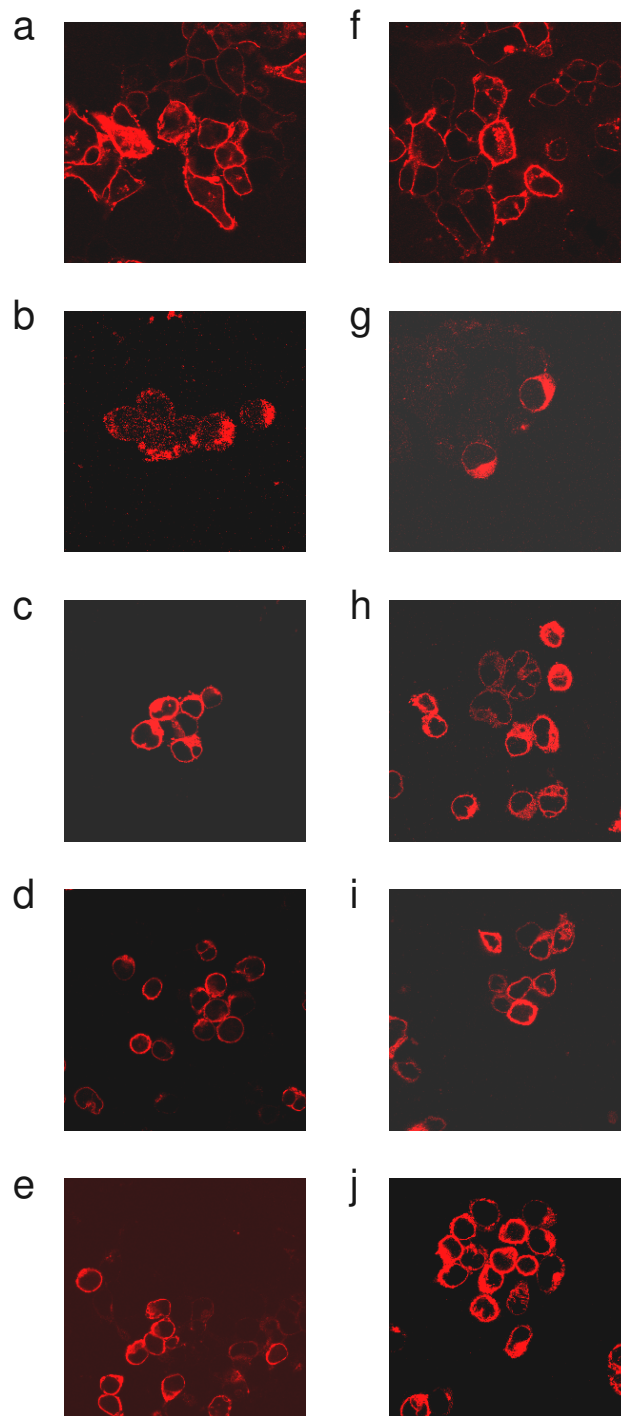
Figure 16. Intracellular expression of La-modified VSV-G.

HEK293wt cells transfected at 32 °C (a-e) or 37 °C (f-j) with La-modified VSV-G-encoding plasmids: a, f: VSV-G wt; b, g: VSV-G La 17; c, h: VSV-G La 31; d, i VSV-G La 209; e, j VSV-G La 271. Fixed and permeabilized cells were stained with anti-VSV-G antibody coupled to Cy3.

6.3.3.2.   Surface expression of La epitope-modified VSV-G proteins

HEK 293wt cells transfected with La-modified VSVG encoding plasmids were analyzed for the surface expression. HEK293wt cells were transfected at 32°C or 37°C with La-modified VSV-G-encoding plasmids. Cells were first stained for DNA with Hoechst 33342 and then for La epitope with 4B6 antibody. The staining was performed on non-fixed, non-permeabilized cells. Subsequently, cells were fixed and pictures were taken with Zeiss LSM Meta 510 Laser Scanning Confocal Microscope (Figure 17). Among the four La-modified VSV-G proteins, only two (VSV-G La 209 and VSV-La 271) were expressed on the plasma membrane.
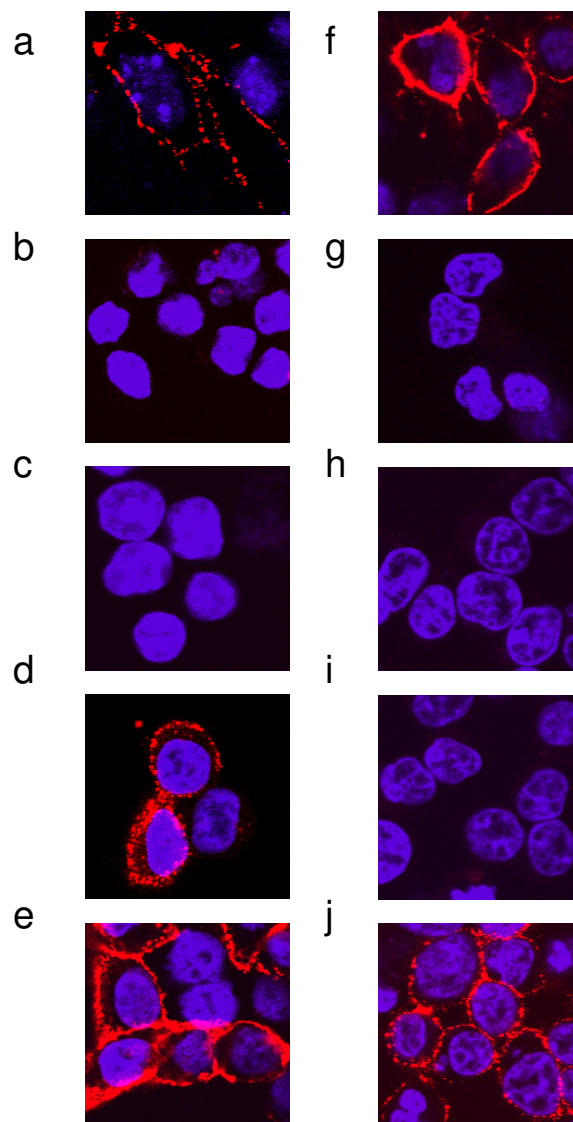

Figure 17. Surface expression of La-modified VSV-G.

HEK293wt cells transfected with La-modified VSV-G-encoding plasmids at 37°C (a-e) and 32°C (f-j). DNA counter staining was performed with Hoechst 33342. La-epitope was detected using anti-VSV-G antibody (17-2-21-4) and goat anti-mouse Cy3 antibody. a, f: VSV-G wt ; b, g: VSV-G La 17; c, h: VSV-G La 31; d, i: VSV-G La 209; e, j: VSV-G La 271.

6.3.3.3. Accessibility of La epitope on La-modified VSV-G proteins

Next, the accessibility of the La epitope was analyzed. HEK293wt cells transfected with VSV-G wt or VSV-G La protein-encoding vectors. First, the DNA counter-staining was performed with Hoechst 33342. Then the cells were stained natively with a monoclonal anti-La antibody (4B6, provided by Prof. Bachmann, Dresden) and goat anti-mouse secondary antibody coupled to Cy3. Only the VSV-G protein modified at amino acid position 271 exposed La epitope, and it did so only at 32 °C (Figure 18). Table 13 summarizes the feature of La-modified VSV-G proteins.
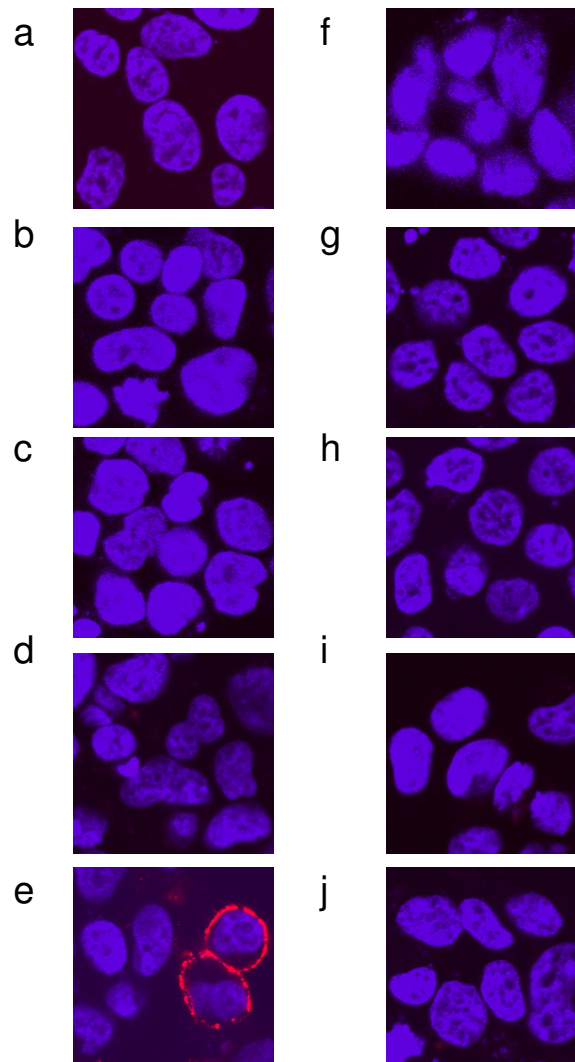

Figure 18. Detection of La epitope on VSV-G La-expressing cells.

HEK293wt cells transfected with La-modified VSV-G-encoding plasmids. DNA counter staining was performed with Hoechst 33342 prior to anti-La staining. La-epitope was detected with anti-La antibody (4B6) and goat anti-mouse Cy3 secondary antibody. Transfections were performed at 32 °C (a-e) and 37 °C (f-j). a, f: VSV-G wt detected with anti-La antibody; b, f: VSV-G La 17; c, h: VSV-G La 31; d, i: VSV-G La 209; e, j: VSV-G La 271.

Designation	Intracellular expression	Surface expression	La epitope accessibility
VSV G wt	+	+	-
VSV G La 17	Only at 37°C	-	-
VSV G La 31	+	-	-
VSV G La 209	+	+	-
VSV G La 275	+	+	Only at 37°C

Table 13. The overall summary of intracellular and surface expression of La-modified VSV-G proteins.

Also given is the accessibility of La epitope. The mutants whose specified feature was dependent on the transfection temperature are indicated with the temperature at which positive staining was observed.

6.4. Fusogenic activity of epitope-modified VSV-G proteins

Onset of the VSV-G-mediated entry into target cells is the VSV-G binding to the cellular receptor. Bound virus is then internalized into the endosomal vesicles, which in turn acidifies. The acidic pH leads to a conformational change in VSVG protein. In this low-pH form of VSVG, the fusion peptide is exposed and this results in the fusion of viral membrane with that of the endosomal vesicle. This fusion step is critical for the success of gene delivery using VSV-G-pseudotyped viral particles. Therefore, the fusogenic capacities of the modified VSV-G proteins, which were transported to the cell membrane and exposed the respective epitope, were evaluated. To resemble the acidic conditions present in the endosomal vesicle, the cells were incubated with PBS, whose pH was adjusted to a certain value. HEK293T cells were co-transfected with VSV-G wt or modified VSV-G- and EGFP-encoding plasmids. A pH range (pH 5.0 to pH 7.5 in 0.5 intervals) including the optimal pH of VSV-G wt was tested. Transfections were performed both at permissive and restrictive temperatures and fusion assay was performed. Syncytium formation was observed and documented with Zeiss Axiovert 200M microscope.

6.4.1. Membrane fusion assay with *myc*-modified VSV-G mutants

The results of the fusion assay at representative pH values are depicted in Figure 19 for myc-modified VSV-G proteins. VSV-G wt has an optimal fusion pH range of 5.8 to 6.2 and the temperature of transfection does not affect its fusogenic capacity. VSV-G myc 17 was fusogenic at both permissive and restrictive

temperature with an optimum pH of 5.5 (Table 14). As expected, VSV-G myc 28, which was only transported to the cell surface at 32°C, induced membrane fusion also only at this temperature. Like VSV-G myc 17, VSV-G myc 28 had an optimal fusion pH lower than that of VSV-G wt. Interestingly VSV-G myc 278 exhibited no fusion at any pH regardless of the temperature although this protein was transported to the cell surface at both 32°C and 37°C. Consequently, VSV-G myc 278 protein was not included in further experiments.
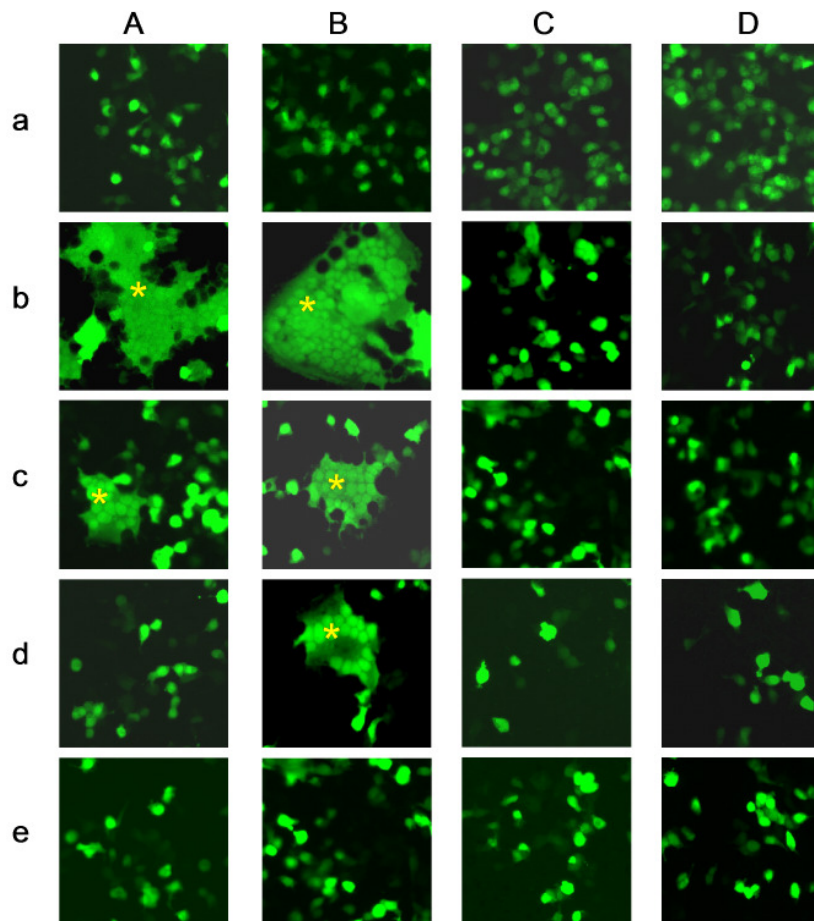

Figure 19. Fusion assay with the myc-modified VSV-G proteins.

HEK 293T cells were co-transfected at 37 °C (A,C) and 32°C (B,D) with EGFP and VSVG (wt or myc-modified) protein-encoding plasmids. 2 days after transfection, fusion was induced by incubating the cells with pH-adjusted PBS for 10min at RT. Cells were then incubated with fresh culture medium for 3hours at 32°C or 37°C, before repeating the procedure. Finally, cells were fixed and observed with Zeiss Axiovert 200M microscope. For each transfection and pH value three random areas are photographed only one of which is depicted in the figure. For determination of the optimal fusion pH, a pH range from 5.0 to 7.5 in 0.5 point intervals was tested. Here pH values A, B: 5.5; C, D: 7.0 are illustrated. Cells were transfected with plasmids encoding a: EGFP; b: VSVG wt; c: VSV-G myc 17; d: VSVG myc 28; e: VSV-G myc 278. Fused cells display distinguished morphology; several nuclei concentrated in the centre of the syncytium (stars).

A

Protein	Syncytium formation at **32ºC** at pH					
	5.0	5.5	6.0	6.5	7.0	7.5
VSV G wt	+	+	+	-	-	-
VSV G myc 17	+	+	-	-	-	-
VSV G myc 28	-	+	-	-	-	-
VSV G myc 278	-	-	-	-	-	-

B

Protein	Syncytium formation at **37ºC** at pH					
	5.0	5.5	6.0	6.5	7.0	7.5
VSV G wt	+	+	+	-	-	-
VSV G myc 17	-	+	-	-	-	-
VSV G myc 28	-	-	-	-	-	-
VSV G myc 278	-	-	-	-	-	-

Table 14. The fusogenic activities of VSV-G proteins.

Fusogenic capacities of VSV-Gwt- and *myc*-modified VSV-G proteins were analyzed in pH range 5.0-7.5 (in 0.5 intervals) and at 32°C (A) and 37°C (B) are summarized.

6.4.2. Membrane fusion assay with La-modified VSV-G mutants

Next, the fusion capacity of VSV-G La 271 protein was analyzed on transfected cells. The protein was subjected to the same fusion assay as the myc-modified VSV-G proteins. Unfortunately, the VSV-G La 271 was not capable of inducing cell-to-cell fusion (Figure 20 and Table 15). Therefore, this mutant was not included in further analyses.
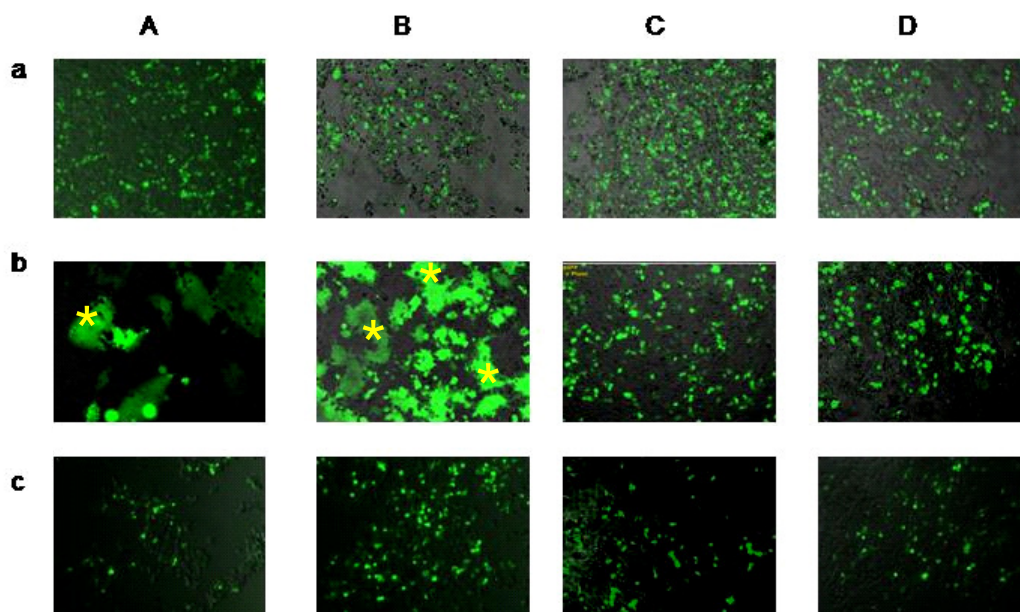
Figure 20. Fusion assay with La-modified VSV-G proteins.

HEK 293T cells were co-transfected at 32 °C (A, C) and 37°C (B, D) with EGFP and VSVG (wt or La-modified) protein-encoding plasmids. 2 days after transfection, fusion was induced by incubating the cells with pH-adjusted PBS for 10min at RT. Cells were then incubated with fresh culture medium for 3hours at 32°C or 37°C, before repeating the procedure. Finally, cells were fixed and observed with Zeiss Axiovert 200M microscope. For each transfection and pH value three random areas are photographed only one of which is depicted in the figure. For determination of the optimal fusion pH, a pH range from 5.0 to 7.5 in 0.5 point intervals was tested. Here pH values A, B: 5.5; C, D: 7.0 are illustrated. Cells were transfected with plasmids encoding a: EGFP; b: VSVG wt; c: VSVG La 271. Fused cells display distinguished morphology; several nuclei concentrated in the centre of the syncytium (stars).

A

	Syncytium formation at 32°C at pH					
	5.0	5.5	6.0	6.5	7.0	7.5
VSV-Gwt	+	+	+	-	-	-
VSV-G La 275	-	-	-	-	-	-

B

	Syncytium formation at 37°C at pH					
	5.0	5.5	6.0	6.5	7.0	7.5
VSV-Gwt	+	+	+	-	-	-
VSV-G La 275	-	-	-	-	-	-

Table 15. The fusogenic capacity of La-modified VSV-G proteins.

VSV-G wt and La epitope-modified VSV-G protein (VSV-G La 271) was analyzed for fusogenic capacity in the pH range 5.0-7.5. Fusion assays were performed at 32°C (A) and 37°C (B).

6.5.   Generation of viral particles pseudotyped with mutant VSV-G proteins

6.5.1. Assembly of VSV-G protein into viral particles (packaging)

The fusogenic myc epitope-modified G proteins were next studied with respect to their capacity to be incorporated into viral particles. Virus assembly was performed at 32°C, which enabled packaging of not only VSV-G wt and VSV-G myc 17 but also the temperature-sensitive protein VSV-G myc 28. The retroviral particles were generated as described in chapter 5.4.2 (Figure 21).
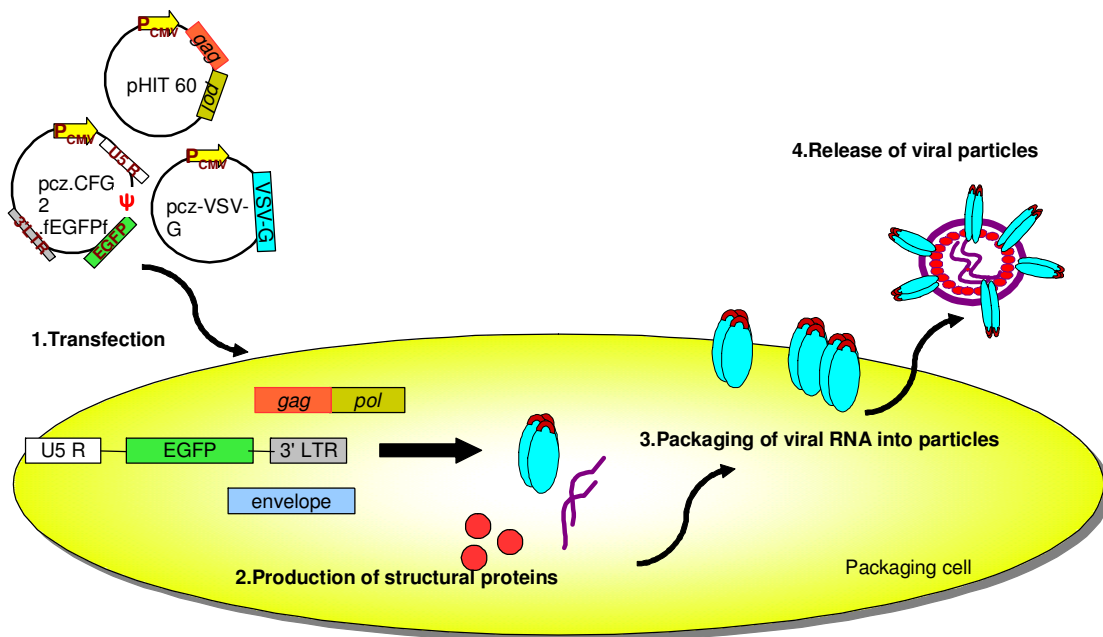

Figure 21. Three-vector packaging system according to Soneoka _et al_. [3].

Packaging cells are co-transfected with three vectors to generate replication-deficient viral particles. One plasmid encodes the gene of interest, which also contains the packaging signal, one plasmid codes for envelope protein and the third plasmid encodes _gag_-pol proteins.

Total cell lysates from the packaging cells were prepared and analyzed by Western blotting. The membrane was incubated with an anti-VSV-G antibody and secondary rabbit anti-mouse Ig HRP antibody. Detection was accomplished via chemiluminescence. All packaging cells except the packaging without envelope protein (Δenv; pHIT 60 and pcz-CFG2-fEGFPf co-transfection) expressed the VSV-G protein (Figure 22).
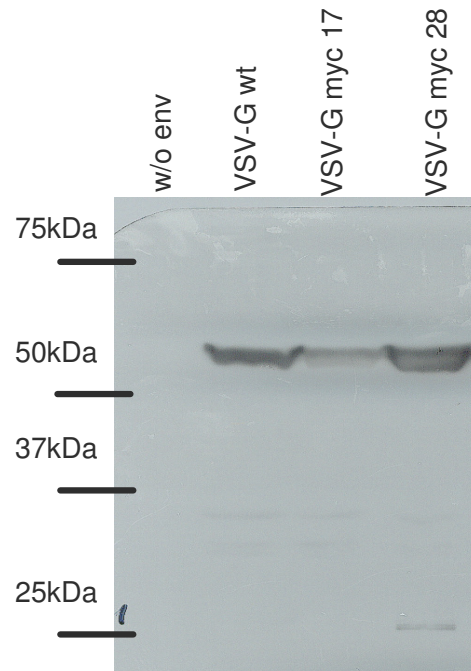
Figure 22 Immunoblot analysis of total cell lysates from packaging cells..

HEK293T cells were co-transfected with pHIT 60, pcz-CFG2-fEGFP alone (Δenv) or with VSV-G wt or myc-modified VSV-G. Cell lysates were separated by SDS-PAGE and proteins were transferred to PVDF membranes. Proteins were detected with anti-VSV-G antibody and rabbit anti-mouse Ig HRP antibody using ECL.

6.6. Concentration and purification of retroviral particles

6.6.1. Concentration of viral particles via ultracentrifugation

The viral particles were concentrated form the packaging cell medium by ultracentrifugation 100.00g with a Beckman Coulter Ultracentrifuge (SW40Ti or SW28 rotor) at 4°C for 2hrs. Following ultracentrifugation, the supernatant was discarded carefully and the viral particles were re-suspended in SDS sample buffer for SDS-PAGE analysis or in culture medium for further use. The viral particles were analyzed by 10% SDS-PAGE and blotted onto PVDF membranes. Presence of viral particles was demonstrated (Figure 23) using the anti-VSV-G (P5D4) and horseradish peroxidase (HRP)-coupled rabbit anti-mouse Ig antibodies.
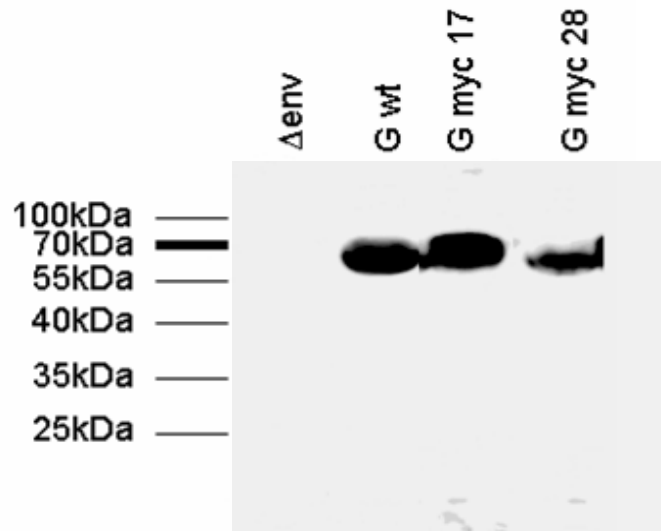
Figure 23. Immunoblot analysis of viral particles following ultracentrifugation.

Ultracentrifuge-concentrated supernatants from packaging cells were analyzed. Packaging cells were co-transfected with pHIT 60, pcz-CFG2-fEGFP alone or with VSV-G wt or myc-modified VSV-G. Viral particles were separated by SDS-PAGE and proteins were transferred to PVDF membranes. Proteins were detected with anti-VSV-G antibody and rabbit anti-mouse Ig HRP antibody with ECL Plus using LAS 3000 (Fuji). Δenv: Packaging cells were co-transfected only with pHIT60 and pcz-CFG2-fEGFPf.

6.6.2. Purification of *myc*-modified-viral particles

Anti-myc antibody-coupled magnetic beads (Miltenyi Biotec) were used to capture retroviral particles pseudotyped with the myc-modified envelope from the packaging cell supernatant. Eluates from the magnetic bead purification were first analyzed with the anti-VSV-G antibody P5D4 and rabbit anti-mouse Ig HRP antibody. Purified myc-modified viral particles displayed a protein band around 67kDa corresponding to VSV-G protein Figure 24A. As expected there was no band representing the VSV-G protein in the supernatants of cells which were not transfected with the wild-type envelope protein. The secondary anti-mouse HRP conjugate also detects the heavy and the light chains of anti-myc antibody, which was coupled to the magnetic beads and was, probably, co-eluted by the hot sample buffer. There is no immunoreactivity against VSV-G wt-pseudotyped retroviral particles, since they are washed away from the anti-myc column. To demonstrate that the envelope proteins, which were observed in viral eluates, represent viral particles and not viral envelope proteins shed from the packaging cells, the membrane was stripped an re-probed with a polyclonal goat anti-p30 serum. Figure 24B shows the presence of the p30 capsid protein in the modified-G protein pseudotyped viral eluates, whereas no bands corresponding to that protein were observed in samples from packaging without envelope or with VSV-G wt. An

additional band of ~65kDa was detectable in the samples, which was probably the precursor of capsid protein, p65*gag*. Also other anti-MLV capsid antibodies have been described that recognize this precursor [177].
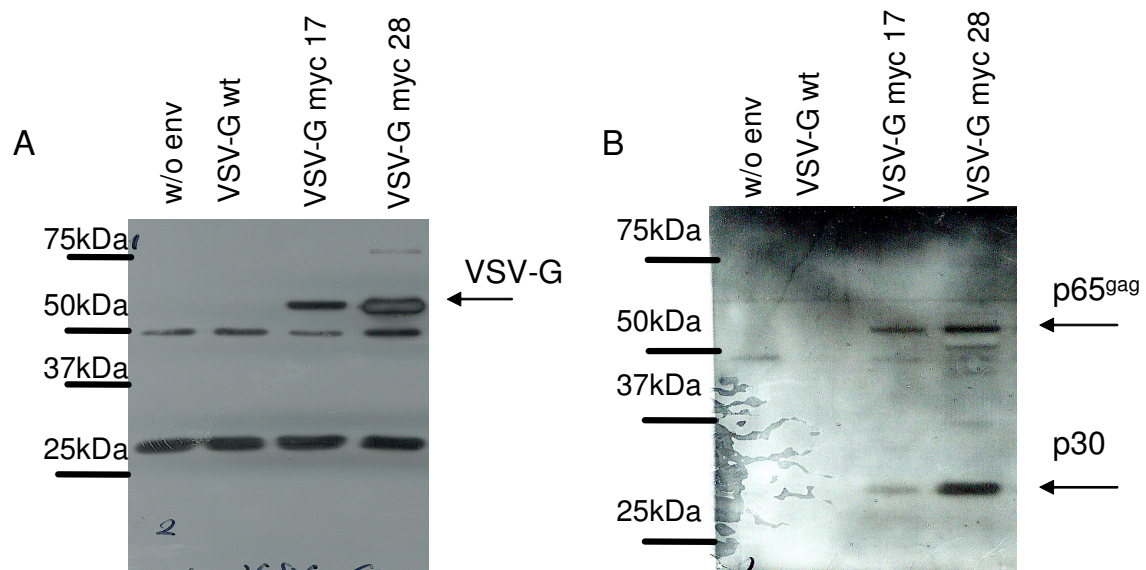

Figure 24. Immunoblot analysis of packaging cells supernatant purified with anti-myc antibody coupled-magnetic bead.

Eluates from purification were separated in SDS-PAGE and proteins were transferred to PVDF membrane. A: VSV-G proteins in eluates were detected with anti-VSV-G antibody and HRP conjugated rabbit anti-mouse Ig antibody. The same membrane was used to detect the capsid protein after stripping under stringent conditions and overnight blocking. B: Capsid protein detection was conducted with anti-p30 serum and HRP conjugated rabbit anti-goat antibody. Blots were visualized in both cases with ECL Plus visualization kit and light-sensitive Hyperfilm.

6.7. Transduction of HEK293T cells with VSV-G–pseudotyped retroviral particles

VSV-G wt-pseudotyped viral particles have a broad target cell range owing to a still undefined ubiquitously expressed cellular receptor. Therefore, it was necessary to analyze whether the epitope insertion has any effect on the wild-type tropism and transduction efficiency. Briefly, VSV-G wt- or modified VSV-G-pseudotyped retroviral particles encoding EGFP were packaged. 48hrs and 72hrs after transfection supernatants were harvested and pooled. One ml supernatant was used for transduction of the HEK293T cells in the presence of 8µg/ml Polybrene. The transduction efficiency was determined 3 day after transduction by FACS. The packaging was performed at 32°C and the transduction was done at both 32°C and 37°C. Figure 25 shows the transduction efficiencies on HEK293T cells, which were transduced at 37°C (Figure 25 a, c, e, g) or 32°C (Figure 25 b, d, f, h). The average efficiencies of transduction at 32°C and 37°C using retroviral particles produced at 32°C are illustrated in Figure 26. The modified retroviral particles displayed lower transduction efficiencies than the wild-type envelope-

containing particles. However, the particles displayed similar transduction efficiencies both at 37°C and 32°C.
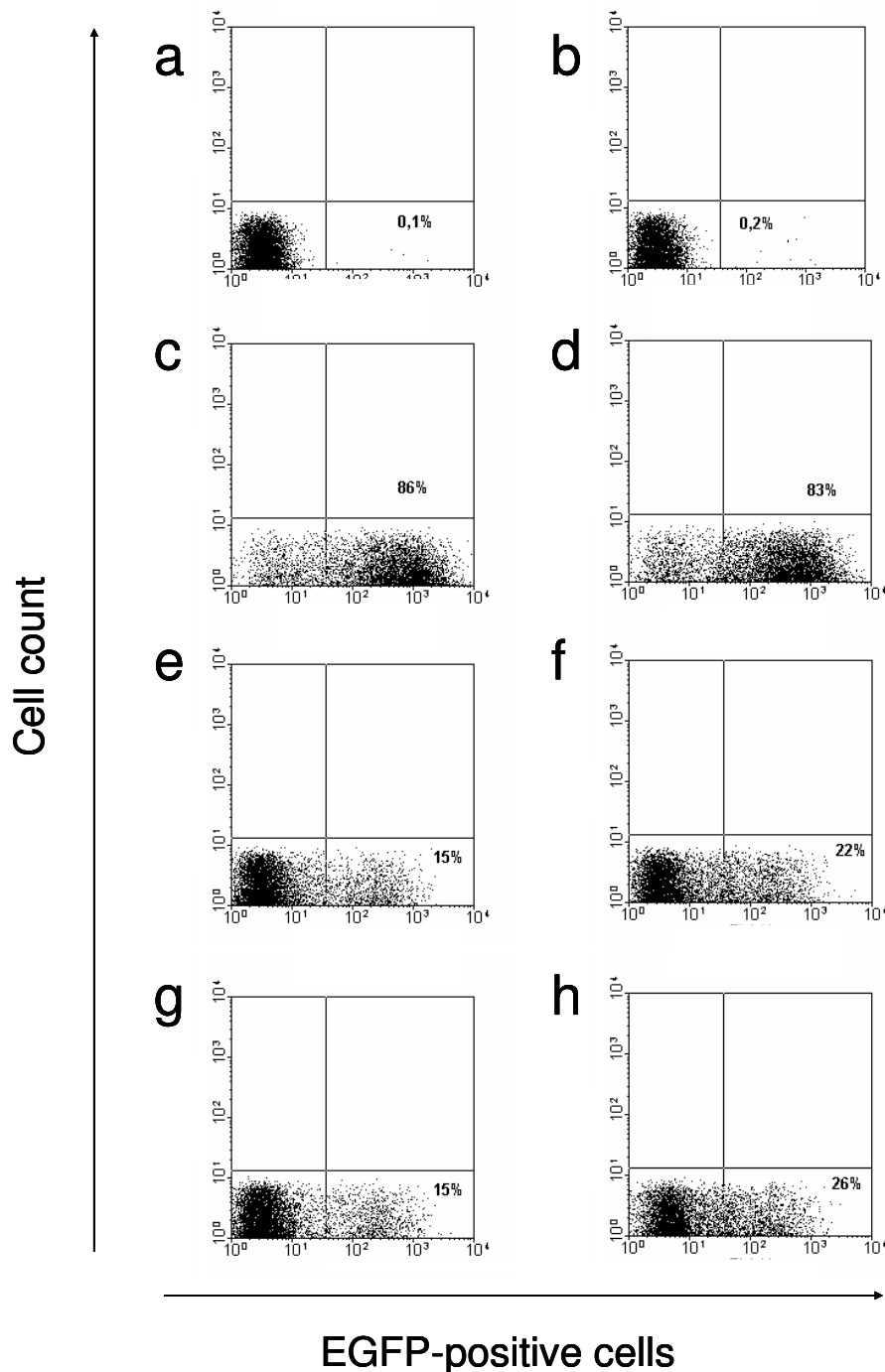

Figure 25. Transduction efficiency of retroviral particles packaged at 32°C.

Packaging of HEK293T cells was performed at 32°C. For packaging pHIT60 and pcz-CFG2-fEGFPf plasmids were used either alone (a, b: Δenv) or with VSVG encoding plasmids where c, d: VSV-Gwt; e, f: VSV-G myc 17; g, h: VSV-G myc 28. The transduction experiments were performed at either 37°C (a, c, e, g) or 32°C (b, d, f, h).
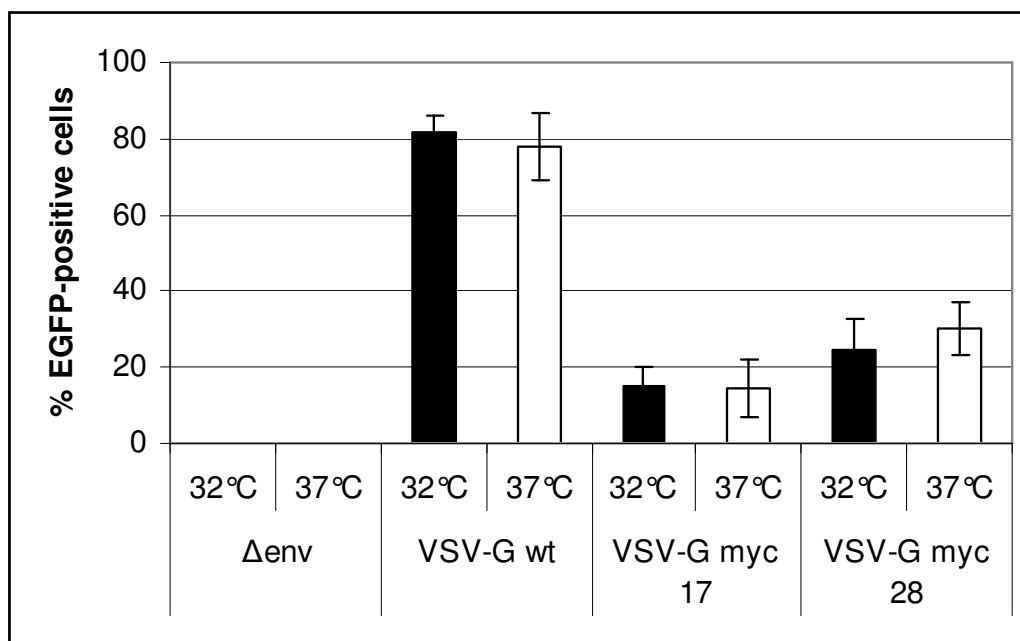
Figure 26. Average transduction efficiency of viral particles packaged at 32°C.

For each envelope protein the mean transduction efficiency of three independent experiments is shown. Transduction temperatures are indicated. Δenv: The packaging without envelope protein.

6.7.1. Effect of anti-*myc* antibody on transduction mediated by *myc*-modified retroviral particles

Next we analyzed whether anti-myc antibody binding can inhibit or reduce transduction efficiency with myc-modified viral particles. The virus production was conducted at 32°C and transduction was performed at 37°C in the presence of one of the following antibodies at a final concentration of 1µg/ml: neutralizing anti-VSVG antibody (8G5, generous gift from Prof. Lyles), anti-myc antibody (Invitrogen) or anti-Xpress tag antibody (Invitrogen), which served as an isotype-matched control. Transduction experiments were carried out in the presence of 8µg/ml Polybrene (final concentration). In Figure 27 results are depicted as normalized to the transduction efficiency obtained with the anti-Xpress antibody Transduction by MLV$^{(G-wt)}$ particles was inhibited by the neutralizing anti-VSV G antibody but was not affected significantly by either anti-myc or anti-Xpress antibodies. On the other hand, transduction with MLV$^{(G-myc\ 17)}$ was not only inhibited by the neutralizing anti-VSV G antibody but also was reduced to 50% when anti-myc antibody was added to the viral particles. The envelope protein VSV-G myc 28-mediated transduction was also diminished by the anti-myc antibody.
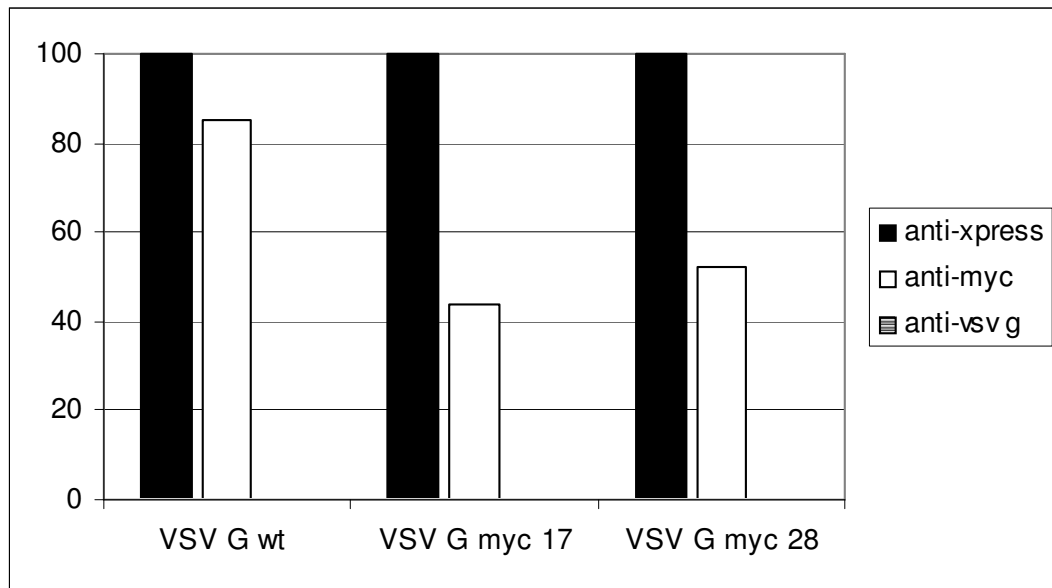
Figure 27. Transduction of HEK293T cells in the presence of anti-myc antibody.

HEK293T cells were transduced with retroviral particles pseudotyped with VSV-G wt, VSV-G myc 17 or VSV-G myc 28. Transduction was performed in the presence of 8µg/ml Polybrene (final concentration), and 1µg/ml of one of the following antibodies: anti-VSVG (neutralizing), anti-myc or anti-Xpress. Anti-Xpress antibody is from the same isotype as the anti-myc antibody and has no binding counterpart either on the viral particle or HEK293T cells. Black column: anti-Xpress antibody; white column: anti-myc antibody; striped column: anti- VSV-G antibody. Results from a representative experiment out of three are shown.

6.8. Effect of nanobeads on the transduction efficiency of myc-modified VSV-G expressing viral particles

The myc-modified retroviral particles can be captured by anti-myc coupled nanoparticles and targeted to PSCA-expressing cells when the nanoparticles are also conjugated to anti-PSCA antibodies. In order to analyze this approach and suggest targeted gene delivery method using modified VSV-G proteins, we used superparamagnetic nanoparticles with a diameter of 200nm and coated with a polysaccharide matrix. These nanoparticles were chemically coupled to monoclonal anti-myc and anti-PSCA antibodies. First of all, the nanobeads were analyzed for their ability to bind to PSCA on engineered and native PSCA-expressing cells. Next, the binding of nanobeads to the myc-modified viral particles was investigated.

6.8.1. anti-PSCA/anti-*myc* superparamagnetic nanobeads (NB)

The anti-PSCA- and anti-myc antibody-coupled magnetic beads can play a vital role in targeted transduction strategy. As bridging molecules, nanobeads must be able to bind PSCA-positive target cells and the myc-epitope of the modified VSV-G

on the virus particle simultaneously. Before scrutinizing the function of nanobeads as linker molecules, first sole interactions of antibodies with their respective targets must be studied.

6.8.2. Binding of anti-PSCA/anti-*myc* nanobeads onto PSCA-positive cells

The PSCA-negative and -positive cells were incubated with the nanobeads and the binding was detected with sheep anti-mouse Cy3 antibody recognizing the antibodies on the nanobeads, which are both of mouse origin. Cells lines tested included PSCA-negative HEK293wt cells, HEK293-PSCA cells engineered to express membrane anchored PSCA, and bladder carcinoma cell lines HT1376 and RT4, which natively express PSCA on their surfaces. Surface PSCA expression was confirmed for PSCA-positive cells by staining with anti-PSCA antibody 7F5 and anti-mouse IgG Cy3 under native conditions (Figure 28B). Specificity of the detection was demonstrated using isotype control as the primary antibody (Figure 28C). HEK293wt cells were devoid of any PSCA expression but HEK293-PSCA as well as RT4 and HT1376 expressed PSCA on the surface. In agreement with the PSCA expression, anti-PSCA/ anti-myc magnetic beads were able to bind only to PSCA-positive cells but not to PSCA-negative HEK293 wt (Figure 28A).
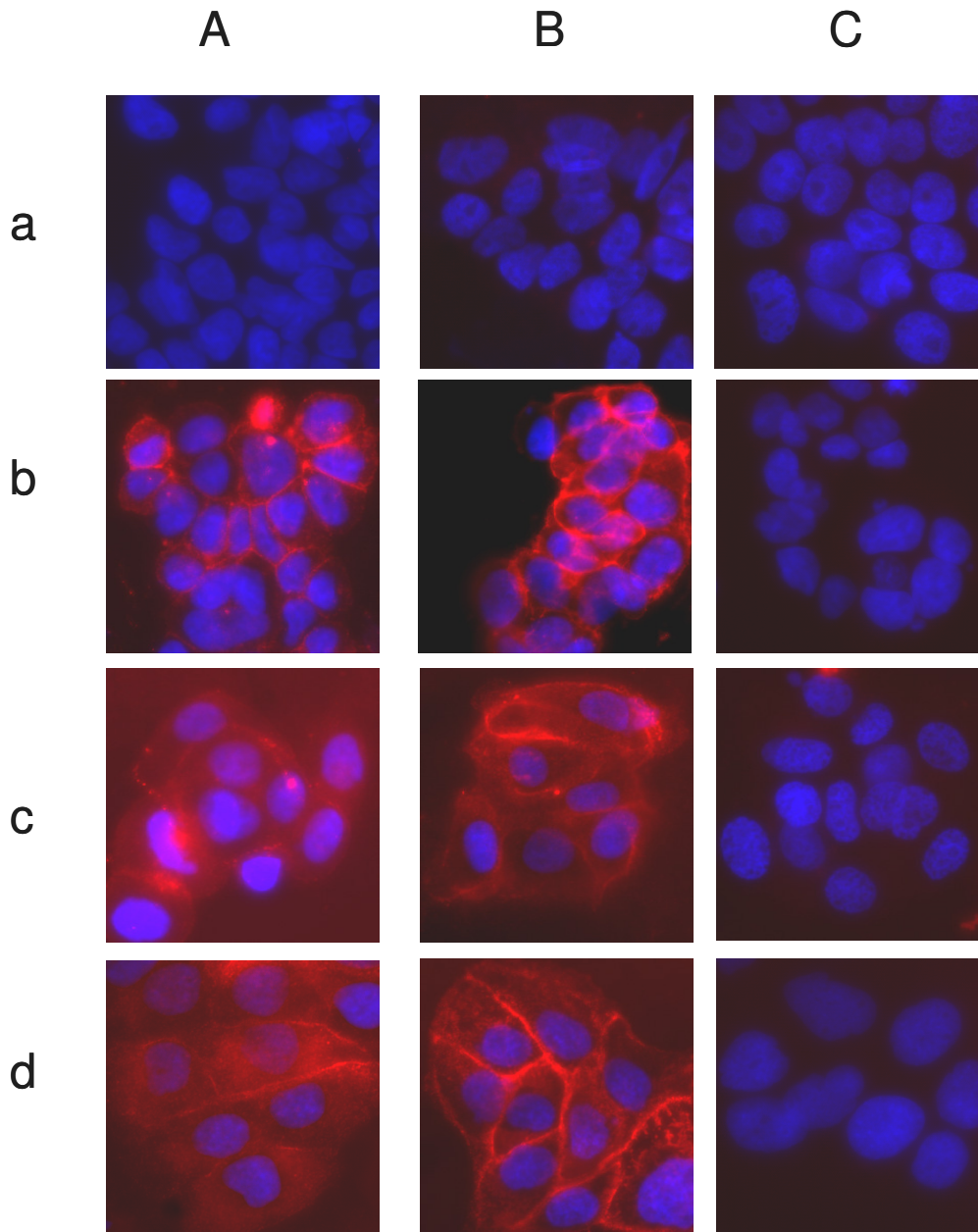
Figure 28. Binding of anti-PSCA and anti-myc antibody-coupled nanobeads onto PSCA-positive cells.

HEK293wt (a), HEK293-PSCA (b), HT1376 (c) and RT4 (d) cells were used to show A: binding of anti-PSCA/anti-myc magnetic beads to PSCA-positive cells after 240min incubation at 37 °C. The staining was performed with sheep anti-mouse IgG antibody coupled to Cy3. B: surface PSCA expression on native cells using anti-PSCA antibody 7F5 and sheep anti-mouse IgG-Cy3. C: the absence of non-specific binding using isotype-matched control antibody and sheep anti-mouse IgG-Cy3. HEK293wt cells (black) were confirmed to be PSCA-negative. Isotype control antibody was used as negative control (green).

6.8.3. Effect of anti-PSCA/ anti-*myc* nanobeads on cell survival

Gu *et al.* [172] and Saffran *et al.* [171] demonstrated that anti-PSCA antibodies induce apoptosis in the tumor cells. Therefore, we analyzed whether the anti-PSCA antibodies coupled to the nanobeads induce apoptosis on PSCA-negative and –positive cells. We analyzed the fraction of cells undergoing internucleosomal DNA-fragmentation by a SubG1 analysis. As illustrated in Figure 29 nanobeads did not induce apoptosis in either PSCA-negative or PSCA-positive cells.
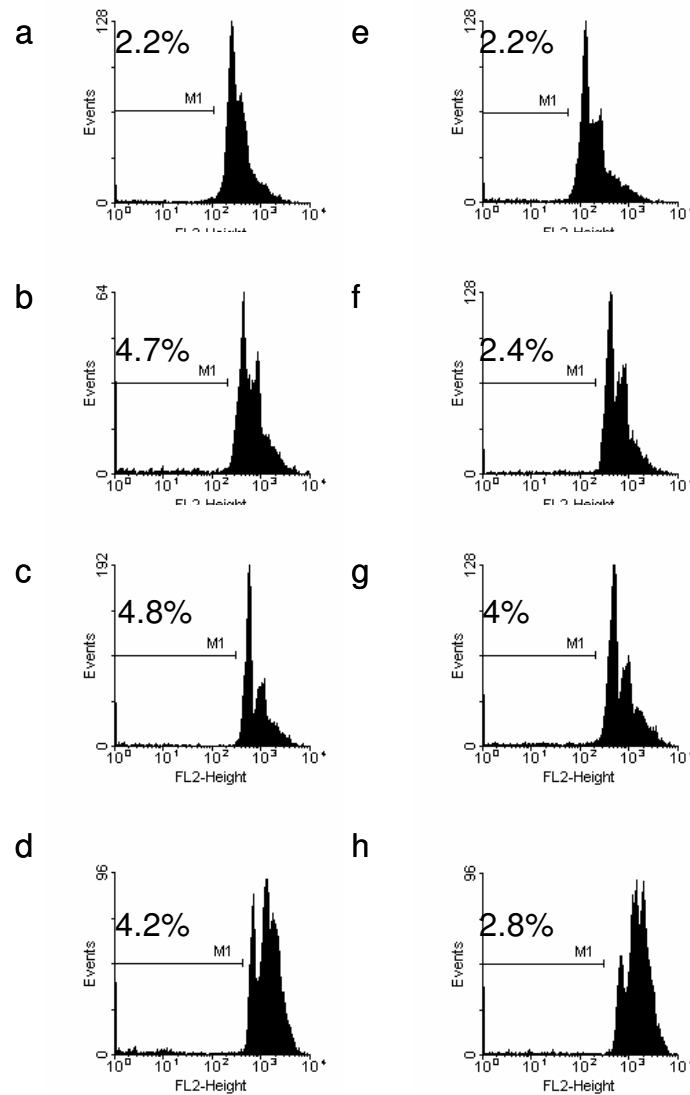

Figure 29. Effect of anti-PSCA/ anti-myc nanobeads on the survival of PSCA-negative and PSCA-positive cells.

PSCA-negative HEK293wt (a, e); and PSCA-positive cells HEK293-PSCA (b, f); RT4 (c, g); HT1376 (d, h) cells were analyzed. a-d: Cells were incubated with IgG1 isotype control antibody (control to the anti-PSCA and anti-myc antibodies bound to nanobeads). e-h: cells were incubated with anti-PSCA/ anti-myc nanobeads. DNA fragmentation was measure by propidium iodide staining. Apoptotic cells are indicated in the area M1 and the percentage of apoptotic cells are displayed on respective histogram.

6.8.4. Binding of anti-PSCA/ anti-*myc* nanobeads onto *myc*-modified retroviral particles

Since we revealed that the anti-PSCA/ anti-myc magnetic beads are able to bind PSCA-positive cells specifically, we analyzed in the next experiment the binding of the magnetic beads to the viral particles pseudotyped with myc-modified VSV-G proteins. The viral particles were harvested from packaging cells at 32°C and incubated with magnetic beads in an orbital shaker for 30min at 37°C. The mixture was then centrifuged at 14000 rpm at 4°C for 30min in a regular bench-top centrifuge. The pellet containing beads and virus bound to beads was used for SDS-PAGE and subsequent Western blotting. The associated virus was detected with the anti-p30 antibody (for the capsid protein of MLV) and the HRP-conjugated rabbit anti-goat IgG antibody (Figure 30). VSV wt-pseudotyped particles lacked the myc-epitope and therefore did not bind to the nanobeads. These particles were thus not precipitated into the pellet. On the other hand, the myc epitope-containing viral particles were detected as shown by the presence of ~30kDa band corresponding to the capsid protein. In conclusion, anti-myc/anti-PSCA nanobeads were capable of binding to the myc epitope and PSCA, separately.
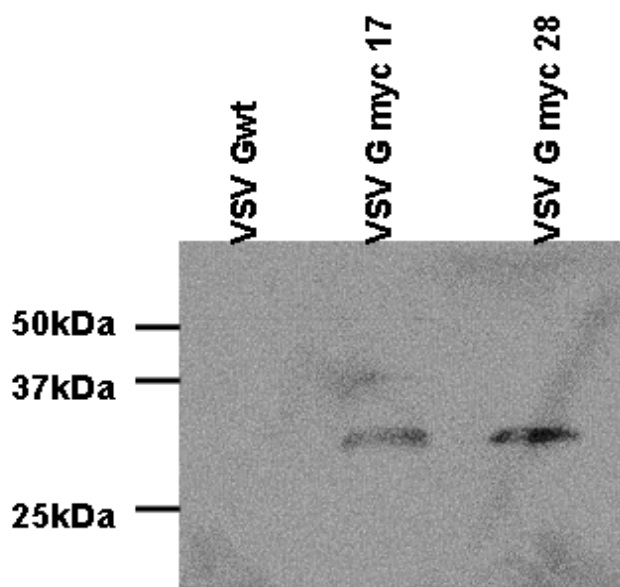

Figure 30. Binding of anti-PSCA / anti-myc nanobeads to myc-modified viral particles.

Supernatants containing viral particles were incubated with anti-PSCA / anti-myc nanobeads. The mixture was centrifuged to precipitate bead/virus complex. The pellet was analyzed by SDS-PAGE and western blot using anti-p30 serum and rabbit anti-goat IgG HRP antibody. The blot was developed with ECL Plus kit and visualization was performed with Fuji LAS 3000.

6.8.5. Effect of nanobeads on transduction with VSV-G wt-pseudotyped particles

To exclude any negative effects of the nanobeads on transduction efficiencies we mixed nanobeads to retroviral particles pseudotyped with wild-type VSV-G and transduced HEK293wt cells. For comparison we included non-treated particles. Figure 31 illustrates the mean transduction efficiencies of three experiments. The experiments revealed that the VSV-G wt mediated transduction efficiency was not influenced by the presence of nanobeads.
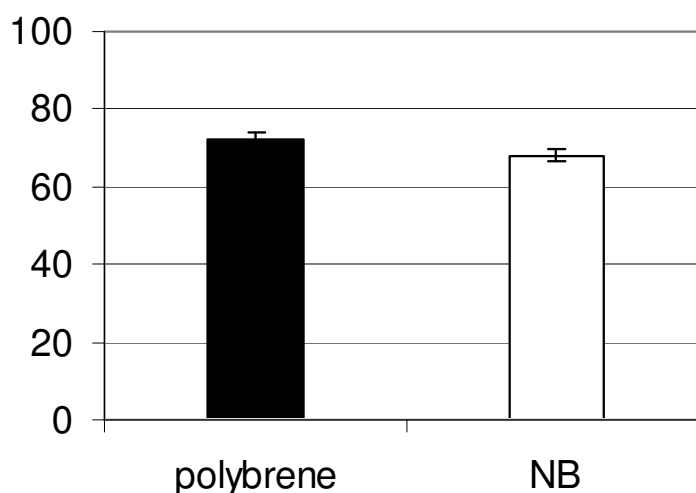

Figure 31. Transduction analysis with VSV-G wt-pseudotyped retroviral particles in the presence of nanobeads.

Retroviral particles pseudotyped with VSV-Gwt were used to transduce HEK293wt cells in the absence or in the presence of nanobeads (NB). Polybrene was added only in the absence of nanobeads.

6.8.6. Transduction with myc-modified viruses in the presence of nanobeads

In the next experiment we sought to investigate whether the myc-modified retroviral particles were still infectious when bound to nanobeads. Virus production was performed at 37°C and the viral particles were concentrated 100-fold by ultracentrifugation. Virus titer was determined on HEK293wt cells to be 3×10^7 for VSVG wt–pseudotyped particles and 3×10^6 for VSV-G myc 17-pseudotyped particles. We then assumed that at least five myc-modified viral particles can bind to a single nanoparticle without completely covering the surface. These complexes made of 5 viruses and 1 nanobead act as a single virus because each such complex can get access to a single target cell. Therefore in calculating the multiplicity of infection (MOI) one complex was considered as a single virus and MOI of 3.4 was used for VSV-G myc17 particles. In case of VSV-G wt–

pseudotyped retroviral particles the amount of virus particles was kept constant. Since these viral particles do not bind to the nanobeads MOI was 17. As depicted in Figure 32, both wild-type and myc-modified VSV-G expressing particles were infectious on PSCA-negative and –positive cells. However there was no enhanced transduction on PSCA-positive cells.

In a separate experiment we demonstrated the internalization of nanobeads selectively by PSCA-positive cells transduced with MLV$^{(G-myc\ 17)}$ particles. We used MLV$^{(G-wt)}$ and MLV$^{(G-myc\ 17)}$ particles for transduction in the excess of nanobeads. The transduced cells were cultivated for a week, in which the cells were splitted and washed intensively with PBS. Then the cells were re-suspended in PBS and dried on Whatman paper. The cells transduced with the MLV$^{(G-wt)}$ particles were not visible as well as the HEK293 cells transduced MLV$^{(G-myc\ 17)}$. However, HEK293-PSCA cells transduced with MLV$^{(G-myc\ 17)}$ were detectable as brown dots, which was due to the presence of brown-colored nanobeads (Figure 33).
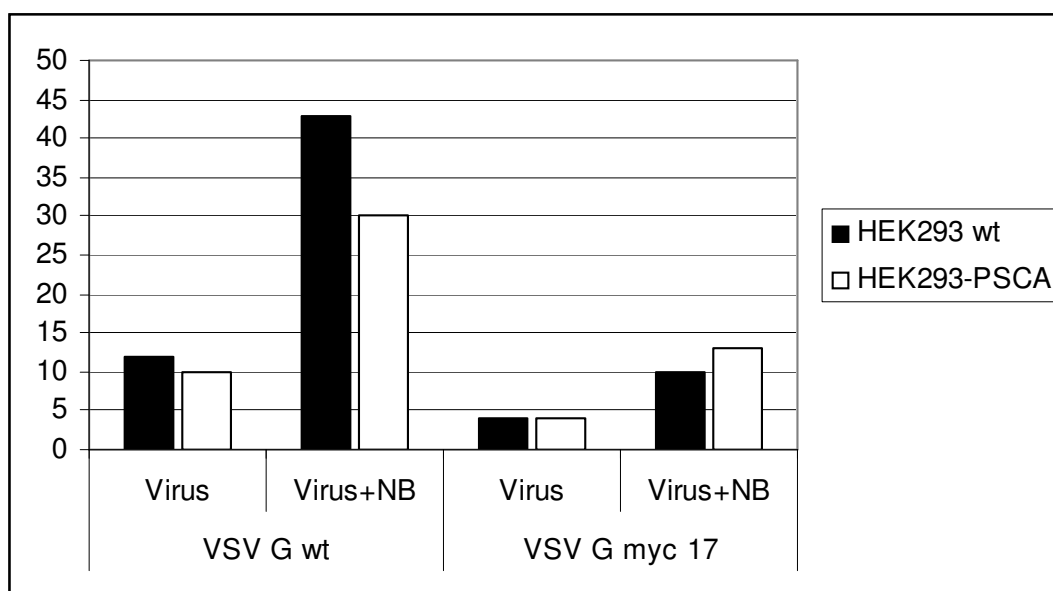

Figure 32. Transduction of PSCA-positive cells with myc-modified viral particles in the presence of nanobeads.

Viral particles concentrated 100x with ultracentrifugation were used for transduction. Transduction was performed either only with viral particles (Virus) or using viral particles incubated with the nanobeads (Virus +NB). The number of viral particles was kept constant therefore MOI was either 3.4, except for c and d in the case of MLV$^{(VSV-G\ wt)}$ transduction. PSCA-negative HEK293wt (Black) and PSCA-positive HEK293-PSCA (white) cells were transduced.
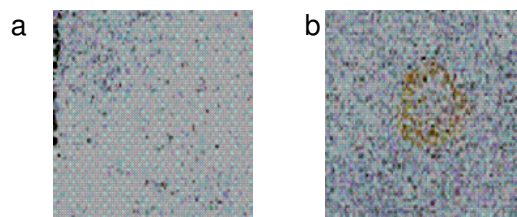
Figure 33. Internalization of nanobead:virus complexes by PSCA-positive cells.

HEK293 (a) and HEK293-PSCA (b) cells were transduced with MLV$^{(G-myc\ 17)}$ particles in the presence of nanoparticles and cultured for a week. Later the cells were harvested in PBS and aliquots were dried on Whatman paper.

Recently, Chan *et al.* [155] reported concentration of VSV-G wt pseudotyped lentiviral vectors, which gained biotinylated membrane from the packaging cells, via streptavidin-coated magnetic beads. In this study authors purified the lentiviral particles in the excess of nanobeads. We have repeated the transduction experiments, and this time used overload of nanobeads. The viral particles were mixed with the nanobeads and were used to transduce PSCA-positive and-negative cells without prior concentration or purification. As depicted in Figure 34, the presence of nanobeads significantly inhibited the transduction with myc-modified VSV-pseudotyped particles on both PSCA-positive and –negative cells.
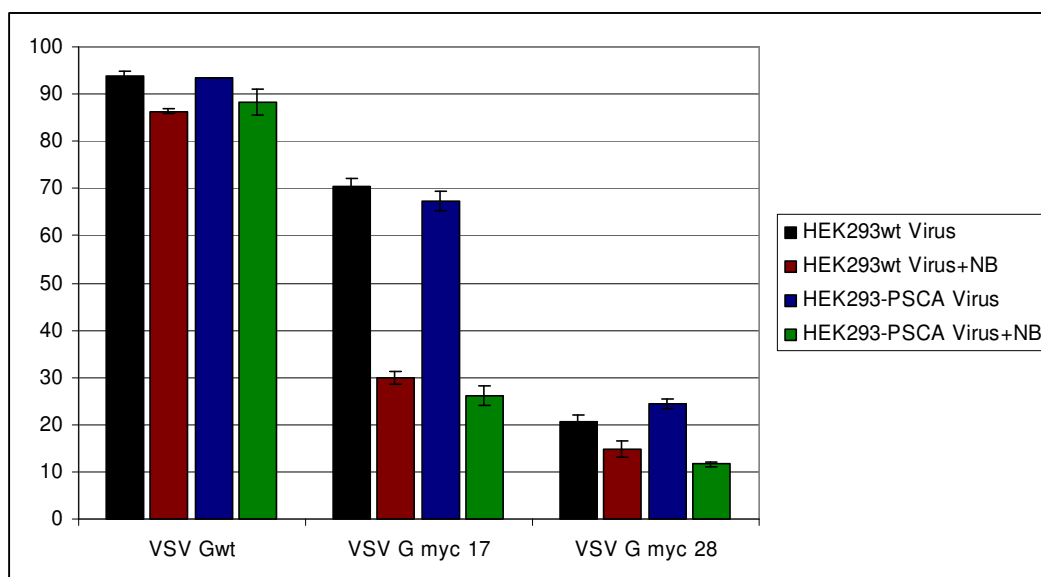

Figure 34. Transduction efficiency of myc-modified retroviral particles in the presence of excess nanobeads.

The retroviral particles were used alone (black and blue) or in the excess of nanobeads to transduce HEK293wt (Black and red) and HEK293-PSCA (blue and green) cells.

We then purified myc-modified viral particles via incubation on a magnet. The viral particles were concentrated by ultracentrifugation (100fold) and titers were determined. Both VSV-Gwt and VSV-G myc 17-pseudotyped DsRed-expressing particles were incubated with 2fold excess of nanobeads and the nanobead: particle complexes were precipitated on a magnet for 1hr. the precipitate and the supernatant parts were used to transfected a mixed culture of PSCA-positive and –negative cells. For this experiment we generated PSCA-positive EGFP-expressing cells by transient transfection of HEK293 cells with pRevCMV_PSCA_IRES2_EGFP vector. VSV-G wt-expressing particles were found to be only in supernatant but not in the precipitate (Figure 35). In case of MLV$^{(G-myc\ 17)}$ particles the transduction efficiency with the supernatant was the same as in the mock-transduced cells (Fig. 36e; transduced with medium from envelope deficient packaging). Although the viral titers were very low, we observed an increase in the transduction efficiency on PSCA-positive cells with the precipitate containing VSV-G myc 17-particles and nanobeads. We also confirmed these results by confocal laser scanning microscopy. The wild type VSV-G-containing particles infected both PSCA-positive and –negative cells (Figure 36A). However, the purified MLV $^{VSV\ G\ myc\ 17}$ particles showed a tendency to transduce PSCA-positive cells (Figure 36B).

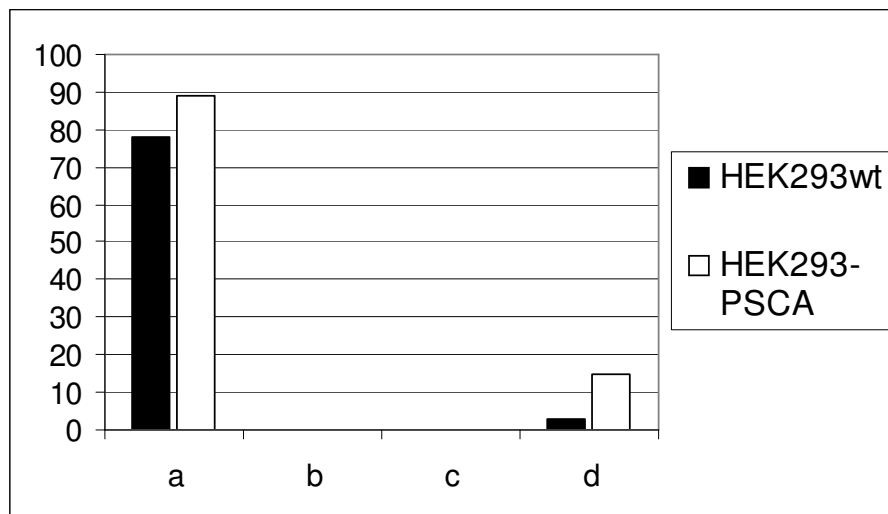**Figure 35. Enhanced transduction of PSCA-positive cells with MLV$^{(G-myc\ 17)}$ particles purified with nanobeads.**

MLV$^{(G-wt)}$ (a, b) and MLV$^{(G-myc\ 17)}$ particles were incubated with nanobeads and particles bound to the nanobeads were precipitated on magnet. The supernatant from the purification (a, c) and the precipitate (b, d) were used to transduce HEK293 (Black column) and HEK293-PSCA (striped column) cells.
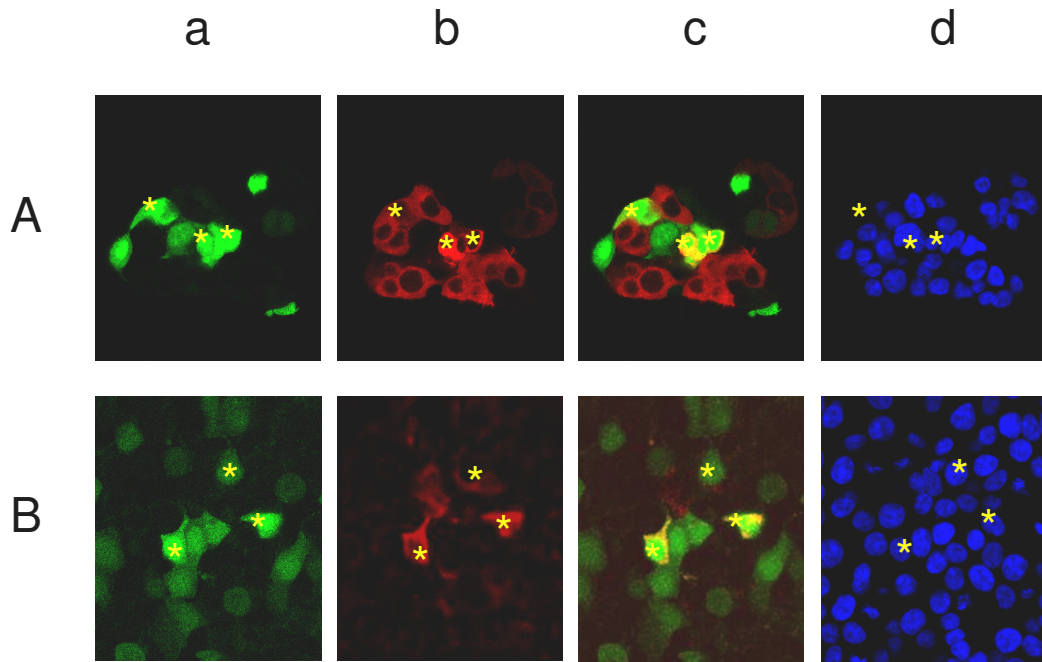
Figure 36. Nanobead mediated-transduction of PSCA-positive cells with MLV(G-myc 17) particles.

Retroviral particles encoding for DsRed were produced with (A) VSV-G wt or (B) VSV-G myc 17 envelope protein. PSCA-positive EGFP encoding cells and PSCA-negative cells were transduced. (a): PSCA-positive cells expressing EGFP; (b): DsRed expressing transduced cells: (c): overlay of "a" and "b"; (d): DNA staining with Hoechst 33342. Stars indicate PSCA-positive transduced cells.

7.   DISCUSSION

VSV-G is among the most commonly used envelope proteins for pseudotyping viruses [94,116] . VSV-G –pseudotyped MoMuLV vectors were shown to be highly stable and capable of infecting diverse cell types ranging from fish to mammals [94]. Retroviral particles containing VSV-G as envelope protein can be produced at high titers. All these characteristics indicate VSV-G as a useful tool for gene delivery purposes. However an anti-tumor gene therapy requires specificity to the target cell type. Therefore it is necessary to identify sequences in VSV-G which may tolerate modification and mutations and may be used for altering virus target tropism.

In this project the aim was to generate modified VSV-G proteins and to evaluate their utility in targeted gene therapy. The evaluation was performed in six steps. First the expression of mutant protein in transfected cells was shown. Second the proteins were analyzed for the intracellular transport to the plasma membrane in transfected cells. Next the proteins, which were transported to the cell surface, were subjected to fusion assay, where the fusion of viral envelope with the endosomal vesicle membrane was simulated. Fourth step was the incorporation of mutant VSV-G proteins into viral particles, which was shown by Western blot analysis of supernatants from the packaging cells. Then infectivity of the viral particles pseudotyped with mutant proteins was examined. Last but not least, using nanoparticles the feasibility of the mutant VSV-G-pseudotyped viral particles for targeted gene delivery was assessed.

7.1.   Generation of modified VSV-G proteins

7.1.1. Generation of scFv anti-PSCA / VSV-G fusion protein

We have started this project with the generation of a fusion protein that consisted of a single chain antibody fragment against the tumor-associated antigen PSCA and VSV-G. ScFv anti-PSCA possesses the same binding specificity as the parental anti-PSCA antibody. ScFv molecules have only one binding part for their antigens and therefore have a lower binding force compared to the parental antibodies. ScFv anti-PSCA was fused N-terminally to VSV-G. Four different fusion proteins were cloned. Two of the proteins contained full-length VSV-G whereas the other two contained N-terminally truncated VSV-G proteins (Figure 10). All four mutant proteins failed to be transported to the cell membrane (Figure 12A). Normal cultivation of cell lines takes place at 37°C, at which also the transfection experiments were performed. However, there are examples of mutant VSV-G proteins whose surface expression is dependent on the temperature. These so-called temperature-sensitive mutants are misfolded at the restrictive temperature 37°C but this can be rescued when the temperature is lowered. None

of the scFv anti-PSCA / VSV-G fusion proteins was transported to the plasma membrane at 37°C and this failure in transport could not be rescued by lowering the incubation temperature to 32°C (Figure 12B).

A single-chain antibody fragment has a molecular weight around 30kDa. Probably linking of such a big protein to the VSV-G was destructive to the protein folding. It is known that the only correctly folded trimers can leave the ER and be transported to the Golgi where post-translational modifications are processed [124]. In 2006 Dreja *et al.* [149] inserted a scFv against human MHC-I and demonstrated the successful incorporation of the fusion protein into lentiviral particles. The authors performed the fusion also on the N-terminus of the mature VSV-G protein and although we have similar constructs (the two fusion proteins with full length VSV-G) our results were rather different. The differences between the fusion proteins this study and those published by the authors are in the linker sequence and the leader peptide. The former may play a role in independent folding of both proteins allowing the correct conformation for each. The latter should not be the decisive factor for the failure of transport since the leader sequence used in our constructs is widely used in mammalian expression vectors for effective secretion of proteins.

7.1.2. Generation of myc epitope modified VSV-G proteins

The fusion of the scFv to the VSV-G protein resulted in a retention of the protein in the ER. Therefore we decided to modify VSV-G with a smaller sequence, which later can be used for targeting. VSV-G is known to be intolerant even to small epitope insertions or single amino acid substitutions [126,129,146,178]. Therefore, we compared the G protein sequences of VSV mutants and natural isolates (Table 10). VSV-G protein has shown to be accumulate mutations also in antigenic epitopes [175]. From the comparison of six VSV strains it was possible to deduce four regions for epitope insertion (Table 11). Additionally the N-terminal part of the mature protein, namely the amino acid number 17 in the precursor protein, and another position at the N-terminus (amino acid 28) were included. All of the myc-epitope modified VSV-G proteins were expressed in transfected cells (Figure 13) but only two of the myc-modified VSV-G proteins were transported to the plasma membrane (Figure 14). Moreover, a third mutant displayed a temperature-sensitive phenotype. Here, the intracellular transport could be rescued by lowering the incubation temperature to 32°C (Figure 14). The other two mutants most probably aggregated in the ER and were only detected in the perinuclear regions of permeabilized cells. The mutants, which were transported to the cell membrane, also exposed the myc epitope (Figure 15). During the completion of this thesis work Roche *et al.* succeeded in the elucidation of the crystal structure of the low-pH and the pre-fusion forms of the VSV-G protein [2,179]. This new information now enables a better understanding of the characteristics of our VSV-G mutants.

The low-pH crystal structure of VSV-G revealed four distinct domains (Figure 37). Domain I is composed of two segments, residues 1 to 17 and residues 310 to 383. Domain II is involved in trimerization of the top of the molecule and is made up of the residues 18 to 35, 259 to 309 and 384 to 405. Domain III, which consists of the segments 36 to 50 and 181 to 258, is inserted into domain II. Domain III has the Pleckstrin homology (PH) domain fold. The only single-segmented domain, the domain IV, covers the residues 51 to 181. It is the fusion domain of the molecule and makes the stem part.
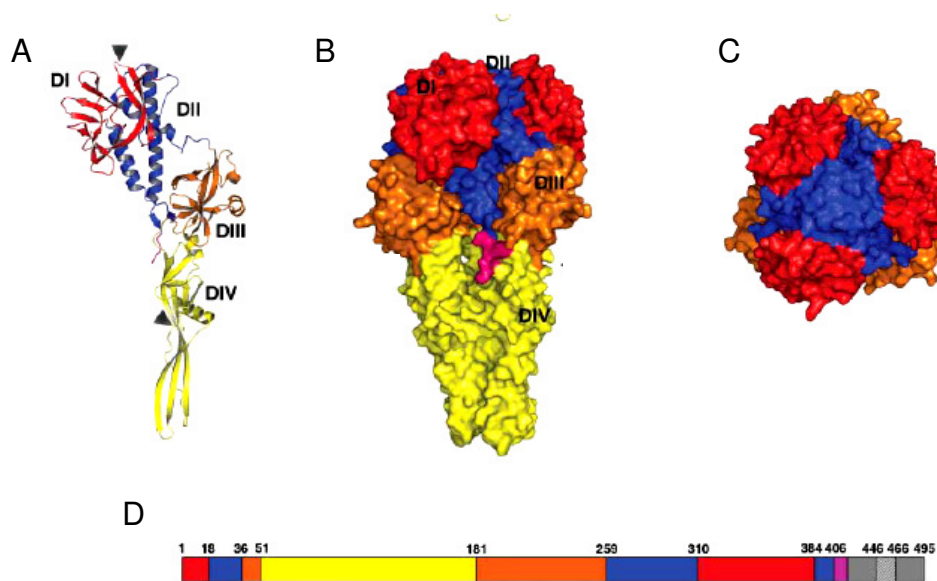

Figure 37. Domain architecture of the VSV-G low-pH form

A: Domain organization in VSV-G monomer. B: VSV-G trimer side view. C: VSV-G trimer viewed from the top. D: Regions forming the four domains in VSVG, colored scheme was used for also A-C. Triangles indicate the glycosylation sites.

The c-myc epitope insertions were performed at five different positions in the G protein of VSV Indiana (Table 11, Figure 38). The modified VSV-G proteins were designated according to the number of amino acid in the mature VSV-G protein after which the insertion is made. The first insertion was made after the signal sequence at position 17. VSV-G myc 17 protein showed intracellular and surface staining patterns similar to wild type protein (Figure 13 and Figure 14), which fits pretty well the structural data, since domain I was reported to be located on the top of the trimer and exposed to the exterior. Amino acid 17 was newly reported to tolerate 13 amino acid long epitope and the mutant proteins were incorporated into viral particles [150]. Furthermore, in the same study authors could purify retroviral particles pseudotyped VSV-G modified at position 17 via Nickel-Nitriltriacetic acid (Ni-NTA). We could also demonstrate myc epitope insertion at position 17 gave rise to a transport- and fusion-competent mutant (Figure 19). For wild type VSV-G optimum pH range is between 5.6 to 6.0 [124]. VSV-G myc 17 has a lower

fusogenic activity than VSV-G wt as can be seen from the number and size of the syncytia. More to the point, VSV-G myc 17 has a lower optimum pH and a smaller pH range for fusion. While VSV-G wt induced membrane fusion at pH 6.0, syncytium formation starts with VSV-G myc 17 only at pH 5.5 (Table 14). Thus, the 10fold lower titer observed with the MLV[(G-myc 17)] particles is probably due to inefficient fusion. The myc epitope insertion at position 17 did not alter the natural tropism of VSV-G as seen by the infection of HEK293wt cell. However, when the infection was performed in the presence of anti-myc antibodies, VSV-G myc 17-mediated transduction efficiency was significantly impaired (Figure 27). This suggests that a proper linker molecule, which would connect the myc epitope and a cellular target may benefit from the reduction of wild type specificity. At this point we decided to generate a single-chain antibody fragment against myc epitope to use as the linking molecule, such as a diabody, between the modified viral particles and the target cells. Unfortunately, we could not obtain scFv molecules with binding affinity to myc epitope from the available hybridoma clone (CT9 B7.3) (data not shown).
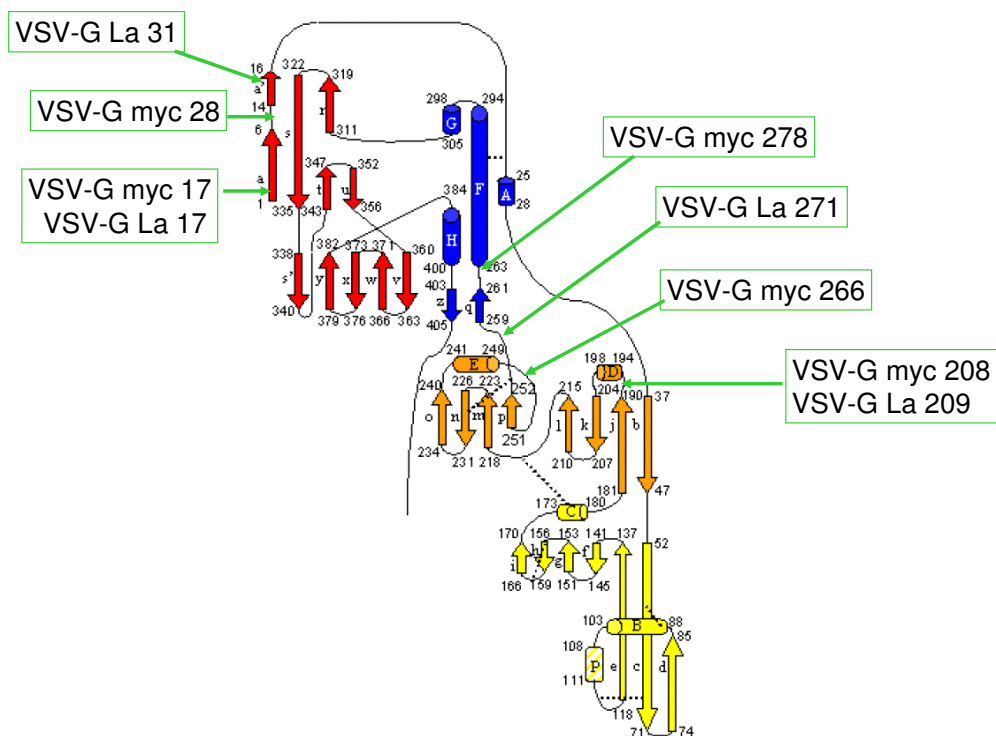

Figure 38. Epitope insertion positions in the ectodomain of VSV-G

Amino acid numbering corresponds to the mature peptide after the cleavage of 16 amino acid-long signal peptide in ER. Secondary structures are: Arrows show ß strands; cylinders indicate helices; and dotter lines indicate the disulfide bridges. Picture adopted from Roche *et al.* [179].

The second insertion was performed at position 28 also in domain I, between the β strands a and a'. This modified VSV-G proteins has a temperature-sensitive phenotype in which it acts like wild type VSV-G at a permissive temperature (Figure 14). The VSV-G myc 28 also exposed the myc epitope on the cell membrane in transfected cells and can be used to package retroviral particles (Figure 15). However, at restrictive temperature (37°C) VSV-G myc 28 is detected only in perinuclear compartments. It has been shown that epitope insertion at position 24 [147] also exhibited temperature-sensitive phenotype. In the interpretation of the domains in the VSV-G, Roche *et al.* [179] described that the ß strands a and a' is wrapped by the three antiparallel ß sheets forming the domain I. since position 28 corresponds to the region prior to ß strand a', it is highly probable that such an insertion interferes with the correct folding. At the permissive temperature VSV-G myc 28 was fusogenic albeit not as efficient as VSV-Gwt or VSV-G myc 17 (Figure 19). VSV-G myc 28-mediated membrane fusion resulted in small syncytia and fusion was observed only at pH 5.5 (Table 14).

Next, two insertions at positions 208 and 266 were made. Both positions reside in the domain III. Domain III contains a typical Pleckstrin Homology (PH) domain. PH domain-containing proteins can bind to phosphatidylinositol lipids in the membranes, which suggest that this domain may play an important role in interactions with the membrane [180,181]. In the low-pH conformation of VSV-G domain III is located in the interior of domain II, which renders this domain inflexible in accommodation of additional sequences. This may explain why the insertion mutants at positions 208 and 266 are not transported beyond the perinuclear areas (Figure 13 and Figure 14). Furthermore, in the mature protein there is a disulfide bridge between residues C^{219} and C^{253} and the insertion at position 266 (in precursor protein; in the mature protein position 250) may inhibit this interaction. This position was recently shown to be intolerant even to smaller epitope (six amino acid long) by Schlehuber and Rose [147].

The last myc epitope insertion was made at position 278. This mutant displayed wild type surface expression characteristics (Figure 14). Also the myc epitope was readily detectable on natively stained cells (Fig.16). However, this mutant failed to induce any membrane fusion (Figure 19). Position 278 is located in the beginning of helix F in the domain II, which is responsible for the trimerization of the protein. During the conformational changes in fusion helix F undergoes major refolding and re-organization (Figure 39). These re-positioning events also include amino acid residues that are very close to the insertion at position 278 (Figure 39). Therefore it is possible that the insertion does not affect the initial folding and transport of the protein to the cell membrane, but at low-pH this insertion inhibits the necessary conformational changes.

In conclusion, we have identified two epitope insertion sites in the VSV-G protein, which are successfully incorporated into retroviral particles. The myc epitope enabled the purification of MLV[(G-myc 17)], and MLV[(G-myc 28)] particles from the culture medium (Figure 24). This suggests an alternative to the recently published purification via the His-tag [150]. Moreover, we demonstrated with anti-myc antibody selective inhibition of MLV[(G-myc 17)], and MLV[(G-myc 28)].
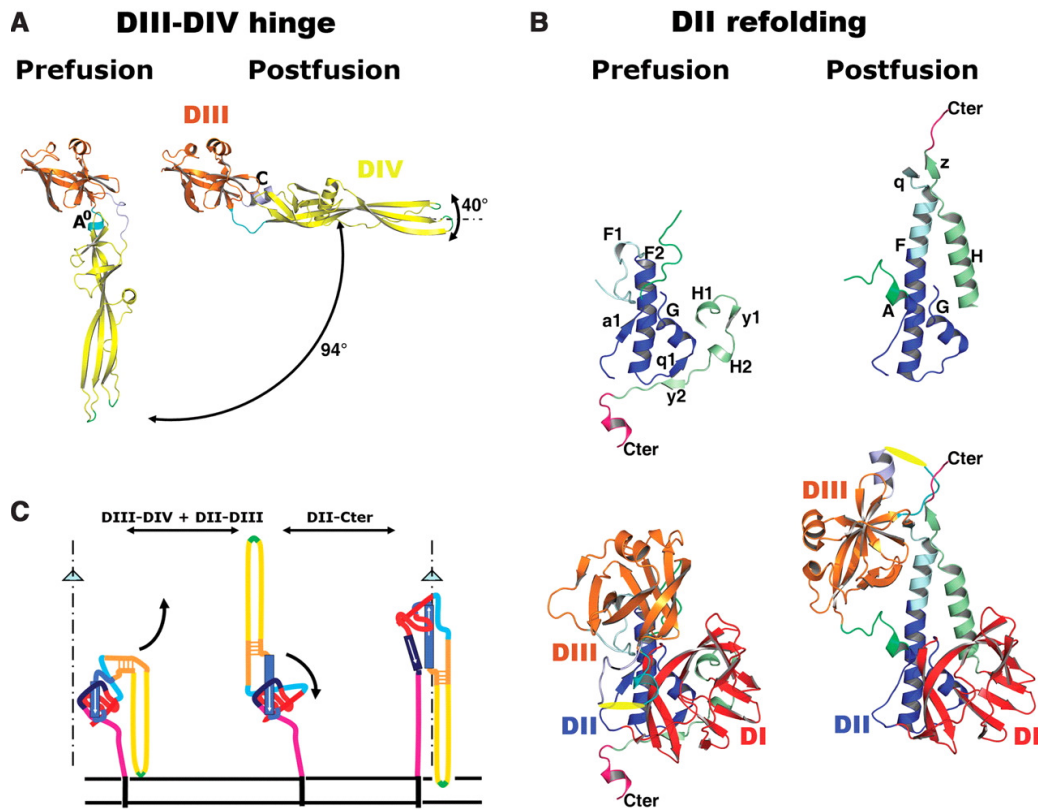

Figure 39. Conformational changes in the ectodomain of VSV-G protein during low pH-induced fusion [2].

A: The pre- and post-fusion conformation of the hinge region between the domains III and IV. B: Refolding of domain II during the fusion. Description of domains. C: Reorganization of domains in the VSV-G protein and their relative positions in the pre- and post-fusion states [2], domains were colored as in Figure 37.

7.1.3. Generation of La epitope modified VSV-G proteins

The lack of functional scFv against the myc epitope, which can be used for generation of bispecific diabodies, we included the La epitope into our analyses. In our institute, scFv molecules against La epitope are already available. Insertion of La epitope into the ectodomain of VSV-G was performed at four different positions, close to myc epitope insertion positions (Table 11). The insertions were localized

to three domains in the protein. Two of the La mutants were transported to the cell membrane but only one exposed the epitope (Figure 16, Figure 17 and Figure 18). Insertion at position 17 (in precursor protein) locates to domain I. This mutant was only detectable in permeabilized cells at 37°C and was not transported to the cell surface. The low level of expression and the failure in transport to the plasma membrane with this La mutant implies the importance of epitope length that can be tolerated at a certain position.

The second La epitope insertion was made at position 31, which corresponds to position 17 in the mature protein and lies in domain II (Figure 38). This mutation is located in the N-terminal part of the first segment that belongs to domain II. Although in the crystal structure this position seems to be in a relatively free position, it may have interfered with correct folding and subsequent trimerization of VSV-G.

The last two insertions were performed positions residing in domain III. Mutants with La epitope at positions 209 and 271 were produced by the transfected cells though at lower levels than VSV-G wt (Figure 16). And interestingly both mutant proteins were detected with anti-VSV-G antibody recognizing the external epitope although this domain is hidden in the domain II and insertion of the small myc epitope in very close positions interfered with the transport (Figure 17). A possible explanation may be the flexibility gained by the insertion of a longer epitope. The myc epitope may introduce a stretch of amino acids which sterically hinders correct folding, but it is possible that the two times longer La epitope gave enough flexibility by looping out and leaving the domain more or less intact. This is also supported by the detection of La epitope in native staining on VSV-G La 271-transfected cells (Figure 18). It is likely that the location of La epitope relative to the insertion position, which has to form a loop, is also important since VSV-G La 209 did not expose the epitope. These two mutations also confirm the important role of the introduced epitope length.

Finally, the fusion activity of La-modified VSV-G protein, which was expressed on the cell surface and exposed La epitope, was analyzed (Figure 20). In the fusion assay, pH values between 5.0 and 7.5 were tested but VSV-G La 271 failed to induce any fusion. This position is close to the ß-sheet "q" which re-positions itself in the last steps of conformational changes during fusion and may therefore hinder the re-organization necessary to achieve a fusion active state.

7.1.4. Conclusion of mutational analysis of VSV-G

VSV-G protein production is tightly controlled and therefore the protein does not contain many permissive sites for modifications. VSV-G still possesses several advantages as a pseudotyping envelope protein over other viral proteins. However the main drawback, the ubiquitous infection mediated by VSV-G must be restricted

to the target cells in order to exploit the potential of VSV-G. Therefore ligand-modification of VSV-G is an interesting and exciting area. Unfortunately the intensive intramolecular interactions set hurdles to the selection of the insertion permissive regions. Together with the recently published crystal structures of pre- and post-fusion conformations of VSV-G our results point out two suitable sites for targeting of VSV-G pseudotyped particles to a defined cell type. As it has been shown also by other groups, the N-terminal region of VSV-G is permissive to epitope insertions [147,149,150]. It is interesting that within a very small region of amino acid residues 24-28 in the precursor protein, two different populations of mutant VSV-G proteins were obtained. The first population had the wild type characteristics and was transported to the membrane at 37°C, whereas the second population displayed temperature-sensitive phenotype that can be rescued at permissive temperature. This underscores the importance of precise location of the epitope inserted into VSV-G.

A major problem with ligand-modified VSV-G-pseudotyped particles is the inefficient transduction. This is mainly due to the reduced fusion capacity of the mutant VSV-G proteins. This appears to be an ordinary problem of viral particles. Tai *et al.* overcame this problem with ecotropic and amphotropic MLV vectors modified by insertion of ZZ domain in the envelope protein by co-expressing the wild type envelope protein [108]. In case of VSV-G this strategy may result in the loss of ligand-specificity and therefore must be considered with care. And yet it will be interesting to see the capacity of fusion-defective mutant VSV-G myc 278 to target retroviral particles in the presence of a fusion-competent envelope.

In conclusion, the two positions we have chosen (positions 17 and 28) regarding the sequence difference between VSV strains appear plausible for modifications studies also according to the crystal structure elucidated in 2006. Since the VSV-G undergoes an extensive series of re-folding and domain organizations, these two positions, which locate to the free N-terminal part of the protein prove to be suitable modification sites.

7.1.5. Outlook into nanotechnology

Although we have functional scFv against the La epitope, none of our mutants induced fusion. Thus, we have turned our attention to the myc mutants and decided to analyze them for regarding the purification of viral particles and targeted transduction of PSCA-positive cells using nanoparticles coupled to antibodies.

Nanotechnology has long being used in gene delivery by gene bombarding. The advancements in bioengineering also allowed modification of this technology to make it more specific, in which ligand molecules were incorporated into the matrix of nanoparticles. VSV-G proteins modified at amino acid positions 17 and 28 are

suitable targets for ligand-directed gene delivery. In order to gain a standpoint on the benefits of these mutants nanoparticles chemically coupled to anti-PSCA and anti-myc antibodies were used. The idea behind is to capture myc-modified retroviral particles via the anti-myc antibodies and to connect them to PSCA-expressing target cells using anti-PSCA antibodies. For this purpose, first of all it is necessary to demonstrate binding of both moieties to their respective ligand. This was achieved for PSCA by incubating PSCA-positive and PSCA-negative cells with nanobeads and then detecting the antibodies coupled to nanobeads with a secondary anti-mouse antibody (Figure 28). After showing the binding to the target cells, we evaluated the effect of nanobeads on the survival of cells. In an apoptosis assay we confirmed that upon binding and internalization nanobeads do not induce apoptosis of PSCA-positive and of PSCA-negative cells (Figure 29).

Next, binding of nanobeads to modified retroviral particles was analyzed with a simple capture assay. MLV$^{(G-wt)}$, MLV$^{(G-myc\ 17)}$, and MLV$^{(G-myc\ 28)}$ particles were incubated in the presence of nanobeads and the complex was then precipitated. In Western blot analysis we could show precipitation of myc-modified particles, which were detected by using an anti-MLV capsid serum (Figure 30). As expected MLV$^{(G-wt)}$ particles were not precipitated.

MLV$^{(G-wt)}$ particles were used for transduction of HEK293wt cells in the presence or absence of nanobeads and as expected transduction efficiencies were comparable (Figure 31). Thus nanobeads exert no unspecific adverse effect on the transduction when viral particles and the target cells display no binding partner. In case of transduction of PSCA-positive cells (Figure 32) a small decrease in efficiency was observed with MLV$^{(G-wt)}$ particles in the presence of nanobeads, which may due to the binding of nanobeads onto PSCA-positive cells and reduce the available surface area that can interact with the viral particles. When MLV$^{(G-myc\ 17)}$ particles were used for transduction in the excess of nanobeads, we observed an inhibition similar to that seen with anti-myc antibody (Figure 34). And there was no significant increase in the specificity of transduction was observed when PSCA-positive cells were used (only 4% increase). These results contradict the outcomes of a recent report by Chan *et al.* [155]. They have demonstrated an effective concentration and purification of biotinylated lentiviral vector via streptavidin-coated nanoparticles where the nanoparticles were at least 10^3 in excess of the viral particles. We assume that an overload of nanoparticles will cover the surface of the viral particles. Such masked particles would never get in contact to the cellular membranes (Figure 40). Therefore, the viral envelope is not capable of undergoing the structural changes necessary for the fusion.

And yet the results are encouraging because by optimizing the virus-capture conditions for VSV-G myc 17, targeted transduction of PSCA-positive cells can be achieved. It may be worthwhile to titrate more precisely the number of viral particles that can be bound to a single nanobead to enable effective binding onto

PSCA-positive cells via the anti-PSCA antibody. Moreover, as shown by Capra and Ednumdson [182], antibody molecules are very small in size compared to the viral particles and the nanobeads (Figure 41). When the viral particle binds to the nanobead via antibody recognizing the modified envelope protein, the second antibody recognizing the target antigen on the tumor cells may not be able to contact the TAA. Thus it may also be useful to anchor target antigen-binding antibodies onto the nanobeads via bigger hinge regions to allow better projection of these molecules towards the target cells.
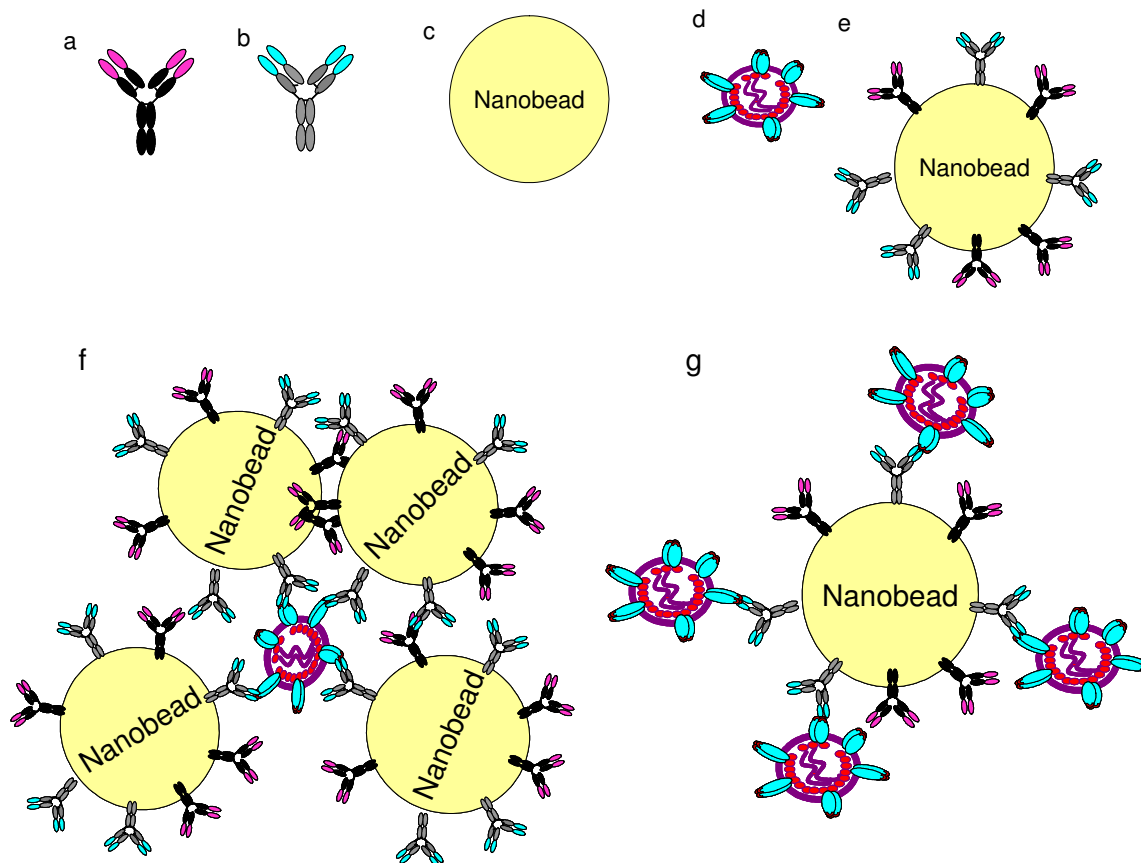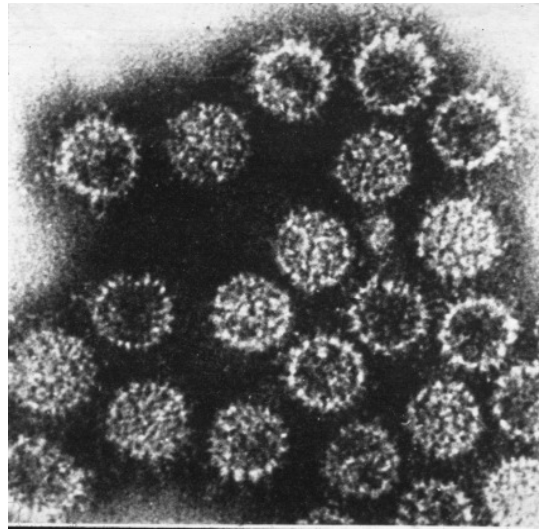

Figure 40. Complex formation between the nanobeads and the viral particles.

a: anti-PSCA antibody; b: anti-myc antibody; c: the nanobead; d: the modified viral particle; e: nanobead coupled to anti-myc and anti-PSCA antibodies; f: complex formation in the excess of nanobeads; g: complex formation in the excess of viral particles.
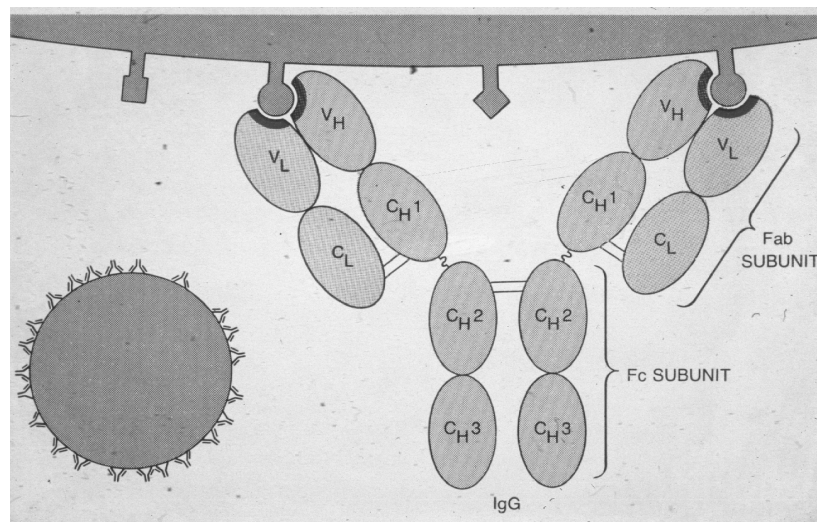
A

B

Figure 41. Antibody molecules bound to a virus.

A: Electron microscope picture of antibody molecules bound to viral particles. B. Illustration of antibody molecules bound to a viral particle regarding the size [182]

Another approach to use the epitope-modified VSV-G mutants is to generate bispecific diabodies. Diabodies are antibody fragments composed of two single-chain antibody fragments. It is possible to generate diabodies which bind with one scFv part to the epitope on the viral envelope protein, and with the other scFv to the tumor associated antigen on the tumor cells (Figure 42). This allows direct targeting of the viral particle. Moreover, diabodies lack the Fc region of the parental antibody and therefore may be particularly useful in clinical applications since they avoid the host immune response against the Fc-portion.
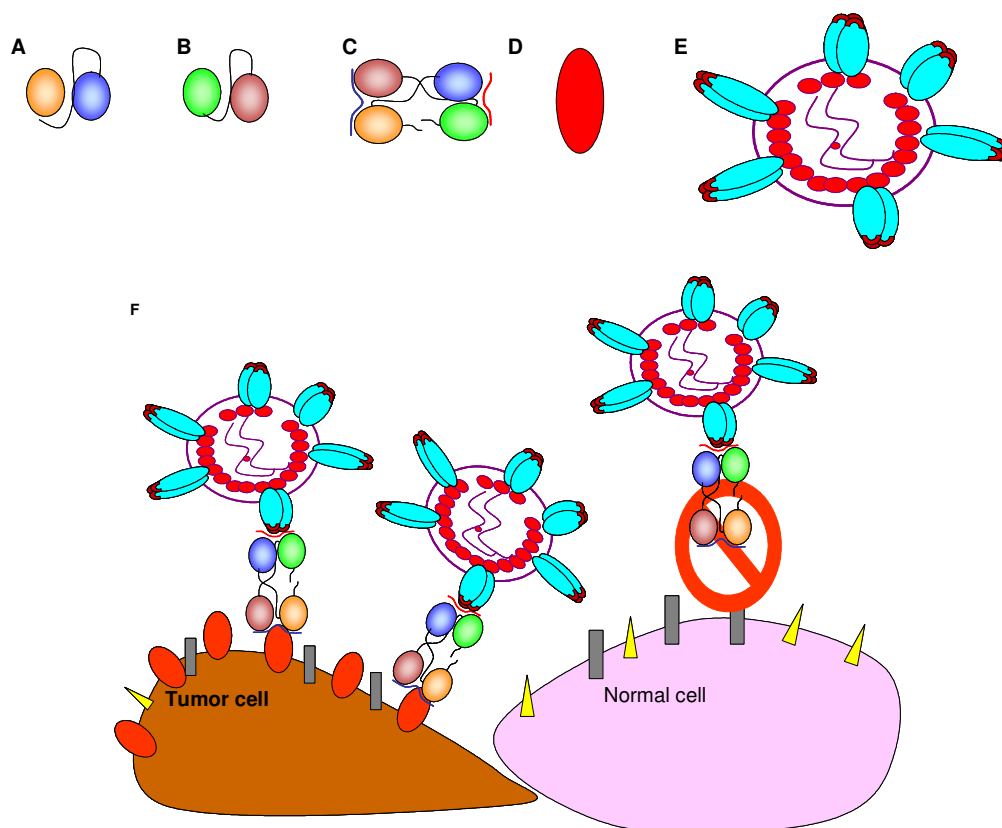
Figure 42. Targeting strategy with bispecific diabodies

scFv against the myc epitope in the VSV-G (A) and PSCA (B) can be fused to generated a bispecific diabody (C). This diabody is capable of recognizing the PSCA (D) and recruiting the modified viral particle (E) to the tumor cells for a targeted anti-tumor therapy (F).

An alternative strategy involves the over-expression of the linker molecule such as the scFv recognizing the TAA in the packaging cell line. As shown by Chan *et al.*, viral particles gather the proteins expressed on the packaging cell membrane during the budding process. These proteins are then available for a targeting procedure. For instance, the scFv anti-PSCA can be over-expressed on the packaging cell line. Thus, we can generate retroviral particles, which contain the myc-modified VSV-G protein for purification and the scFv anti-PSCA for the targeting. Expression of the scFv as a separate membrane protein instead of a fusion moiety to the VSV-G overcomes the problems in the folding and fusion therefore allows the production of fully functional VSV-G proteins. Anchoring the scFv to a hinge region for a better projection should facilitate the target antigen binding.

8.   CONCLUSION

As to our knowledge, up to now, there only few successful modifications of VSV-G protein, which confined the specificity [146,147,149]. However, in these studies the mutant VSV-G proteins lacked the wild-type fusion or packaging capacity. Thus, although in both studies specific binding was demonstrated, the transduction levels were insufficient. In another recent report, His-tag was inserted into the VSV-G and these mutants were successfully incorporated into viral particles, which in turn were purified via Ni-NTA chromatography. Unfortunately, the mutant protein retained the wild-type tropism and is therefore is not applicable for targeted therapy. On the other hand, our mutational analyses have revealed two epitope-permissive sites in the ectodomain of VSV-G protein, which allows viral assembly and purification using antibodies. This suggests an alternative to the recently published purification via the His-tag [150]. The fact that the MLV$^{(G\text{-}myc\ 17)}$, and MLV$^{(G\text{-}myc\ 28)}$ mediated transductions were inhibited by anti-myc antibody and increased transduction efficiency on PSCA-positive cells with these particles implies their potential as targeting vectors.

9. REFERENCES

1. www.wiley.co.uk.   2007.
   Ref Type: Generic

2. Roche S, Rey FA, Gaudin Y, Bressanelli S: **Structure of the prefusion form of the vesicular stomatitis virus glycoprotein G.** *Science* 2007, **315:** 843-848.

3. Soneoka Y, Cannon PM, Ramsdale EE, Griffiths JC, Romano G, Kingsman SM *et al.*: **A transient three-plasmid expression system for the production of high titer retroviral vectors.** *Nucleic Acids Res* 1995, **23:** 628-633.

4. Rosenberg SA, Packard BS, Aebersold PM, Solomon D, Topalian SL, Toy ST *et al.*: **Use of tumor-infiltrating lymphocytes and interleukin-2 in the immunotherapy of patients with metastatic melanoma. A preliminary report.** *N Engl J Med* 1988, **319:** 1676-1680.

5. Anderson WF: **Human gene therapy.** *Science* 1992, **256:** 808-813.

6. Blaese RM, Culver KW, Miller AD, Carter CS, Fleisher T, Clerici M *et al.*: **T lymphocyte-directed gene therapy for ADA- SCID: initial trial results after 4 years.** *Science* 1995, **270:** 475-480.

7. Edelstein ML, Abedi MR, Wixon J, Edelstein RM: **Gene therapy clinical trials worldwide 1989-2004-an overview.** *J Gene Med* 2004, **6:** 597-602.

8. Dummer R, Hassel JC, Fellenberg F, Eichmuller S, Maier T, Slos P *et al.*: **Adenovirus-mediated intralesional interferon-gamma gene transfer induces tumor regressions in cutaneous lymphomas.** *Blood* 2004, **104:** 1631-1638.

9. Jantscheff P, Herrmann R, Spagnoli G, Reuter J, Mehtali M, Courtney M *et al.*: **Gene therapy with cytokine-transfected xenogenic cells (Vero-IL-2) in patients with metastatic solid tumors: mechanism(s) of elimination of the transgene-carrying cells.** *Cancer Immunol Immunother* 1999, **48:** 321-330.

10. Schreiber S, Kampgen E, Wagner E, Pirkhammer D, Trcka J, Korschan H *et al.*: **Immunotherapy of metastatic malignant melanoma by a vaccine consisting of autologous interleukin 2-transfected cancer cells: outcome of a phase I study.** *Hum Gene Ther* 1999, **10:** 983-993.

11. Moolten FL: **Tumor chemosensitivity conferred by inserted herpes thymidine kinase genes: paradigm for a prospective cancer control strategy.** *Cancer Res* 1986, **46:** 5276-5281.

12. Rochlitz CF: **Gene therapy of cancer.** *Swiss Med Wkly* 2001, **131:** 4-9.

13. Wolff JA, Malone RW, Williams P, Chong W, Acsadi G, Jani A *et al.*: **Direct gene transfer into mouse muscle in vivo.** *Science* 1990, **247:** 1465-1468.

14. Wolff JA, Ludtke JJ, Acsadi G, Williams P, Jani A: **Long-term persistence of plasmid DNA and foreign gene expression in mouse muscle.** *Hum Mol Genet* 1992, **1:** 363-369.

15. Wells DJ: **Gene therapy progress and prospects: electroporation and other physical methods.** *Gene Ther* 2004, **11:** 1363-1369.

References

16. Heller LC, Ugen K, Heller R: **Electroporation for targeted gene transfer.** *Expert Opin Drug Deliv* 2005, **2:** 255-268.

17. Keating A, Toneguzzo F: **Gene transfer by electroporation: a model for gene therapy.** *Prog Clin Biol Res* 1990, **333:** 491-498.

18. Spandidos DA: **Electric field-mediated gene transfer (electroporation) into mouse Friend and human K562 erythroleukemic cells.** *Gene Anal Tech* 1987, **4:** 50-56.

19. Yang NS, Burkholder J, Roberts B, Martinell B, McCabe D: **In vivo and in vitro gene transfer to mammalian somatic cells by particle bombardment.** *Proc Natl Acad Sci U S A* 1990, **87:** 9568-9572.

20. Song W, Lahiri DK: **Efficient transfection of DNA by mixing cells in suspension with calcium phosphate.** *Nucleic Acids Res* 1995, **23:** 3609-3611.

21. Graham FL, van der Eb AJ: **A new technique for the assay of infectivity of human adenovirus 5 DNA.** *Virology* 1973, **52:** 456-467.

22. Felgner PL, Gadek TR, Holm M, Roman R, Chan HW, Wenz M *et al.*: **Lipofection: a highly efficient, lipid-mediated DNA-transfection procedure.** *Proc Natl Acad Sci U S A* 1987, **84:** 7413-7417.

23. Felgner PL, Ringold GM: **Cationic liposome-mediated transfection.** *Nature* 1989, **337:** 387-388.

24. Gao X, Huang L: **Cationic liposome-mediated gene transfer.** *Gene Ther* 1995, **2:** 710-722.

25. Huebner S, Battersby BJ, Grimm R, Cevc G: **Lipid-DNA complex formation: reorganization and rupture of lipid vesicles in the presence of DNA as observed by cryoelectron microscopy.** *Biophys J* 1999, **76:** 3158-3166.

26. Kamau SW, Hassa PO, Steitz B, Petri-Fink A, Hofmann H, Hofmann-Amtenbrink M *et al.*: **Enhancement of the efficiency of non-viral gene delivery by application of pulsed magnetic field.** *Nucleic Acids Res* 2006, **34:** e40.

27. Koltover I, Salditt T, Radler JO, Safinya CR: **An inverted hexagonal phase of cationic liposome-DNA complexes related to DNA release and delivery.** *Science* 1998, **281:** 78-81.

28. Koltover I, Salditt T, Safinya CR: **Phase diagram, stability, and overcharging of lamellar cationic lipid-DNA self-assembled complexes.** *Biophys J* 1999, **77:** 915-924.

29. Futaki S, Masui Y, Nakase I, Sugiura Y, Nakamura T, Kogure K *et al.*: **Unique features of a pH-sensitive fusogenic peptide that improves the transfection efficiency of cationic liposomes.** *J Gene Med* 2005, **7:** 1450-1458.

30. Hart SL: **Lipid carriers for gene therapy.** *Curr Drug Deliv* 2005, **2:** 423-428.

31. Xu Y, Szoka FC, Jr.: **Mechanism of DNA release from cationic liposome/DNA complexes used in cell transfection.** *Biochemistry* 1996, **35:** 5616-5623.

32. Garnett MC: **Gene-delivery systems using cationic polymers.** *Crit Rev Ther Drug Carrier Syst* 1999, **16:** 147-207.

33. Ahn CH, Chae SY, Bae YH, Kim SW: **Biodegradable poly(ethylenimine) for plasmid DNA delivery.** *J Control Release* 2002, **80:** 273-282.

34. Godbey WT, Wu KK, Mikos AG: **Poly(ethylenimine) and its role in gene delivery.** *J Control Release* 1999, **60:** 149-160.

35. Godbey WT, Wu KK, Mikos AG: **Tracking the intracellular path of poly(ethylenimine)/DNA complexes for gene delivery.** *Proc Natl Acad Sci U S A* 1999, **96:** 5177-5181.

36. Wang S, Ma N, Gao SJ, Yu H, Leong KW: **Transgene expression in the brain stem effected by intramuscular injection of polyethylenimine/DNA complexes.** *Mol Ther* 2001, **3:** 658-664.

37. Erbacher P, Zou S, Bettinger T, Steffan AM, Remy JS: **Chitosan-based vector/DNA complexes for gene delivery: biophysical characteristics and transfection ability.** *Pharm Res* 1998, **15:** 1332-1339.

38. Jiang HL, Kim YK, Arote R, Nah JW, Cho MH, Choi YJ *et al.*: **Chitosan-graft-polyethylenimine as a gene carrier.** *J Control Release* 2007, **117:** 273-280.

39. Koping-Hoggard M, Tubulekas I, Guan H, Edwards K, Nilsson M, Varum KM *et al.*: **Chitosan as a nonviral gene delivery system. Structure-property relationships and characteristics compared with polyethylenimine in vitro and after lung administration in vivo.** *Gene Ther* 2001, **8:** 1108-1121.

40. Guo W, Lee RL: **Receptor-targeted gene delivery via folate-conjugated polyethylenimine.** *AAPS PharmSci* 1999, **1:** E19.

41. Schaffer DV, Fidelman NA, Dan N, Lauffenburger DA: **Vector unpacking as a potential barrier for receptor-mediated polyplex gene delivery.** *Biotechnol Bioeng* 2000, **67:** 598-606.

42. Buchschacher GL, Jr.: **Introduction to retroviruses and retroviral vectors.** *Somat Cell Mol Genet* 2001, **26:** 1-11.

43. Hemminki A, Kanerva A, Liu B, Wang M, Alvarez RD, Siegal GP *et al.*: **Modulation of coxsackie-adenovirus receptor expression for increased adenoviral transgene expression.** *Cancer Res* 2003, **63:** 847-853.

44. Medina-Kauwe LK: **Endocytosis of adenovirus and adenovirus capsid proteins.** *Adv Drug Deliv Rev* 2003, **55:** 1485-1496.

45. Meier O, Greber UF: **Adenovirus endocytosis.** *J Gene Med* 2004, **6 Suppl 1:** S152-S163.

46. Mathias P, Wickham T, Moore M, Nemerow G: **Multiple adenovirus serotypes use alpha v integrins for infection.** *J Virol* 1994, **68:** 6811-6814.

47. Wickham TJ, Mathias P, Cheresh DA, Nemerow GR: **Integrins alpha v beta 3 and alpha v beta 5 promote adenovirus internalization but not virus attachment.** *Cell* 1993, **73:** 309-319.

48. Berns KI, Giraud C: **Adenovirus and adeno-associated virus as vectors for gene therapy.** *Ann N Y Acad Sci* 1995, **772:** 95-104.

49. Brody SL, Crystal RG: **Adenovirus-mediated in vivo gene transfer.** *Ann N Y Acad Sci* 1994, **716:** 90-101.

50. Danthinne X, Imperiale MJ: **Production of first generation adenovirus vectors: a review.** *Gene Ther* 2000, **7:** 1707-1714.

51. Jornot L, Petersen H, Lusky M, Pavirani A, Moix I, Morris *et al.*: **Effects of first generation E1E3-deleted and second generation E1E3E4-deleted/modified adenovirus vectors on human endothelial cell death.** *Endothelium* 2001, **8:** 167-179.

52. Lusky M, Christ M, Rittner K, Dieterle A, Dreyer D, Mourot B *et al.*: **In vitro and in vivo biology of recombinant adenovirus vectors with E1, E1/E2A, or E1/E4 deleted.** *J Virol* 1998, **72:** 2022-2032.

53. Mizuguchi H, Kay MA: **A simple method for constructing E1- and E1/E4-deleted recombinant adenoviral vectors.** *Hum Gene Ther* 1999, **10:** 2013-2017.

54. Schaack J: **Adenovirus vectors deleted for genes essential for viral DNA replication.** *Front Biosci* 2005, **10:** 1146-1155.

55. Alba R, Bosch A, Chillon M: **Gutless adenovirus: last-generation adenovirus for gene therapy.** *Gene Ther* 2005, **12 Suppl 1:** S18-S27.

56. Fallaux FJ, Kranenburg O, Cramer SJ, Houweling A, van OH, Hoeben RC *et al.*: **Characterization of 911: a new helper cell line for the titration and propagation of early region 1-deleted adenoviral vectors.** *Hum Gene Ther* 1996, **7:** 215-222.

57. Fallaux FJ, Bout A, van dV, I, Van den Wollenberg DJ, Hehir KM, Keegan J *et al.*: **New helper cells and matched early region 1-deleted adenovirus vectors prevent generation of replication-competent adenoviruses.** *Hum Gene Ther* 1998, **9:** 1909-1917.

58. Graham FL, Smiley J, Russell WC, Nairn R: **Characteristics of a human cell line transformed by DNA from human adenovirus type 5.** *J Gen Virol* 1977, **36:** 59-74.

59. Schiedner G, Hertel S, Kochanek S: **Efficient transformation of primary human amniocytes by E1 functions of Ad5: generation of new cell lines for adenoviral vector production.** *Hum Gene Ther* 2000, **11:** 2105-2116.

60. Palmer D, Ng P: **Improved system for helper-dependent adenoviral vector production.** *Mol Ther* 2003, **8:** 846-852.

61. Parks RJ, Chen L, Anton M, Sankar U, Rudnicki MA, Graham FL: **A helper-dependent adenovirus vector system: removal of helper virus by Cre-mediated excision of the viral packaging signal.** *Proc Natl Acad Sci U S A* 1996, **93:** 13565-13570.

62. Sato M, Suzuki S, Kubo S, Mitani K: **Replication and packaging of helper-dependent adenoviral vectors.** *Gene Ther* 2002, **9:** 472-476.

63. **Gene therapy for cystic fibrosis utilizing a replication deficient recombinant adenovirus vector to deliver the human cystic fibrosis transmembrane conductance regulator cDNA to the airways. A phase I study.** *Hum Gene Ther* 1994, **5:** 1019-1057.

64. Cohen EE, Rudin CM: **ONYX-015. Onyx Pharmaceuticals.** *Curr Opin Investig Drugs* 2001, **2:** 1770-1775.

65. Heise C, Sampson-Johannes A, Williams A, McCormick F, Von Hoff DD, Kirn DH: **ONYX-015, an E1B gene-attenuated adenovirus, causes tumor-specific cytolysis and antitumoral efficacy that can be augmented by standard chemotherapeutic agents.** *Nat Med* 1997, **3:** 639-645.

66. Kirn D, Hermiston T, McCormick F: **ONYX-015: clinical data are encouraging.** *Nat Med* 1998, **4:** 1341-1342.

67. Nemunaitis J, Khuri F, Ganly I, Arseneau J, Posner M, Vokes E *et al.*: **Phase II trial of intratumoral administration of ONYX-015, a replication-selective adenovirus, in patients with refractory head and neck cancer.** *J Clin Oncol* 2001, **19:** 289-298.

68. Zabner J, Couture LA, Gregory RJ, Graham SM, Smith AE, Welsh MJ: **Adenovirus-mediated gene transfer transiently corrects the chloride transport defect in nasal epithelia of patients with cystic fibrosis.** *Cell* 1993, **75:** 207-216.

69. Kotin RM, Siniscalco M, Samulski RJ, Zhu XD, Hunter L, Laughlin CA *et al.*: **Site-specific integration by adeno-associated virus.** *Proc Natl Acad Sci U S A* 1990, **87:** 2211-2215.

70. Samulski RJ, Zhu X, Xiao X, Brook JD, Housman DE, Epstein N *et al.*: **Targeted integration of adeno-associated virus (AAV) into human chromosome 19.** *EMBO J* 1991, **10:** 3941-3950.

71. Ponnazhagan S, Erikson D, Kearns WG, Zhou SZ, Nahreini P, Wang XS *et al.*: **Lack of site-specific integration of the recombinant adeno-associated virus 2 genomes in human cells.** *Hum Gene Ther* 1997, **8:** 275-284.

72. Samulski RJ, Chang LS, Shenk T: **Helper-free stocks of recombinant adeno-associated viruses: normal integration does not require viral gene expression.** *J Virol* 1989, **63:** 3822-3828.

73. Aitken ML, Moss RB, Waltz DA, Dovey ME, Tonelli MR, McNamara SC *et al.*: **A phase I study of aerosolized administration of tgAAVCF to cystic fibrosis subjects with mild lung disease.** *Hum Gene Ther* 2001, **12:** 1907-1916.

74. Flotte TR, Zeitlin PL, Reynolds TC, Heald AE, Pedersen P, Beck S *et al.*: **Phase I trial of intranasal and endobronchial administration of a recombinant adeno-associated virus serotype 2 (rAAV2)-CFTR vector in adult cystic fibrosis patients: a two-part clinical study.** *Hum Gene Ther* 2003, **14:** 1079-1088.

75. Gura T: **Hemophilia. After a setback, gene therapy progresses...gingerly.** *Science* 2001, **291:** 1692-1697.

References

76. Glorioso JC, DeLuca NA, Fink DJ: **Development and application of herpes simplex virus vectors for human gene therapy.** *Annu Rev Microbiol* 1995, **49:** 675-710.

77. Croen KD, Ostrove JM, Dragovic LJ, Smialek JE, Straus SE: **Latent herpes simplex virus in human trigeminal ganglia. Detection of an immediate early gene "anti-sense" transcript by in situ hybridization.** *N Engl J Med* 1987, **317:** 1427-1432.

78. Dobson AT, Sederati F, vi-Rao G, Flanagan WM, Farrell MJ, Stevens JG *et al.*: **Identification of the latency-associated transcript promoter by expression of rabbit beta-globin mRNA in mouse sensory nerve ganglia latently infected with a recombinant herpes simplex virus.** *J Virol* 1989, **63:** 3844-3851.

79. Goins WF, Sternberg LR, Croen KD, Krause PR, Hendricks RL, Fink DJ *et al.*: **A novel latency-active promoter is contained within the herpes simplex virus type 1 UL flanking repeats.** *J Virol* 1994, **68:** 2239-2252.

80. Izumi KM, McKelvey AM, vi-Rao G, Wagner EK, Stevens JG: **Molecular and biological characterization of a type 1 herpes simplex virus (HSV-1) specifically deleted for expression of the latency-associated transcript (LAT).** *Microb Pathog* 1989, **7:** 121-134.

81. Wu N, Watkins SC, Schaffer PA, DeLuca NA: **Prolonged gene expression and cell survival after infection by a herpes simplex virus mutant defective in the immediate-early genes encoding ICP4, ICP27, and ICP22.** *J Virol* 1996, **70:** 6358-6369.

82. Papanastassiou V, Rampling R, Fraser M, Petty R, Hadley D, Nicoll J *et al.*: **The potential for efficacy of the modified (ICP 34.5(-)) herpes simplex virus HSV1716 following intratumoural injection into human malignant glioma: a proof of principle study.** *Gene Ther* 2002, **9:** 398-406.

83. Markert JM, Medlock MD, Rabkin SD, Gillespie GY, Todo T, Hunter WD *et al.*: **Conditionally replicating herpes simplex virus mutant, G207 for the treatment of malignant glioma: results of a phase I trial.** *Gene Ther* 2000, **7:** 867-874.

84. Montelaro RC, Bolognesi DP: **Structure and morphogenesis of type-C retroviruses.** *Adv Cancer Res* 1978, **28:** 63-89.

85. Pages JC, Bru T: **Toolbox for retrovectorologists.** *J Gene Med* 2004, **6 Suppl 1:** S67-S82.

86. Varmus H: **Retroviruses.** *Science* 1988, **240:** 1427-1435.

87. Vile RG, Russell SJ: **Retroviruses as vectors.** *Br Med Bull* 1995, **51:** 12-30.

88. Shaunak S, Weber JN: **The retroviruses: classification and molecular biology.** *Baillieres Clin Neurol* 1992, **1:** 1-21.

89. Buchschacher GL, Jr., Wong-Staal F: **Development of lentiviral vectors for gene therapy for human diseases.** *Blood* 2000, **95:** 2499-2504.

90. Boettiger D: **Animal virus pseudotypes.** *Prog Med Virol* 1979, **25:** 37-68.

91. Spector DH: **Potential host range expansion of the retroviruses.** *Dev Biol Stand* 1992, **76:** 153-164.

92. Zavada J: **Viral pseudotypes and phenotypic mixing.** *Arch Virol* 1976, **50:** 1-15.

93. Emi N, Friedmann T, Yee JK: **Pseudotype formation of murine leukemia virus with the G protein of vesicular stomatitis virus.** *J Virol* 1991, **65:** 1202-1207.

94. Yee JK, Friedmann T, Burns JC: **Generation of high-titer pseudotyped retroviral vectors with very broad host range.** *Methods Cell Biol* 1994, **43 Pt A:** 99-112.

95. Burns JC, Friedmann T, Driever W, Burrascano M, Yee JK: **Vesicular stomatitis virus G glycoprotein pseudotyped retroviral vectors: concentration to very high titer and efficient gene transfer into mammalian and nonmammalian cells.** *Proc Natl Acad Sci U S A* 1993, **90:** 8033-8037.

96. Onodera M, Ariga T, Kawamura N, Kobayashi I, Ohtsu M, Yamada M *et al.*: **Successful peripheral T-lymphocyte-directed gene transfer for a patient with severe combined immune deficiency caused by adenosine deaminase deficiency.** *Blood* 1998, **91:** 30-36.

97. Braakman E, van B, V, van Krimpen BA, Fischer A, Bolhuis RL, Valerio D: **Genetic correction of cultured T cells from an adenosine deaminase-deficient patient: characteristics of non-transduced and transduced T cells.** *Eur J Immunol* 1992, **22:** 63-69.

98. Hoogerbrugge PM, van B, V, Fischer A, Debree M, le DF, Perignon JL *et al.*: **Bone marrow gene transfer in three patients with adenosine deaminase deficiency.** *Gene Ther* 1996, **3:** 179-183.

99. Muul LM, Tuschong LM, Soenen SL, Jagadeesh GJ, Ramsey WJ, Long Z *et al.*: **Persistence and expression of the adenosine deaminase gene for 12 years and immune reaction to gene transfer components: long-term results of the first clinical gene therapy trial.** *Blood* 2003, **101:** 2563-2569.

100. Onodera M, Nelson DM, Sakiyama Y, Candotti F, Blaese RM: **Gene therapy for severe combined immunodeficiency caused by adenosine deaminase deficiency: improved retroviral vectors for clinical trials.** *Acta Haematol* 1999, **101:** 89-96.

101. Hacein-Bey-Abina S, Von KC, Schmidt M, le DF, Wulffraat N, McIntyre E *et al.*: **A serious adverse event after successful gene therapy for X-linked severe combined immunodeficiency.** *N Engl J Med* 2003, **348:** 255-256.

102. Hacein-Bey-Abina S, Von KC, Schmidt M, McCormack MP, Wulffraat N, Leboulch P *et al.*: **LMO2-associated clonal T cell proliferation in two patients after gene therapy for SCID-X1.** *Science* 2003, **302:** 415-419.

103. Gazit G, Kane SE, Nichols P, Lee AS: **Use of the stress-inducible grp78/BiP promoter in targeting high level gene expression in fibrosarcoma in vivo.** *Cancer Res* 1995, **55:** 1660-1663.

104. Vile R, Miller N, Chernajovsky Y, Hart I: **A comparison of the properties of different retroviral vectors containing the murine tyrosinase promoter to**

achieve transcriptionally targeted expression of the HSVtk or IL-2 genes. *Gene Ther* 1994, **1:** 307-316.

105. Haynes C, Erlwein O, Schnierle BS: **Modified envelope glycoproteins to retarget retroviral vectors.** *Curr Gene Ther* 2003, **3:** 405-410.

106. Ohno K, Meruelo D: **Retrovirus vectors displaying the IgG-binding domain of protein A.** *Biochem Mol Med* 1997, **62:** 123-127.

107. Ohno K, Sawai K, Iijima Y, Levin B, Meruelo D: **Cell-specific targeting of Sindbis virus vectors displaying IgG-binding domains of protein A.** *Nat Biotechnol* 1997, **15:** 763-767.

108. Tai CK, Logg CR, Park JM, Anderson WF, Press MF, Kasahara N: **Antibody-mediated targeting of replication-competent retroviral vectors.** *Hum Gene Ther* 2003, **14:** 789-802.

109. Morizono K, Xie Y, Ringpis GE, Johnson M, Nassanian H, Lee B *et al.*: **Lentiviral vector retargeting to P-glycoprotein on metastatic melanoma through intravenous injection.** *Nat Med* 2005, **11:** 346-352.

110. Martin F, Neil S, Kupsch J, Maurice M, Cosset F, Collins M: **Retrovirus targeting by tropism restriction to melanoma cells.** *J Virol* 1999, **73:** 6923-6929.

111. Martin F, Chowdhury S, Neil S, Phillipps N, Collins MK: **Envelope-targeted retrovirus vectors transduce melanoma xenografts but not spleen or liver.** *Mol Ther* 2002, **5:** 269-274.

112. Kahl CA, Pollok K, Haneline LS, Cornetta K: **Lentiviral vectors pseudotyped with glycoproteins from Ross River and vesicular stomatitis viruses: variable transduction related to cell type and culture conditions.** *Mol Ther* 2005, **11:** 470-482.

113. Kiem HP, Heyward S, Winkler A, Potter J, Allen JM, Miller AD *et al.*: **Gene transfer into marrow repopulating cells: comparison between amphotropic and gibbon ape leukemia virus pseudotyped retroviral vectors in a competitive repopulation assay in baboons.** *Blood* 1997, **90:** 4638-4645.

114. Watson DJ, Kobinger GP, Passini MA, Wilson JM, Wolfe JH: **Targeted transduction patterns in the mouse brain by lentivirus vectors pseudotyped with VSV, Ebola, Mokola, LCMV, or MuLV envelope proteins.** *Mol Ther* 2002, **5:** 528-537.

115. Movassagh M, Desmyter C, Baillou C, Chapel-Fernandes S, Guigon M, Klatzmann D *et al.*: **High-level gene transfer to cord blood progenitors using gibbon ape leukemia virus pseudotype retroviral vectors and an improved clinically applicable protocol.** *Hum Gene Ther* 1998, **9:** 225-234.

116. Lee H, Song JJ, Kim E, Yun CO, Choi J, Lee B *et al.*: **Efficient gene transfer of VSV-G pseudotyped retroviral vector to human brain tumor.** *Gene Ther* 2001, **8:** 268-273.

117. Perletti G, Osti D, Marras E, Tettamanti G, de EM: **Generation of VSV-G pseudotyped lentiviral particles in 293T cells.** *J Cell Mol Med* 2004, **8:** 142-143.

References

118. Yang Y, Vanin EF, Whitt MA, Fornerod M, Zwart R, Schneiderman RD *et al.*: **Inducible, high-level production of infectious murine leukemia retroviral vector particles pseudotyped with vesicular stomatitis virus G envelope protein.** *Hum Gene Ther* 1995, **6:** 1203-1213.

119. Okimoto T, Friedmann T, Miyanohara A: **VSV-G envelope glycoprotein forms complexes with plasmid DNA and MLV retrovirus-like particles in cell-free conditions and enhances DNA transfection.** *Mol Ther* 2001, **4:** 232-238.

120. Jang JE, Shaw K, Yu XJ, Petersen D, Pepper K, Lutzko C *et al.*: **Specific and stable gene transfer to human embryonic stem cells using pseudotyped lentiviral vectors.** *Stem Cells Dev* 2006, **15:** 109-117.

121. Leurs C, Jansen M, Pollok KE, Heinkelein M, Schmidt M, Wissler M *et al.*: **Comparison of three retroviral vector systems for transduction of nonobese diabetic/severe combined immunodeficiency mice repopulating human CD34+ cord blood cells.** *Hum Gene Ther* 2003, **14:** 509-519.

122. Relander T, Karlsson S, Richter J: **Oncoretroviral gene transfer to NOD/SCID repopulating cells using three different viral envelopes.** *J Gene Med* 2002, **4:** 122-132.

123. Barrette S, Douglas J, Orlic D, Anderson SM, Seidel NE, Miller AD *et al.*: **Superior transduction of mouse hematopoietic stem cells with 10A1 and VSV-G pseudotyped retrovirus vectors.** *Mol Ther* 2000, **1:** 330-338.

124. Coll JM: **The glycoprotein G of rhabdoviruses.** *Arch Virol* 1995, **140:** 827-851.

125. de SA, Braakman I, Helenius A: **Posttranslational folding of vesicular stomatitis virus G protein in the ER: involvement of noncovalent and covalent complexes.** *J Cell Biol* 1993, **120:** 647-655.

126. Doms RW, Ruusala A, Machamer C, Helenius J, Helenius A, Rose JK: **Differential effects of mutations in three domains on folding, quaternary structure, and intracellular transport of vesicular stomatitis virus G protein.** *J Cell Biol* 1988, **107:** 89-99.

127. Machamer CE, Florkiewicz RZ, Rose JK: **A single N-linked oligosaccharide at either of the two normal sites is sufficient for transport of vesicular stomatitis virus G protein to the cell surface.** *Mol Cell Biol* 1985, **5:** 3074-3083.

128. Machamer CE, Rose JK: **Influence of new glycosylation sites on expression of the vesicular stomatitis virus G protein at the plasma membrane.** *J Biol Chem* 1988, **263:** 5948-5954.

129. Machamer CE, Rose JK: **Vesicular stomatitis virus G proteins with altered glycosylation sites display temperature-sensitive intracellular transport and are subject to aberrant intermolecular disulfide bonding.** *J Biol Chem* 1988, **263:** 5955-5960.

130. de Silva AM, Balch WE, Helenius A: **Quality control in the endoplasmic reticulum: folding and misfolding of vesicular stomatitis virus G protein in cells and in vitro.** *J Cell Biol* 1990, **111:** 857-866.

131. Hammond C, Helenius A: **Folding of VSV G protein: sequential interaction with BiP and calnexin.** *Science* 1994, **266:** 456-458.

132. Nehls S, Snapp EL, Cole NB, Zaal KJ, Kenworthy AK, Roberts TH *et al.*: **Dynamics and retention of misfolded proteins in native ER membranes.** *Nat Cell Biol* 2000, **2:** 288-295.

133. Schlegel R, Willingham MC, Pastan IH: **Saturable binding sites for vesicular stomatitis virus on the surface of Vero cells.** *J Virol* 1982, **43:** 871-875.

134. Schlegel R, Tralka TS, Willingham MC, Pastan I: **Inhibition of VSV binding and infectivity by phosphatidylserine: is phosphatidylserine a VSV-binding site?** *Cell* 1983, **32:** 639-646.

135. Coil DA, Miller AD: **Phosphatidylserine is not the cell surface receptor for vesicular stomatitis virus.** *J Virol* 2004, **78:** 10920-10926.

136. Carneiro FA, Lapido-Loureiro PA, Cordo SM, Stauffer F, Weissmuller G, Bianconi ML *et al.*: **Probing the interaction between vesicular stomatitis virus and phosphatidylserine.** *Eur Biophys J* 2006, **35:** 145-154.

137. Coll JM: **Synthetic peptides reveal a phospholipid binding domain in the glycoprotein of VHSV, a salmonid rhabdovirus.** *Vet Res* 1995, **26:** 399-407.

138. Coll JM: **Synthetic peptides from the heptad repeats of the glycoproteins of rabies, vesicular stomatitis and fish rhabdoviruses bind phosphatidylserine.** *Arch Virol* 1997, **142:** 2089-2097.

139. Estepa A, Coll JM: **Pepscan mapping and fusion-related properties of the major phosphatidylserine-binding domain of the glycoprotein of viral hemorrhagic septicemia virus, a salmonid rhabdovirus.** *Virology* 1996, **216:** 60-70.

140. Carneiro FA, Ferradosa AS, Da Poian AT: **Low pH-induced conformational changes in vesicular stomatitis virus glycoprotein involve dramatic structure reorganization.** *J Biol Chem* 2001, **276:** 62-67.

141. Carneiro FA, Stauffer F, Lima CS, Juliano MA, Juliano L, Da Poian AT: **Membrane fusion induced by vesicular stomatitis virus depends on histidine protonation.** *J Biol Chem* 2003, **278:** 13789-13794.

142. Hoekstra D: **Membrane fusion of enveloped viruses: especially a matter of proteins.** *J Bioenerg Biomembr* 1990, **22:** 121-155.

143. Kielian M: **Class II virus membrane fusion proteins.** *Virology* 2006, **344:** 38-47.

144. Schibli DJ, Weissenhorn W: **Class I and class II viral fusion protein structures reveal similar principles in membrane fusion.** *Mol Membr Biol* 2004, **21:** 361-371.

145. Da Poian AT, Carneiro FA, Stauffer F: **Viral membrane fusion: is glycoprotein G of rhabdoviruses a representative of a new class of viral fusion proteins?** *Braz J Med Biol Res* 2005, **38:** 813-823.

146. Guibinga GH, Hall FL, Gordon EM, Ruoslahti E, Friedmann T: **Ligand-modified vesicular stomatitis virus glycoprotein displays a temperature-sensitive intracellular trafficking and virus assembly phenotype.** *Mol Ther* 2004, **9:** 76-84.

References

147. Schlehuber LD, Rose JK: **Prediction and identification of a permissive epitope insertion site in the vesicular stomatitis virus glycoprotein.** *J Virol* 2004, **78:** 5079-5087.

148. Fredericksen BL, Whitt MA: **Vesicular stomatitis virus glycoprotein mutations that affect membrane fusion activity and abolish virus infectivity.** *J Virol* 1995, **69:** 1435-1443.

149. Dreja H, Piechaczyk M: **The effects of N-terminal insertion into VSV-G of an scFv peptide.** *Virol J* 2006, **3:** 69.

150. Yu JH, Schaffer DV: **Selection of novel vesicular stomatitis virus glycoprotein variants from a peptide insertion library for enhanced purification of retroviral and lentiviral vectors.** *J Virol* 2006, **80:** 3285-3292.

151. Bharali DJ, Klejbor I, Stachowiak EK, Dutta P, Roy I, Kaur N *et al.*: **Organically modified silica nanoparticles: a nonviral vector for in vivo gene delivery and expression in the brain.** *Proc Natl Acad Sci U S A* 2005, **102:** 11539-11544.

152. Dobson J: **Gene therapy progress and prospects: magnetic nanoparticle-based gene delivery.** *Gene Ther* 2006, **13:** 283-287.

153. Scherer F, Anton M, Schillinger U, Henke J, Bergemann C, Kruger A *et al.*: **Magnetofection: enhancing and targeting gene delivery by magnetic force in vitro and in vivo.** *Gene Ther* 2002, **9:** 102-109.

154. Takeda S, Terazono B, Mishima F, Nakagami H, Nishijima S, Kaneda Y: **Novel drug delivery system by surface modified magnetic nanoparticles.** *J Nanosci Nanotechnol* 2006, **6:** 3269-3276.

155. Chan L, Nesbeth D, Mackey T, Galea-Lauri J, Gaken J, Martin F *et al.*: **Conjugation of lentivirus to paramagnetic particles via nonviral proteins allows efficient concentration and infection of primary acute myeloid leukemia cells.** *J Virol* 2005, **79:** 13190-13194.

156. Huber DL: **Synthesis, properties, and applications of iron nanoparticles.** *Small* 2005, **1:** 482-501.

157. Zhang J, Sapp CM: **A novel retroviral vector that allows the magnetic selection of infected cells.** *J Virol Methods* 2001, **94:** 1-6.

158. Okon E, Pouliquen D, Okon P, Kovaleva ZV, Stepanova TP, Lavit SG *et al.*: **Biodegradation of magnetite dextran nanoparticles in the rat. A histologic and biophysical study.** *Lab Invest* 1994, **71:** 895-903.

159. Johannsen M, Gneveckow U, Thiesen B, Taymoorian K, Cho CH, Waldofner N *et al.*: **Thermotherapy of Prostate Cancer Using Magnetic Nanoparticles: Feasibility, Imaging, and Three-Dimensional Temperature Distribution.** *Eur Urol* 2006.

160. Kohler N, Sun C, Wang J, Zhang M: **Methotrexate-modified superparamagnetic nanoparticles and their intracellular uptake into human cancer cells.** *Langmuir* 2005, **21:** 8858-8864.

161. Jemal A, Siegel R, Ward E, Murray T, Xu J, Smigal C *et al.*: **Cancer statistics, 2006.** *CA Cancer J Clin* 2006, **56:** 106-130.

References

162. Kaliberov SA, Buchsbaum DJ: **Gene delivery and gene therapy of prostate cancer.** *Expert Opin Drug Deliv* 2006, **3:** 37-51.

163. Dannull J, Diener PA, Prikler L, Furstenberger G, Cerny T, Schmid U *et al.*: **Prostate stem cell antigen is a promising candidate for immunotherapy of advanced prostate cancer.** *Cancer Res* 2000, **60:** 5522-5528.

164. Elsamman E, Fukumori T, Kasai T, Nakatsuji H, Nishitani MA, Toida K *et al.*: **Prostate stem cell antigen predicts tumour recurrence in superficial transitional cell carcinoma of the urinary bladder.** *BJU Int* 2006, **97:** 1202-1207.

165. Elsamman EM, Fukumori T, Tanimoto S, Nakanishi R, Takahashi M, Toida K *et al.*: **The expression of prostate stem cell antigen in human clear cell renal cell carcinoma: a quantitative reverse transcriptase-polymerase chain reaction analysis.** *BJU Int* 2006, **98:** 668-673.

166. Gu Z, Thomas G, Yamashiro J, Shintaku IP, Dorey F, Raitano A *et al.*: **Prostate stem cell antigen (PSCA) expression increases with high gleason score, advanced stage and bone metastasis in prostate cancer.** *Oncogene* 2000, **19:** 1288-1296.

167. Lam JS, Yamashiro J, Shintaku IP, Vessella RL, Jenkins RB, Horvath S *et al.*: **Prostate stem cell antigen is overexpressed in prostate cancer metastases.** *Clin Cancer Res* 2005, **11:** 2591-2596.

168. Reiter RE, Gu Z, Watabe T, Thomas G, Szigeti K, Davis E *et al.*: **Prostate stem cell antigen: a cell surface marker overexpressed in prostate cancer.** *Proc Natl Acad Sci U S A* 1998, **95:** 1735-1740.

169. Ross S, Spencer SD, Holcomb I, Tan C, Hongo J, Devaux B *et al.*: **Prostate stem cell antigen as therapy target: tissue expression and in vivo efficacy of an immunoconjugate.** *Cancer Res* 2002, **62:** 2546-2553.

170. Amara N, Palapattu GS, Schrage M, Gu Z, Thomas GV, Dorey F *et al.*: **Prostate stem cell antigen is overexpressed in human transitional cell carcinoma.** *Cancer Res* 2001, **61:** 4660-4665.

171. Saffran DC, Raitano AB, Hubert RS, Witte ON, Reiter RE, Jakobovits A: **Anti-PSCA mAbs inhibit tumor growth and metastasis formation and prolong the survival of mice bearing human prostate cancer xenografts.** *Proc Natl Acad Sci U S A* 2001, **98:** 2658-2663.

172. Gu Z, Yamashiro J, Kono E, Reiter RE: **Anti-prostate stem cell antigen monoclonal antibody 1G8 induces cell death in vitro and inhibits tumor growth in vivo via a Fc-independent mechanism.** *Cancer Res* 2005, **65:** 9495-9500.

173. Hanahan D: **Studies on transformation of Escherichia coli with plasmids.** *J Mol Biol* 1983, **166:** 557-580.

174. Holmes DS, Quigley M: **A rapid boiling method for the preparation of bacterial plasmids.** *Anal Biochem* 1981, **114:** 193-197.

175. VandePol SB, Holland JJ: **Evolution of vesicular stomatitis virus in athymic nude mice: mutations associated with natural killer cell selection.** *J Gen Virol* 1986, **67 (Pt 3):** 441-451.

176. VandePol SB, Lefrancois L, Holland JJ: **Sequences of the major antibody binding epitopes of the Indiana serotype of vesicular stomatitis virus.** *Virology* 1986, **148:** 312-325.

177. Epstein LB, Knight RA: **Studies on mouse Moloney virus induced tumours: I. The detection of p30 as a cytotoxic target on murine Moloney leukaemic spleen cells, and on an in vitro Moloney sarcoma line by antibody mediated cytotoxicity.** *Br J Cancer* 1975, **31:** 499-512.

178. Gallione CJ, Rose JK: **A single amino acid substitution in a hydrophobic domain causes temperature-sensitive cell-surface transport of a mutant viral glycoprotein.** *J Virol* 1985, **54:** 374-382.

179. Roche S, Bressanelli S, Rey FA, Gaudin Y: **Crystal structure of the low-pH form of the vesicular stomatitis virus glycoprotein G.** *Science* 2006, **313:** 187-191.

180. Ma AD, Brass LF, Abrams CS: **Pleckstrin associates with plasma membranes and induces the formation of membrane projections: requirements for phosphorylation and the NH2-terminal PH domain.** *J Cell Biol* 1997, **136:** 1071-1079.

181. Touhara K, Inglese J, Pitcher JA, Shaw G, Lefkowitz RJ: **Binding of G protein beta gamma-subunits to pleckstrin homology domains.** *J Biol Chem* 1994, **269:** 10217-10220.

182. Capra JD, Edmundson AB: **The antibody combining site.** *Sci Am* 1977, **236:** 50-59.
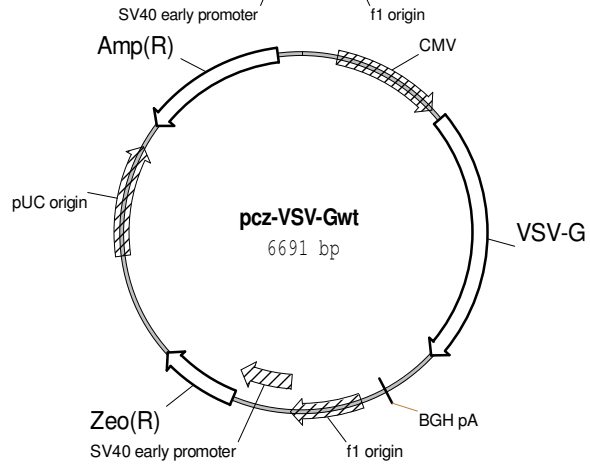
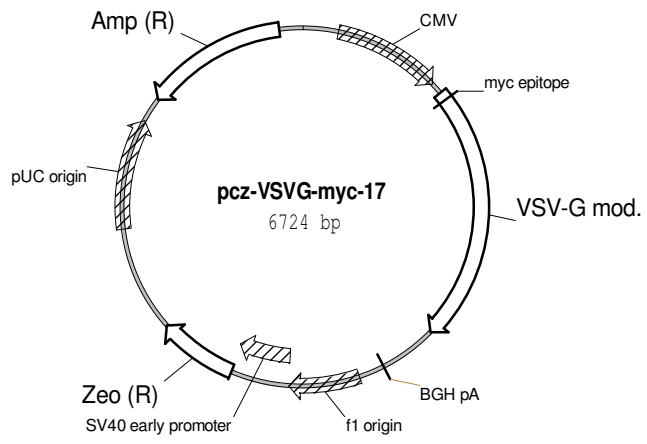# 10. APPENDIX

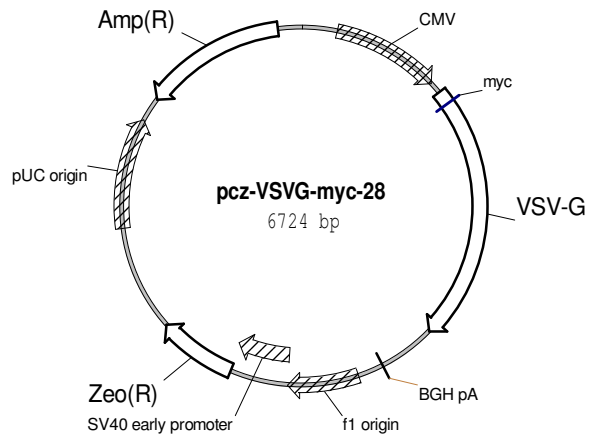## 10.1. Vector maps

pAMI-G
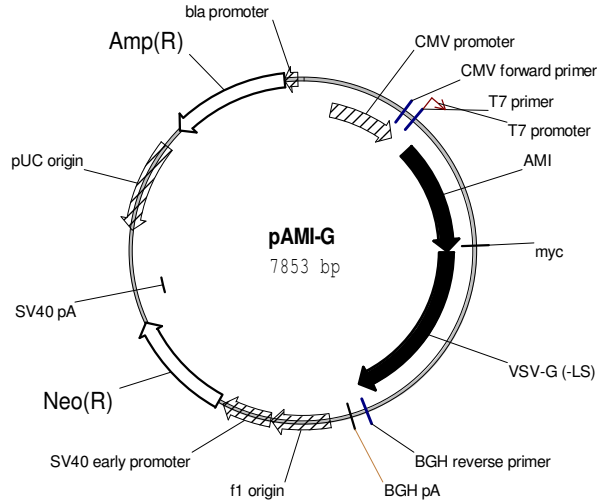
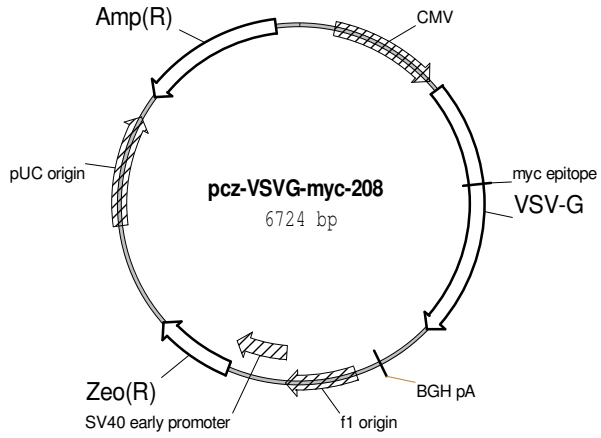pAMI-L-G
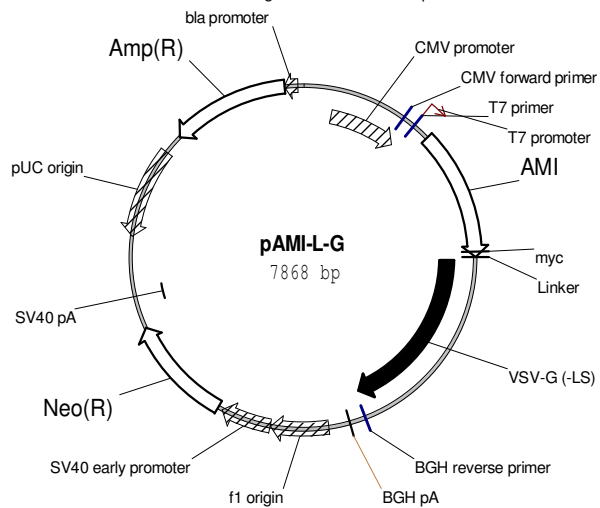
pAMI-L-sG1
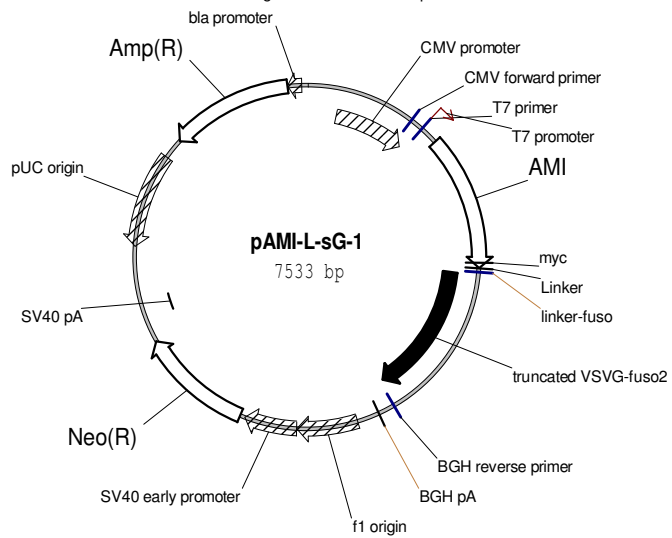
pAMI-L-sG2
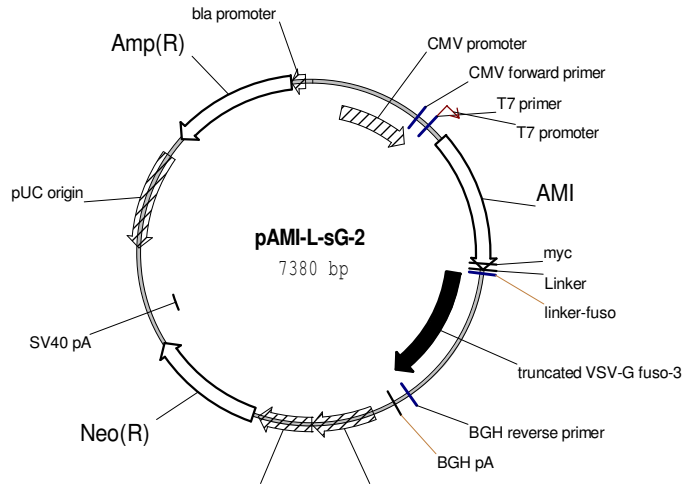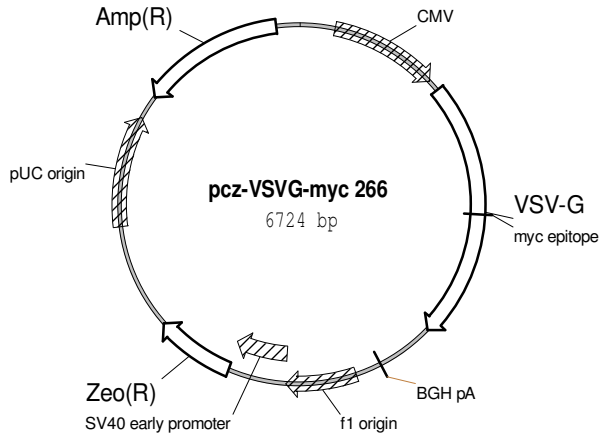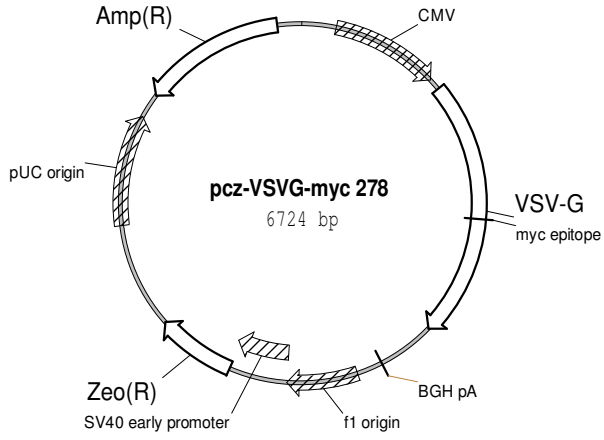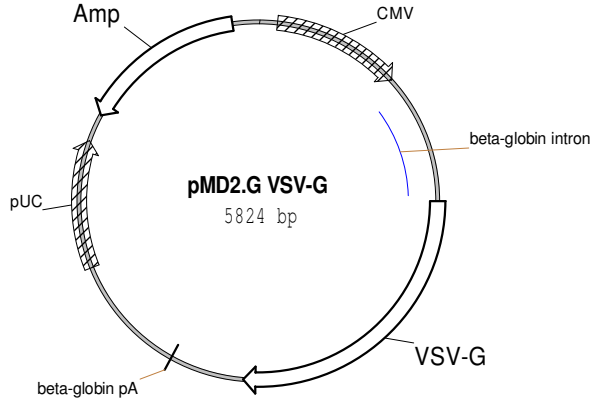

pcz-VSV-Gwt

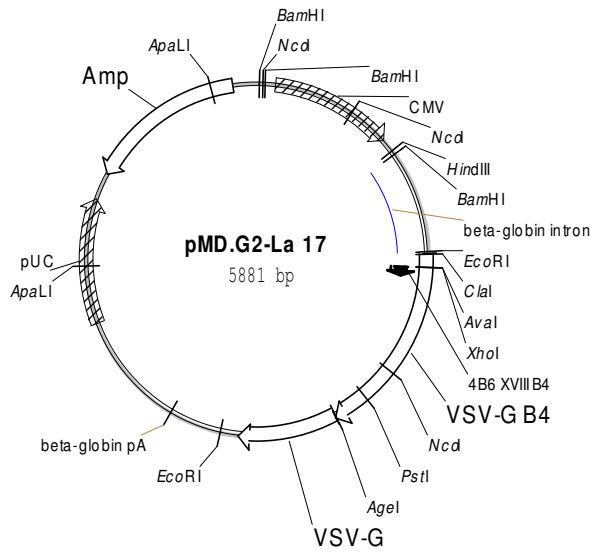pcz-VSV-G myc 17

pcz-VSV-G myc 28
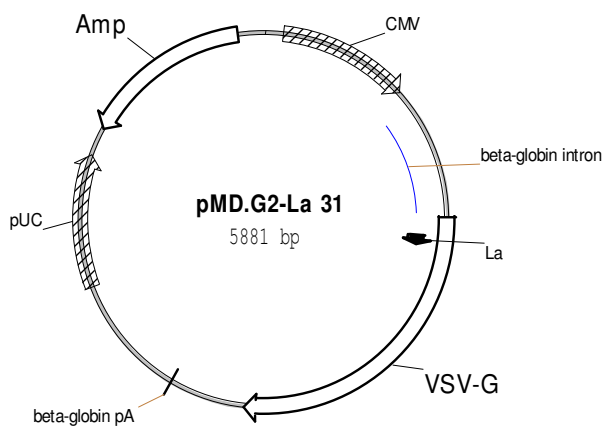
pcz-VSV-G myc 208
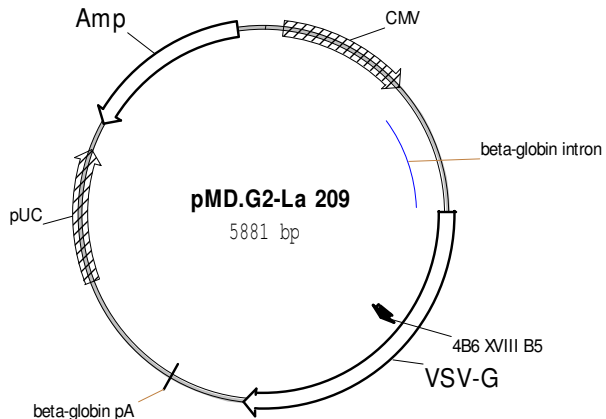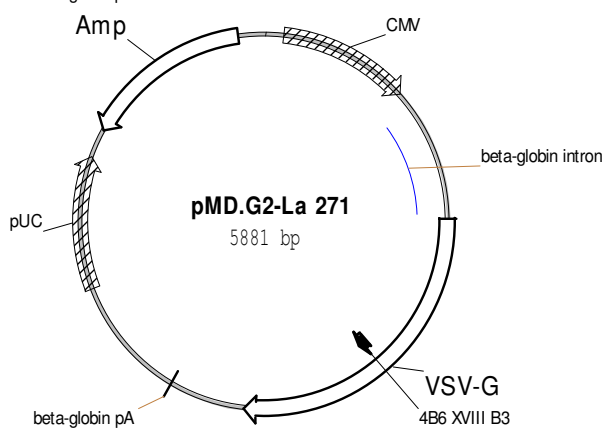

pcz-VSV-G myc 266

pcz-VSV-G myc 278

pMD.G2

pMD.G2-La 17

pMD.G2-La 17
5881 bp

pMD.G2-La 31

pMD.G2-La 31
5881 bp

pMD.G2-La 209

pMD.G2-La 209
5881 bp

pMD.G2-La 271

pMD.G2-La 271
5881 bp

Versicherung

Hiermit versichere ich, dass ich die vorliegende Arbeit ohne unzulässige Hilfe Dritter und ohne Benutzung anderer als der angegebenen Hilfsmittel angefertigt habe. Die aus fremden Quellen direkt oder indirekt übernommenen Gedanken sind als solche kenntlich gemacht. Die Arbeit wurde weder im Inland noch im Ausland in gleicher oder ähnlicher Form einer anderen Prüfungsbehörde vorgelegt.

Die vorliegende Arbeit wurde am Institut für Immunologie der Technischen Universität Dresden unter wissenschaftlicher Betreuung von Prof. Dr. med. habil. E. P. Rieber angefertigt.

Die Promotionsordnung wird anerkannt.

Dresden, den 25.06.2007

Serap Güneş